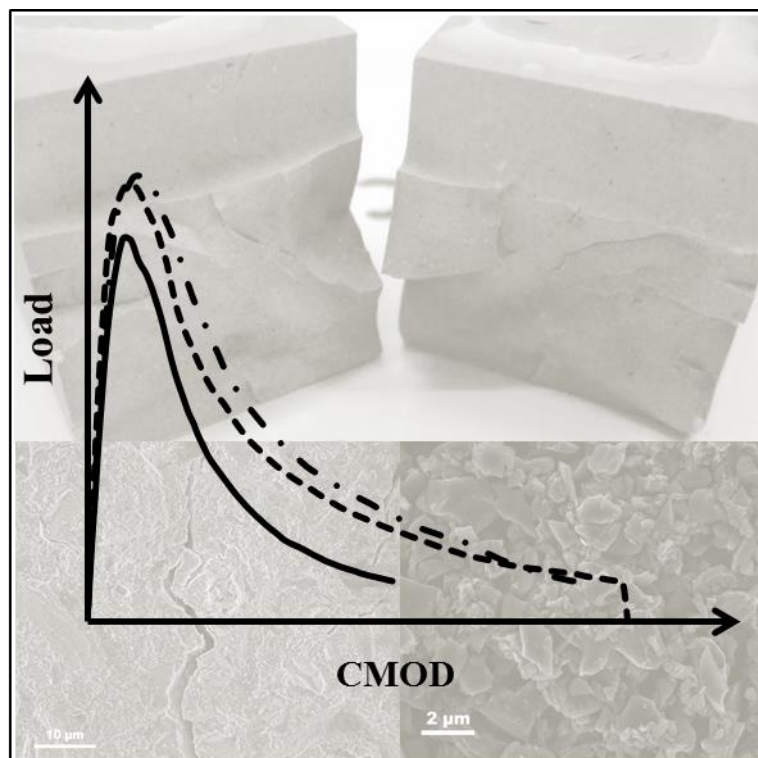


Sajjad Ahmad

Innovative mix design of cementitious materials for enhancing strength and ductility



Dottorato di Ricerca in Ingegneria delle Strutture
Politecnico di Torino

Sajjad Ahmad

**Innovative mix design of cementitious
materials for enhancing strength and
ductility**

Tesi per il conseguimento del titolo di Dottore di Ricerca
XXVII Ciclo (2012 - 2013 - 2014)



Dottorato di Ricerca in Ingegneria delle Strutture
Politecnico di Torino

Dicembre 2014

Dottorato di Ricerca in Ingegneria delle Strutture
Politecnico di Torino, Corso Duca degli Abruzzi 24, 10129 Torino, Italy

Tutori: Prof. Giuseppe Andrea Ferro, Prof. Jean-Marc Tulliani

Coordinatore: Prof. Alberto Carpinteri

Dedicated to my family

Acknowledgements

All praises be to Allah Almighty, the Merciful, the Beneficent, Who blesses us with His kindness, mercy and help that made me capable to accomplish my studies.

I feel great privilege to express my deep gratitude to my supervisors Professor Giuseppe Andrea Ferro (Department of Structural, Geotechnical and Building Engineering - DISEG) and Associate Professor Jean-Marc Tulliani (Department of Applied Science and Technology - DISAT) for providing me with the opportunity to research in the field of cementitious composites. I am very thankful for their kind interest, valuable advices and guidance with generous dedication, throughout all the phases of my study at Politecnico di Torino.

I would like to thank Dr. Pravin Jagdale (DISAT) for his support and guidance in the synthesis and characterization of the carbonized materials. I am also thankful to Dr. Guastella Salvatore (DISAT) for FESEM and EDX analysis and Dr. Mauro Giorcelli (DISAT) for Raman analysis of the carbonized materials. I am also grateful to Mr. Marco Costanzo Alessio (DISEG) and Mr. Pietro Paolo Provenzano (DISEG) for their help and cooperation in carrying out laborious testing.

I would like to thank Mr. Lorenzo Bar (Associazione Italiana Bambù), Mr. Felice Giraud (Assocanapa), Dr. Stefano Broggio (Mapei S.p.A.), Dr. Fulvio Canonico (Buzzi Unicem S.p.A.) and Professor Francisco Robles Hernandez (College of Technology, University of Houston, Houston TX, USA) for providing raw bamboo, hemp hurds, super plasticizer, cement and carbon soot for the present research work, respectively.

I would also like to acknowledge the PhD study grant provided by Higher Education Commission Pakistan (Ref no. HRDI-UESTPs/HEC/2012/36) under the project of HRDI-UESTPs.

Summary

Cement based composites i.e. paste, mortar and concrete are the most utilized materials in the construction industry all over the world. Cement composites are quasi-brittle in nature and possess extremely low tensile strength as compared to their compressive strength. Due to their low tensile strength capacity, cracks develop in cementitious composites due to the drying shrinkage, plastic settlements and/or stress concentrations (due to external restrains and/or applied stresses) etc. These cracks developed at the nanoscale may grow rapidly due to the applied stresses and join together to form micro and macro cracks. The growth of cracks from nanoscale to micro and macro scale is very rapid and may lead to sudden failure of the cement composites. Therefore, it is necessary to develop such types of cement composites possessing higher resistance to crack growth, enhanced flexural strength and ductility.

The development of new technologies and materials has revolutionized every field of science by opening new horizons in production and manufacturing. In construction materials, especially in cement and concrete composites, the use of nano/micro particles and fibers in the mix design of these composites has opened new ways from improved mechanical properties to enhanced functionalities. Generally, the production or manufacturing processes of the nano/micro sized particles and fibers are energy intensive and expensive. Therefore, it is very important to explore new methods and procedures to develop less energy intensive, low cost and eco-friendly inert nano/micro sized particles for utilization in the cement composites to obtain better performance in terms of strength and ductility.

The main theme of the present research work was to develop a family of new type of cementitious composites possessing superior performance characteristics in terms of strength, ductility, fracture energy and crack growth pattern by incorporating micro sized inert carbonized particles in the mix design of cementitious composites. To achieve these objectives the micro sized inert carbonized particles were prepared from organic waste materials, namely: Bamboo,

IV

coconut shell and hemp hurds. For comparison purposes and performance optimization needs, another inorganic waste material named as carbon soot was also investigated in the present research.

The experimental investigations for the present study was carried out in two phases; In the first phase of research work, a methodology was developed for the synthesis of the micro sized inert carbonized particles from the above mentioned organic raw materials. In the second phase of research, various mix proportions of the cementitious composites were prepared incorporating the synthesized micro sized inert carbonized particles. For micro sized inert carbonized particles obtained from bamboo and coconut shell three wt.% additions i.e. 0.05, 0.08, 0.20 were investigated and for particles synthesized from hemp hurds 0.08, 0.20, 1.00 and 3.00 wt.% additions were explored.

The cement composites were characterized by third-point bending tests and their fracture parameters were evaluated. The mechanical characterization of specimens suggested that 0.08 wt.% addition of micro sized inert carbonized bamboo particles enhances the flexural strength and toughness of cement composites up to 66% and 103% respectively. The toughness indices I₅, I₁₀ and total toughness of the cement composites were also enhanced. The carbonized particles synthesized from coconut shell resulted in improved toughness and ductility without any increase in the modulus of rupture of the cement composite specimens. Maximum enhancements in I₅ and I₁₀ were observed for 0.08% addition of both carbonized and carbonized-annealed particles. For the carbonized hemp hurds cement composites the results indicate that the micro sized inert carbonized particles additions enhanced the flexural strength, compressive strength and the fracture energy of the cement composites.

The microstructure of the cement composites was also studied with the help of field emission scanning electron microscope (FESEM) by observing small chunks of cement composite paste samples. The FESEM observations indicated that the micro sized inert carbonized particles utilized in the mix design of these mixes were well dispersed in the cement matrix. It was also observed that the fracture paths followed by the cracks were tortures and irregular due the presence of micro particles in the matrix. The cracks during their growth often contoured around the inert particle inclusions and resulted in enhanced energy absorption capacity of the cement composites.

The study was further enhanced to the cement mortar composites and their performances were studied. The results indicated that the energy absorption behavior of the composites was enhanced for all the cement composites containing micro carbonized particles.

Finally, it is concluded that the ductility and toughness properties of the cement composites can be enhanced by incorporating the micro sized inert carbonized particles in the cement matrix. The fracture energy, ductility and toughness properties enhancement of the cement composites greatly depends upon the source and synthesis procedure followed for the production of micro sized inert carbonized particles.

Contents

Acknowledgements	I
Summary	III
Contents	VII
List of figures	XIII
List of tables	XVII
Notations and abbreviations	XIX
Chapter 1 Introduction	1
1.1 Background	1
1.2 Research objectives	3
1.3 Research significance	3
1.4 Thesis organization	5
Chapter 2 Literature review	7
2.1 Cementitious composites	7
2.2 Microstructure of cementitious composites	8
2.3 Fracture mechanism of cement composites	11
2.4 Toughening mechanisms in cement composites	12
2.4.1 Crack deflection	12
2.4.2 Micro cracks	13
2.4.3 Bridging action of inclusions	13

VIII

2.4.4	Crack branching	13
2.4.5	Crack surface resistance	14
2.4.6	Crack tip blunting	14
2.5	Fracture mechanics properties of cementitious composite	15
2.5.1	Toughness indices	16
2.5.2	Brittleness index	17
2.5.3	Characteristic length	18
Chapter 3 Materials and methods		21
3.1	Materials	21
3.1.1	Cement	21
3.1.2	Fine aggregates	22
3.1.3	High range water reducing admixture (HRWRA)	22
3.1.4	Raw materials for the synthesis of carbonized particles	22
3.1.4.1	Bamboo	22
3.1.4.2	Coconut shell	25
3.1.4.3	Hemp hurds	26
3.1.4.4	Carbon soot	27
3.2	Processing of raw materials	29
3.2.1	Pyrolysis of raw materials	29
3.2.1.1	Pyrolysis of bamboo	30
3.2.1.2	Pyrolysis of coconut shell	31
3.2.1.3	Pyrolysis of hemp hurds	32
3.2.2	Grinding of pyrolyzed materials	33
3.3	Preparation of cement composites	34
3.3.1	Water demand and setting time of cement	34
3.3.2	Super-plasticizer demand	34

3.3.3	Mix design of cement paste and mortar composites	35
3.3.4	Cement paste sample preparation	35
3.3.5	Mortar sample preparation	37
3.4	Material's characterization	39
3.4.1	Thermogravimetric analysis	40
3.4.2	Carbonized material characterization	40
3.4.2.1	FESEM analysis	40
3.4.2.2	Raman analysis	40
3.4.2.3	Dispersion of carbonized particles in water	40
3.4.2.4	XRD analysis	41
3.4.3	Mechanical characterization of cement composites	41
3.4.3.1	Three point flexure test	41
3.4.3.2	Compression test of specimens	42
3.4.4	Microstructural characterization of cement composites	43
Chapter 4	Experimental results	45
4.1	Tests on raw materials	45
4.1.1	Thermo-Gravimetric analysis	45
4.1.2	Raman analysis	49
4.1.3	FESEM analysis	50
4.1.4	EDX analysis	54
4.1.5	Dispersion analysis of carbonized materials in water	55
4.2	Mechanical characterization of SCP composites	56
4.2.1	SCP containing micro carbonized bamboo particles	56
4.2.1.1	Three point bending tests	56
4.2.1.2	Evaluation of flexural test results	57
4.2.1.3	Compression tests	59

4.2.1.4	FESEM of SCPs	60
4.2.2	SCPs containing carbonized coconut shell particles	61
4.2.2.1	Three point bending tests	61
4.2.2.2	Evaluation of flexural tests	61
4.2.2.3	Compression tests	64
4.2.2.4	FESEM of SCPs	64
4.2.3	SCPs containing micro carbonized hemp hurds particles	66
4.2.3.1	Three point bending tests	66
4.2.3.2	Evaluation of flexural tests	66
4.2.3.3	Compression tests	69
4.2.3.4	FESEM of SCPs	69
4.2.5	SCPs containing carbon soot particles	70
4.2.5.1	Three point bending tests	70
4.2.5.2	Evaluation of flexural test results	71
4.2.6	SCPs containing micro carbonized particles and carbon soot	73
4.2.6.1	Three point bending test	74
4.2.6.2	Evaluation of flexural test results	74
4.3	Tests on SCMs	76
4.3.1	Third-point bending tests	76
4.3.2	Evaluation of flexural test results	77
4.3.3	Modulus of rupture of mortar composites	81
Chapter 5	Discussion on results	83
5.1	Discussion on carbonized inert particles	83
5.1.1	Pyrolysis kinetics of materials	83
5.1.2	Micro structure and composition	84

5.2	Mechanical results	85
5.2.1	Load-CMOD relation & modulus of rupture	85
5.2.2	Crack surfaces and cement composites microstructure	86
5.2.3	Dispersion of carbonized inert particles	87
5.3	Evaluation of flexural test results	88
Chapter 6 Conclusions		91
References		93

List of figures

Figure 2.1: Direct tensile test of a concrete plate, (left) LVDT responses and (right) stress-displacement curve (Shah et al., 1995)	11
Figure 2.2: Crack deflection around grain boundary; (a) SEM and (b) TEM observations of an alumina composite (Yi et al., 2014)	12
Figure 2.3: Bridging action by solid inclusion (left) and fibers (right)	13
Figure 2.4: Model of a rough crack interface, (a) open crack, (b) slip at contact surfaces (Mróz & Mróz, 2010)	14
Figure 2.5: Crack tip blunting due to pores	15
Figure 2.6: Load-deflection curve for a beam with third-point bending for the evaluation of the toughness indices (ASTM, 1997)	16
Figure 2.7: Description of brittleness index (Topçu, 1997)	18
Figure 3.1: Typical structure of bamboo plant	23
Figure 3.2: Transverse section of a hemp stem	26
Figure 3.3: TEM and schematic images of soot and carbon nano-spheres. (a) An ns-soot particle from diesel particulate matter. (b) Enlarged image of (a). (c) High-resolution image of ns-soot particle from (b). (d) Schematic image of carbonaceous nano-spheres aggregated to form ns-soot. (Buseck et al., 2012)	28
Figure 3.4: Experimental setup for the pyrolysis of organic raw materials	30
Figure 3.5: Schematic overview of pyrolysis process of bamboo	31
Figure 3.6: Schematic overview of pyrolysis process of coconut shell	32
Figure 3.7: (a) As obtained hemp hurds, (b) Carbonized and ground hemp hurds	32
Figure 3.8: Grinding apparatus (a) mortar and pestle, (b) ball mill, (c) attrition mill	33
Figure 3.9: Typical dimensions of mini slump cone (Hagerman's cone)	34
Figure 3.10: Janke & Kunkel homogenizer and (b) Hobart mixer	39
Figure 3.11: Three point flexure tests of (a) paste and (b) mortar composites	42

Figure 3.12: Compression test setup of cement paste composites	43
Figure 4.1: TGA analysis of raw materials in Argon	46
Figure 4.2: TGA analysis of carbonized materials in air	47
Figure 4.3: TGA & DTG curves of raw bamboo in argon (left) and carbonized bamboo in air (right)	48
Figure 4.4: TGA & DTG curves of chemically treated bamboo in argon (left) and chemically treated and carbonized bamboo in air (right)	48
Figure 4.5: TGA & DTG curves of coconut shell in argon (left) and carbonized coconut shell in air (right)	48
Figure 4.6: TGA & DTG curves of carbon soot in argon (left) and in air (right)	49
Figure 4.7: Raman spectrum of carbonized materials	50
Figure 4.8: I_D/I_G variation for carbonized materials	50
Figure 4.9: FESEM of a small bamboo piece after TGA	51
Figure 4.10: FESEM of carbonization and ground bamboo particles	52
Figure 4.11: FESEM of carbonized and ground coconut shell particles	52
Figure 4.12: FESEM of carbonized and ground hemp hurds	53
Figure 4.13: FESEM of carbon soot particles	54
Figure 4.14: Water suspension containing carbonized bamboo particles (a) After 1 h of mixing, (b) After 24 h of mixing	55
Figure 4.15: Typical load-CMOD curves for cement composites with and without carbonized bamboo particles	56
Figure 4.16: Comparison of toughness index I_5 for the cement paste composites containing carbonized bamboo particles	57
Figure 4.17: Comparison of toughness index I_{10} for the cement paste composites containing carbonized bamboo particles	58
Figure 4.18: Comparison of total toughness of cement paste composites containing carbonized bamboo particles	58
Figure 4.19: Comparison of flexural strength of cement paste composites containing carbonized bamboo particles	59
Figure 4.20: Typical fracture surfaces of the cement paste after third-point bending test	59
Figure 4.21: Compressive strength comparison of cement composites containing carbonized bamboo particles	60
Figure 4.22: FESEM of cement composite sample containing carbonized particles	60

Figure 4.23: Typical load-CMOD curves for cement composites with and without carbonized coconut shell particles	61
Figure 4.24: Comparison of toughness index I5 for the cement paste composites containing carbonized coconut shell particles	62
Figure 4.25: Comparison of toughness index I10 for the cement paste composites containing carbonized coconut shell particles	62
Figure 4.26: Comparison of total toughness of cement paste composites containing carbonized coconut shell particles	63
Figure 4.27: Comparison of flexural strength of cement paste composites containing carbonized coconut shell particles	63
Figure 4.28: Typical fracture surfaces of the cement paste containing carbonized coconut shell after third-point bending test	64
Figure 4.29: Compressive strength comparison of cement composites containing carbonized coconut shell particles	64
Figure 4.30: FESEM of cement composite sample containing carbonized 0.2% coconut particles	65
Figure 4.31: Typical load-CMOD curve of control mix and cement composite with 0.08% hemp hurds	66
Figure 4.32: Comparison of toughness index I5 for the cement paste composites containing carbonized hemp hurds particles	67
Figure 4.33: Comparison of toughness index I10 for the cement paste composites containing carbonized hemp hurds particles	67
Figure 4.34: Comparison of flexural strength of cement paste composites containing carbonized hemp hurd particles	68
Figure 4.35: Typical fracture surfaces of the cement composites after third-point bending test (a) control mix, (b) CEM+0.08HH	68
Figure 4.36: Compressive strength comparison of cement composites containing carbonized hemp hurd particles	69
Figure 4.37: FESEM of cement composite sample containing carbonized hemp hurd particles	70
Figure 4.38: Typical load-CMOD curve of control mix and cement composite with 1.0% carbon soot	71
Figure 4.39: Comparison of toughness index I5 for the cement paste composites containing carbon soot particles	71
Figure 4.40: Comparison of toughness index I10 for the cement paste composites containing carbon soot particles	72
Figure 4.41: Comparison of total toughness of cement paste composites containing carbon soot particles	72

Figure 4.42: Comparison of flexural strength of cement paste composites containing carbon soot particles	73
Figure 4.43: Typical fracture surfaces of the cement paste containing carbon soot particles after third-point bending test	73
Figure 4.44: Typical load-CMOD curve of control mix and cement composites containing carbon soot and inert carbonized particles	74
Figure 4.45: Comparison of toughness index I5 for the cement paste composites containing carbon soot and inert carbonized particles	75
Figure 4.46: Comparison of toughness index I10 for the cement paste composites containing carbon soot and inert carbonized particles	75
Figure 4.47: Comparison of total toughness of the cement paste composites containing carbon soot and inert carbonized particles	76
Figure 4.48: Typical load-CMOD relation of cement mortar composites containing various types of carbonized particles	77
Figure 4.49: Load-CMOD curve for the cement composite containing carbon soot particles	77
Figure 4.50: Comparison of toughness index I5 of mortar composites	78
Figure 4.51: Comparison of toughness index I10 of mortar composites	78
Figure 4.52: Comparison of toughness index I20 of mortar composites	79
Figure 4.53: Comparison of residual toughness R(5,10) of cement mortar composites	79
Figure 4.54: Comparison of residual toughness R(10,20) of cement mortar composites	80
Figure 4.55: Total toughness of cement mortar composites	80
Figure 4.56: Modulus of rupture of cement mortar composites	81

List of tables

Table 2.1: Mechanical properties of C-S-H from literature (mean value \pm SD)	8
Table 3.1: Physical properties of ordinary Portland cement	21
Table 3.2: Chemical properties of ordinary Portland cement	21
Table 3.3: Mix proportioning for paste and mortar systems	35
Table 3.4: Composition of cement paste composites with carbonized bamboo particles*	36
Table 3.5: Composition of cement paste composites with carbonized coconut shell particles*	36
Table 3.6: Composition of cement paste composites with carbonized hemp hurds particles*	36
Table 3.7: Composition of cement paste composites with carbon soot particles*	37
Table 3.8: Composition details of cement mortar composites with various carbonized particles*	38
Table 4.1: Mass loss behavior of raw material in Argon	46
Table 4.2: Intensity peak ratios of D and G bands of the carbonized materials and carbon soot in Raman spectrum	49
Table 4.3: Elemental composition of carbonized bamboo particles	54
Table 4.4: Elemental composition of carbonized coconut shell, hemp hurds and carbon soot particles	55

Notations and abbreviations

BI	Brittleness index
CEM	Cement (Ordinary Portland cement)
CH	Calcium hydro-oxide
CMOD	Crack mouth opening displacement
CNFs	Carbon nano fibers
CNTs	Carbon nano tubes
CPB	Chemically treated and pyrolyzed bamboo
CPBA	Chemically treated, pyrolyzed and annealed bamboo
CS	Carbon soot
C-S-H	Calcium silicate hydrate
E	Modulus of elasticity
EDX	Energy-dispersive x-ray
FESEM	Field emission scanning electron microscope
F_{\max}	Maximum vertical force in third-point bending test
FPZ	Fracture process zone
f_t	Tensile strength of cement composites
G_f	Fracture energy
H	Indentation hardness
h	Height of the specimen excluding notch height
HD	High density
HH	Carbonized hemp hurds
HRWRA	High range water reducing admixture

l	Span length in third-point bending test
l_{ch}	Characteristic length
LD	Low density
LVDT	Linear variable differential transformer
M	Indentation modulus
OPC	Ordinary Portland cement
PB	Pyrolyzed bamboo
PBA	Pyrolyzed and annealed bamboo
PC	Pyrolyzed coconut shell
PCA	Pyrolyzed and annealed coconut shell
PP	Polypropylene
PVA	Poly-vinyl alcohol
SCM	Self-consolidating mortar
SCP	Self-consolidating paste
TGA	Thermo-gravimetric analysis
TI	Toughness index
W	Width of specimen
σ_{max}	Modulus of rupture

Chapter 1 Introduction

1.1 Background

The humankind has ever strived to understand and adept at materials behavior and their utilization. Stone, Bronze or Iron Ages are the division of human history named after the materials, is an evident of the fact. If we follow the same naming convention then present age may be regarded as the Concrete Age due to the tremendous amounts of concrete production and utilization all over the world. Concrete is a manmade stone like material, primarily composed of sand, gravel, cementitious material (usually Portland cement) and water (Gambhir, 2004; Neville & Brooks, 2010). The water chemically reacts with the cementitious materials and form hydrated gel. As the gel hardens, it binds all the sand and gravel particles together forming a compact matrix structure (Mehta & Monteiro, 2006).

Concrete is an anisotropic material and exhibits different properties in tension and compression. The properties of cement and concrete composites are derived from their two basic components/phases (i.e. hydration products phase, aggregate phase) and the interaction between them. Cement composites are quasi brittle in nature with very low deformation capacity under tensile stresses but much stronger in compression. So small amount of tensile stresses, which may be due to the mechanically applied loads, environmental loadings, and/or deleterious reactions such as shrinkage, carbonation, Alkali silica reactions etc., can cause cracking in the cement composites. Due to the low deformation capacity and brittle nature of the cement composites, the developed cracks grow rapidly and adversely affect the strength and durability thus reducing the service life span of the structures (Zhang & Ju, 2011). The brittle nature of the cement composites is attributed to the absence of stress relieving mechanisms at the crack tips like dislocation or crazing in metals and polymers. As a result, the stresses required for the propagation of the cracks are much lesser as compared to the stresses required for their initiation (Freiman & Mecholsky, 2012). The large variations in the stresses required for crack initiation

and growth in cement composites leads to unstable and rapid growth of the cracks after their nucleation (Banthia & Sheng, 1996).

The issues of brittleness and crack susceptibility are more pronounced in the high strength cement composites, which have been developed to meet the modern world requirements. As it is a well-known fact that the brittleness of cementitious composites is directly related to their strength (Domone, 2007). Therefore, it is important to enhance the ductility and reduce crack susceptibility of the cementitious composites especially high strength cement composites to enhance the service life span of the structures. The reduction in crack susceptibility and ductility enhancement of the cement composites can be achieved by following the appropriate precautions in design, construction practices and most importantly the materials and their proportioning.

In literature most of the existing research on the ductility enhancement is based on to the utilization of the fibers in the cement composites. There are a large number of fiber types that have been studied for example hemp, sisal, jute, cellulose whiskers, steel, polyvinyl alcohol (PVA), polypropylene (PP), carbon nanotubes (CNTs), carbon nano fibers (CNFs) and many others (Cao, Zhang, & Wei, 2013; Carneiro, Lima, Leite, & Toledo Filho, 2014; Chung, 2000; Hamzaoui, Guessasma, Mecheri, Eshtiaghi, & Bennabi, 2014; Lima, Toledo Filho, & Melo Filho, 2014; Lopez, Ferro, Jagadale, & Tulliani, 2013; Musso, Tulliani, Ferro, & Tagliaferro, 2009; Sedan, Pagnoux, Smith, & Chotard, 2008; Siddique & Mehta, 2014; Yang & Li, 2014). Recent studies also show the utilization of nano materials such as graphene, nano crystalline cellulose, calcium carbonate whiskers and nano SiO₂ particles for improving the ductility and strength of the cement composites (Alkhateb, Al-Ostaz, Cheng, & Li, 2013; Kawashima, Hou, Corr, & Shah, 2013; Kim, Foley, & Reda Taha, 2013; Pourjavadi, Fakoorpoor, Khaloo, & Hosseini, 2012). The fibers in the cement matrix behave as crack arresters and restrain their growth. The crack arresting mechanisms of fibers in cement composites impart toughness and enhance their energy absorption capacity. In the crack arresting mechanism of fibers, two crucial parameters that limit the performance of fibers are their dispersion in the host matrix and the interfacial bonding between the fiber and the composites. The uniform fibers dispersion in the cement matrix is usually a difficult task and requires special procedures, thus greatly reducing their utilization in the cement composites (Konsta-Gdoutos, Metaxa, & Shah, 2010; Martone, Formicola, Giordano, & Zarrelli, 2010; Metaxa, Konsta-Gdoutos, & Shah, 2013).

Therefore, in the present research work another approach was adopted to enhance the ductility as well as the mechanical strength of the cement composites that is to trap the growth of cracks and deflect their paths by the utilization of micro

sized inert carbonized particles in the mix design of cementitious composites. The micro sized particles inclusion brings heterogeneity in the matrix at micro level and results in complex crack tip stresses around the inert particle inclusion. The presence of complex stress fields around the crack tips restricts the in plane movement of the cracks and results in crack deflection and sometimes crack contouring around the particle. The random and multi-plane movement of the crack path results in higher fracture surface area involving more material in the cracking process as compared to the cracking in a single plane. Working on the above-mentioned idea in the present research the carbonized particles were developed from organic waste products i.e. bamboo, coconut shell and hemp hurds and further utilized in the preparation of the cementitious composites.

1.2 Research objectives

The main goal of the present thesis work is to enhance the strength and ductility of the cementitious composites by using an innovative approach of incorporating the micro sized inert carbonized particles in the cement matrix. Keeping in view the environmental aspects and sustainability, the micro sized inert particles were synthesized from organic waste products. The detailed list of objectives is given below:

1. Producing a new class of strong, tough and environmentally friendly self-consolidating cementitious materials for structural applications
2. Optimization of the composition of cement composites to enhance their mechanical strength and ductility by using the micro sized inert carbonized particles
3. Study of the relationship between the fracture toughness of cement composites and the inert particles loading in the cement matrix
4. Development of methodology for the synthesis of micro sized inert carbonized particles from the organic waste products
5. Exploration of the cheap, environmental friendly and sustainable sources for the production of micro sized inert carbonized particles

1.3 Research significance

Cement and concrete composites are produced in abundance all over the world and their production poses heavy load on the environment and sustainability of the

natural resources. The development of the cement composite with superior properties in terms of mechanical strength and ductility will lead to the lesser consumption of natural resources as well as improving the safety and service life of the structure. The improved crack resistance will also have positive influence on the maintenance requirements and subsequently reducing the maintenance and replacement costs of the structures.

Nowadays there are great concerns about the sustainability of the natural resources and environment. The sustainable development is about to following such methodologies that the present world demands should be satisfied while ensuring the capability of the natural resources to fulfill the requirement of the future generations (Awwad, Mabsout, Hamad, Farran, & Khatib, 2012). The development of inert carbonized particles from the plant and agricultural waste is not only sustainable but also environmental friendly. The incorporation of the micro sized inert carbonized particles in the cement matrix results in the packing density enhancement of the paste phase consequently reducing the minimum paste requirement for obtaining the given level of workability. In other words, the increased packing density of the cement composites translates into reduced paste requirement which is essential for the development of the eco-friendly concretes (Abd Elrahman & Hillemeier, 2014; A.K.H. Kwan, Ng, & Huen, 2014; Albert K.H. Kwan & Yeung, 2014; Rizwan, Ahmad, & Bier, 2012; X. Wang, Wang, Taylor, & Morcou, 2014). Besides the lesser paste requirements, the improved ductility of the cement composites leads to the longer service life and improved safety of the structures thus indirectly resulting in the reduced utilization of the natural resources for the maintenance and replacement of the structures. The increased flexure and compressive strength will leads to the smaller member sizes in the structures resulting in the reduced cement and aggregate utilization (A.K.H. Kwan et al., 2014; Mueller, Wallevik, & Khayat, 2014; Rizwan et al., 2012; Tangpagasit, Cheerarot, Jaturapitakkul, & Kiattikomol, 2005; Ulm, 2009; X. Wang et al., 2014).

Alongside the reduced utilization of the natural resources, another positive effect of carbonized particles incorporation in the cement composites on the environment is by the phenomenon of carbon sequestration. The carbon sequestration is defined as the process of depositing the carbon in a reservoir and preventing it from going back to the atmosphere. The residence time of carbon in form of organic char is in the range of hundreds of years therefore, by converting the organic waste into carbonized form and storing it in the concrete matrix will reduce the amounts of carbon going back to atmosphere. This phenomenon will also help in reducing the carbon footprints of cement industry (Choi, Yun, & Lee, 2012).

1.4 Thesis organization

In this thesis, three plant waste materials were processed for the synthesis of the micro sized inert carbonized particles. The developed micro sized particles were utilized in the production of cement paste composites and their performance were studied. Then the study was enhanced to the cement mortar systems and their mechanical performances were also investigated. The first chapter of this thesis briefly describes the introduction, research significance and research objectives. In the second chapter of the dissertation, the background of cementitious composites is provided especially focusing on the viewpoint of fracture mechanics. Third chapter contains the details about the materials utilized in the present research and brief description about the synthesis, and processing of carbonized micro inert particles is given. The preparation of the cement composites and subsequently their testing procedures are also briefly explained. In the fourth chapter, the mechanical test results and physiochemical characterization of the cementitious composites are reported. The discussion on the results is made in fifth chapter of this thesis. In the last chapter, conclusions and recommendations based on the present research activity are reported.

6 Innovative mix design of cementitious materials for enhancing strength and ductility

Chapter 2 Literature review

2.1 Cementitious composites

Nowadays modern cement and concrete composites are widely used in construction industry all over the world. The cement composites are required to possess special performance characteristics to fulfill the stringent requirements of the modern structures. These special requirements may include workability, flow ability, mechanical strengths at early age and/or long term, durability, impermeability, shrinkage, toughness, crack tolerance, higher fracture energy, impact resistance and so on. The high performance cementitious composites fulfilling such special requirements usually require special and/or innovative raw materials accompanied with superior mixing and construction practices. As a fruit of advancements in the materials science and technology, the mechanical strengths of cementitious composites have reached several times higher than it was in the beginning of the 19th century. The development of super-plasticizers and high range water reducers; which are an essential component of the self-consolidating cementitious composites, have paved the way to attain highly workable cement composites even at very low w/c ratio, thus resulting in much higher mechanical strength and better performance characteristics. The increased mechanical strength of the cement composites translates into the reduced sizes of the structural members. The reduction in structural member sizes not only helps in cost saving but also beneficial for the environment and sustainability of the natural resources as the production of Ordinary Portland Cement (OPC) is a major cause of the CO₂ emissions in the atmosphere (Worrell, Price, Martin, Hendriks, & Meida, 2001).

Cement composites are composed of diverse types of materials, possessing different performance characteristics and in cement composites, these materials combine to produce complex microstructure. In this chapter, a brief overview of the microstructure of cement composites is presented and its effect on the fracture properties is discussed.

2.2 Microstructure of cementitious composites

Cement composites are the heterogeneous materials composed of complex micro, mezzo and macro structure. All the properties of the cement composites are derived from their microstructure. Following is a little description of the microstructure of the cement composites.

The cement particles in the fresh mix react with water to form hydrates. These hydrates of cement harden with time and bind the aggregate particles to form a stone like mass. Calcium silicate hydrates (C-S-H); calcium hydro-oxide (CH) and calcium sulfoaluminates (also known as ettringite) are the major cement hydration products (Peled, Castro, & Weiss, 2013; Zhao & Sun, 2014). The C-S-H gel is the main hydration product that makes up about 50-75% volume of the paste. It is crystalline in nature and composed of particles having size range of about 1.0 μm . The C-S-H is the major component that plays important role in imparting the strength to the cement composites (Hu, Han, Gao, Zhang, & Li, 2014; Hu & Li, 2014). The mechanical properties of C-S-H such as hardness and indentation modulus are generally determined by the nanoindentation technique. From literature, some results related to the mechanical properties of C-S-H gel are reported in Table 1.1.

Table 1.1: Mechanical properties of C-S-H from literature (mean value \pm SD)

Sample composition	Indentation modulus (M) (GPa)	Hardness (H) (GPa)	Reference
w/c: 0.30	23.7 \pm 5.9	0.68 \pm 0.18	(Vandamme & Ulm, 2009)
w/c: 0.35	23.4 \pm 3.4 (LD*)	0.73 \pm 0.15	(Zhu, Hughes, Bicanic, & Pearce, 2007)
	31.4 \pm 2.1 (HD**)	1.27 \pm 0.18	
w/c: 0.40	21.7 \pm 2.2 (LD)	-	(Constantinides & Ulm, 2004)
	29.4 \pm 2.4 (HD)	-	
w/c: 0.45	22.89 \pm 0.76 (LD)	0.93 \pm 0.11	(Mondal, Shah, & Marks, 2007)
	41.45 \pm 1.75 (HD)	1.43 \pm 0.29	
w/c: 0.50	18.1 \pm 4.0 (LD)	-	(Jennings, Thomas, Gevrenov, Constantinides, & Ulm, 2007)
	31.0 \pm 4.0 (HD)	-	

* Low density C-S-H

** High density C-S-H

The nano indentation results reveals that the w/c ratio has direct impact on the mechanical strength of the C-S-H. Increased w/c ratio reduces the strength of C-S-H at nano scale and consequently results in lower strengths of cement composites.

The second major hydration product is calcium hydro-oxide (CH) have hexagonal crystals like morphology with size ranging from 0.01 to 0.1 μm and these crystals constitutes about 20-25% of the paste volume. The third component of the cement hydration products is calcium sulfoaluminates or ettringite forms only 10-15% of the paste volume. The ettringite is a crystal type material with long and slender prismatic needles like appearance. Besides these crystals, porosities (C-S-H gel pores and capillary pores) are another major component of the microstructure of hardened cement paste (Stark, 2011). The sizes of these pores may vary from 0.5 to 10 nm and 0.01 to 10 μm for gel and capillary pores, respectively, but they play an important role in the mechanical behavior of the cementitious composites (Shah, Swartz, & Ouyang, 1995).

The structure of cementitious composites may be divided in to two phases based on their physical and mechanical characteristics i.e. paste phase and aggregate phase. These two phases exhibit different microstructure, physical and mechanical properties i.e. strength, elastic modulus, coefficient of thermal expansion etc. As a result of these variations in the properties stresses generates at the interface of these phases in the cement composites (Scrivener, Crumbie, & Laugesen, 2004). The stress concentrations sometimes form nano or micro cracks/flaws in the composite prior to the external loads. The interaction between the paste and aggregate phases and the inherent flaws/micro cracks governs the behavior of cement composites at applied loads/stresses. Thus, many researchers have studied the utilization of nano/micro sized materials in the cementitious composites with the objective of improving the microstructure and consequently making the cement composites more efficient in terms of mechanical strength, durability, economical and ecofriendly.

Literature shows that the use of fly ash, silica fume, ground granulated blast furnace slag, lime stone powder, bentonite, metakaolin, glass powder, rice husk, coconut shell and wheat straw ashes in the cementitious composites as a partial replacement of cement have several positive effects on their performance, such as improved workability, consistency, thixotropy, compressive strength and durability (Abd Elrahman & Hillemeier, 2014; Aly, Hashmi, Olabi, Messeiry, & Hussain, 2011; Grilo et al., 2014; Jayapalan, Lee, & Kurtis, 2013; Kawashima et al., 2013; Khushnood, Rizwan, Memon, Tulliani, & Ferro, 2014; Memon, Arsalan, Khan, & Lo, 2012; Rahman, Baluch, & Malik, 2014; Sinsiri, Kroehong, Jaturapitakkul, & Chindaprasirt, 2012; C. Wang, Yang, Liu, Wan, & Pu, 2012). Depending on the

physical properties (i.e. particle size, gradation and shape) and/or chemical composition, the above-mentioned secondary raw materials (SRMs) either produce hydraulic and/or a pozzolanic activity and the positive effects achieved by their utilization are attributed to the hydraulic or pozzolanic activity. However, concrete is a quasi-brittle material which can be very strong in compression (>200 MPa ultimate strength), but presents generally a low resistance in tension and consequently a limited bending strength. It is also characterized by a relatively low fracture toughness. Studies show that cement, aggregate and mineral admixture can improve the toughness of concrete, but the effect is not obvious (Brandt, 2009).

Therefore, to improve the ductility of cement composites many researchers have tried to use fibers of various sizes for decades. Some examples of fibers that are generally used are steel, sisal, hemp, polyvinyl alcohol (PVA), polypropylene (PP), and many others (Awwad et al., 2012; Hakamy, Shaikh, & Low, 2013, 2014; Lin, Kayali, Morozov, & Sharp, 2014). Moreover, in recent years, particular attention has been paid to the distribution of fibers: very small and well-dispersed fibers may control the micro cracks in the matrix from the very beginning of their opening (Brandt, 2009). To this aim, nanomaterials such as carbon nanotubes (CNTs), carbon nano-fibers (CNFs), graphene, nano-crystalline cellulose, calcium carbonate whiskers and nano-SiO₂ particles were also investigated for improving the ductility and strength of cement composites (Beigi, Berenjian, Lotfi Omran, Sadeghi Nik, & Nikbin, 2013; Cao et al., 2013; Lv et al., 2013; Metaxa et al., 2013; Musso et al., 2009; Onuaguluchi, Panesar, & Sain, 2014; Pourjavadi et al., 2012; Quercia, Spiesz, Hüsken, & Brouwers, 2014). The basic aim of all the above mentioned work is generally the same; that is to improve the microstructure of the cementitious composites so that the crack generation is prevented and their propagation is blocked in the cement composites. Each method has its own pros and cons: some of them are costly and others might be difficult to use. Therefore, it is necessary to look into this issue from another approach such as by using the proposed micro-sized inert carbonized particles that are not only cheap but also easy to work with, contrarily to CNTs, for example. Recent research showed that the use of micro-sized carbonized hemp hurds, bamboo and coconut shell particles in the cement matrix improve the microstructure of the cementitious composites thus enhancing the strength and fracture toughness of cement composites (S. Ahmad, Khushnood, Jagdale, Tulliani, & Ferro, 2015; G. A. Ferro, Ahmad, Khushnood, Restuccia, & Tulliani, 2014; G. Ferro, Tulliani, Lopez, & Jagdale, 2015).

2.3 Fracture mechanism of cement composites

Cement and concrete composites are several times weaker in tension as compared to their compressive strength. The application of tensile stresses results in the developments of new cracks and/or growth of existing flaws in perpendicular direction to the application of loads. The mechanism of crack development and growth may be divided into four stages with respect to the load application. In the initial phase of load application, which is around 30% of the tensile strength of the material, the magnitude of the applied stress are lower and do not cause the initiation or growth of cracks in the composite. In the second phase, which is in between 30% to 80% of the tensile strength, isolated cracks generate in the matrix due the higher applied stresses. In the first and second phase, the material behaves in linear elastic manner. After the development of sufficient isolated cracks in the matrix, they grow and coalesce to form localized damage zones and this results in non-linear behavior of the material. The third phase of stable crack growth is in between 80% to the maximum strength of the material. After the peak load (fourth phase) unstable crack growth occurs leading to the failure of the material (Z. Li, Kulkarni, & Shah, 1993; Shah et al., 1995).

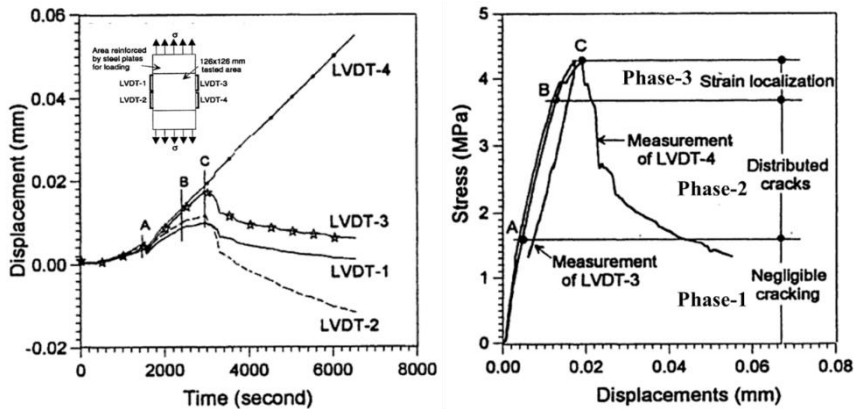


Figure 1.1: Direct tensile test of a concrete plate, (left) LVDT responses and (right) stress-displacement curve (Shah et al., 1995)

2.4 Toughening mechanisms in cement composites

Theoretically speaking the principals of linear elastic fracture mechanics indicate that the stresses at the crack tip approaches infinity. However, in real materials infinite stresses could not develop, so there should be some inelastic region beyond the crack tip in which the inelastic transformations can take place. In metals, this region is referred as yielding zone and for cement composites, it is known as fracture process zone (FPZ) (Jenq & Shah, 1991). Complex mechanisms take place in the FPZ of composites offering resistance to the crack growth. Few of these crack growth resistance or toughening mechanisms are explained below:

2.4.1 Crack deflection

The cement composites are composed of usually disorientated grains. The disorientation of the grains poses hurdle in the growth of a fracture path in a grain and crack has to deflect its path along the boundary of the grain to propagate by following the principal of least fracture resistance path. The increase in the fracture energy is dictated by the amount of deflections the fracture has to go through in the composite. A typical representation of the crack deflection in alumina composite is given in Figure 1.2 (Becker, Cannon, & Ritchie, 2002; Yi et al., 2014).

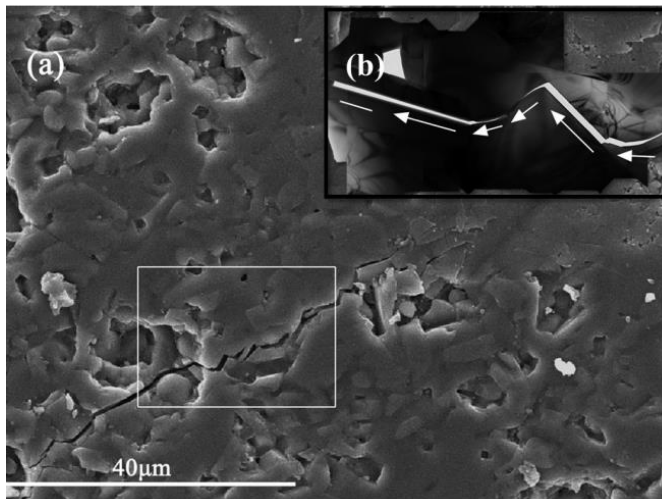


Figure 1.2: Crack deflection around grain boundary; (a) SEM and (b) TEM observations of an alumina composite (Yi et al., 2014)

2.4.2 Micro cracks

In cement composites, micro-cracks develop due to the uneven shrinkage, non-uniform drying and restraints of formwork and/or aggregate particles. The micro-cracks play important role in relieving the high stresses near the crack tip. The micro-cracks act as a shield to the crack tip against the far field stresses by absorbing the energy. Thus, they enhance the total energy requirement of the crack to grow in the composite (V. C. Li & Maalej, 1996a, 1996b).

2.4.3 Bridging action of inclusions

One of the most important phenomena of toughness enhancement is the crack bridging by the inert inclusion in the matrix. The inert inclusions may include aggregates, particle, fibers etc. The crack bridging action comes into play when the crack has already propagated beyond the inclusion and the stresses kept on transmitting through the inclusion until it is pulled out or torn in part (see Figure 1.3). This results in more energy requirement for the crack growth.

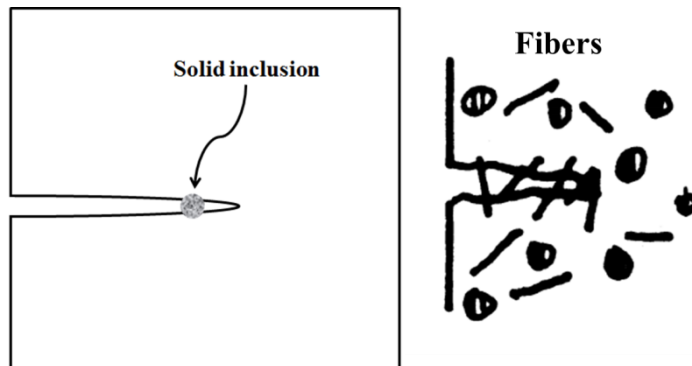


Figure 1.3: Bridging action by solid inclusion (left) and fibers (right)

2.4.4 Crack branching

The crack branching in the composites happens due to their inherent heterogeneity in the fracture process zone. The development of each new branch of the crack, the growth rate of the parent crack slows down and results in the increased fracture energy of the composite.

2.4.5 Crack surface resistance

The pullout of the inert inclusions and crack branching phenomenon results in rough and tortured fracture surfaces (I. Ahmad, Yazdani, & Zhu, 2015). The effect of rough crack surfaces for providing the toughness is more prominent in mode II and III loadings. In fact, the already generated rough crack surfaces by the mode I loading when observe the shear or torsional stresses then the rough surfaces came in to contact and increase the friction between the face requiring more energy for cracks to grow (Mróz & Mróz, 2010). The traction or frictional force also act as shield against the application of stresses to the crack tip (Freiman & Mecholsky, 2012).

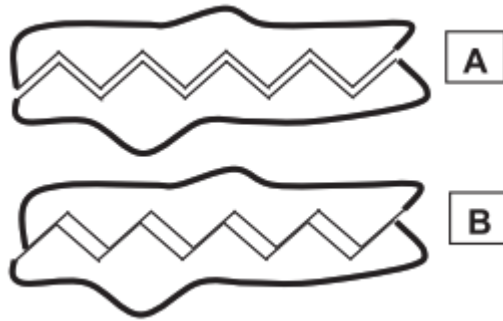


Figure 1.4: Model of a rough crack interface, (a) open crack, (b) slip at contact surfaces (Mróz & Mróz, 2010)

2.4.6 Crack tip blunting

Sometimes the crack tip encounters a void in its path. The voids might occur due to the entrapped air or water during the casting or preparation. The void results in blunting of the crack tip. The blunt tip require higher amount of energy to initiate a new crack from the periphery of the void resulting in improved toughness of the composite.

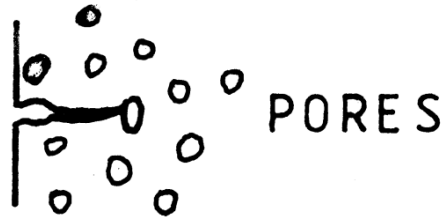


Figure 1.5: Crack tip blunting due to pores

2.5 Fracture mechanics properties of cementitious composite

The fracture energy (G_f) is one of the important characteristic of a material for the explanation of its fracture behavior (Rao & Prasad, 2002). In the fictitious crack model of Hillerborg, it was proposed that the G_f , tensile strength (f_t) and stress-CMOD relations can completely describe the fracture characteristics of cementitious composites (Hillerborg, 1983, 1985). The fracture energy can be defined as the energy required to produce a crack of unit surface area in the direction of propagation of the crack. According to the RILEM technical committee report 50-FMC, three point bending tests performed on notched beam can be used to determine the fracture energy of concrete materials. As the notched beam splits in to two halves, G_f may be evaluated by dividing the total energy dissipated by the surface area of the crack:

$$G_f = W/b(d-a_o) \quad (2.1)$$

Where W is the total energy dissipated, b is the notched beam thickness, d is the total height of beam and a_o is the height of the pre-fabricated notch in the tested beam specimen (Einsfeld & Velasco, 2006).

Bazant stated that the fracture characteristics obtained by the work of fracture method (RILEM 50-FMC) are ambiguous and size dependent so various sizes of the specimens results in different fracture characteristics (Bazant & Pfeiffer, 1987). Therefore, Bazant proposed a size effect method (SEM) for the determination of the fracture energy and other fracture characteristics of the cement composites. Similarly, other alternate parameters and methods that may be used for the

determination of the fracture characteristics of cement composites are described below:

2.5.1 Toughness indices

The fracture resistance of cement composites and various other ceramic materials is increased by the toughening mechanisms (see section 2.4). There are several ways to characterize the energy absorption capability of the cement composites and the toughness indices are one of them. The toughness of material is defined as the total area under the load deflection curve in a three point bending test of a prism. The toughness or load deflection curves are not only related to the material's characteristics but also strongly depends upon the dimensions of the test specimen. The first article based on the idea of a dimension less toughness number was published in 1978 by Henagar (Brandt, 2009). The method was further refined and standardized by ASTM in 1984 as ASTM C 1018 "Standard test method for flexural toughness and first-crack strength of fiber-reinforced concrete (using beam with third-point loading)" (ASTM, 1997).

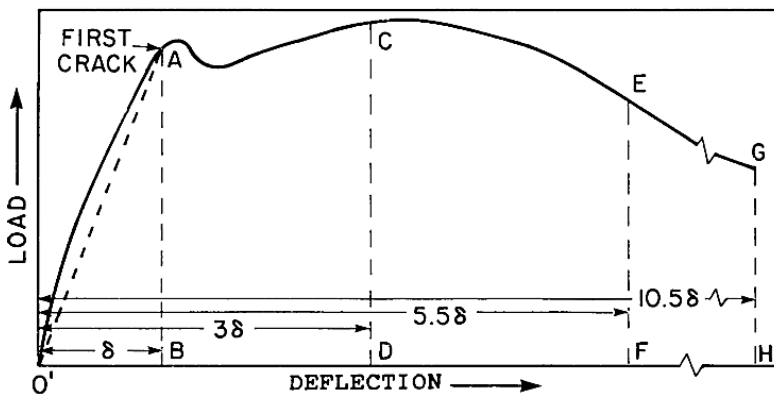


Figure 1.6: Load-deflection curve for a beam with third-point bending for the evaluation of the toughness indices (ASTM, 1997)

The ASTM standard provides evaluation of the three toughness indices indicated as TI_5 , TI_{10} and TI_{20} given by Eq. 2.2, 2.3 and 2.4, respectively.

$$TI5 = \frac{\text{Area under the F-}\delta \text{ curve up to 3times the 1}^{\text{st}} \text{ crack Deflection}}{\text{Area under the F-}\delta \text{ curve up to 1}^{\text{st}} \text{ crack Deflection}} \quad (2.2)$$

$$TI10 = \frac{\text{Area under the F-}\delta \text{ curve up to 5.5times the 1}^{\text{st}} \text{ crack Deflection}}{\text{Area under the F-}\delta \text{ curve up to 1}^{\text{st}} \text{ crack Deflection}} \quad (2.3)$$

$$TI20 = \frac{\text{Area under the F-}\delta \text{ curve up to 10.5times the 1}^{\text{st}} \text{ crack Deflection}}{\text{Area under the F-}\delta \text{ curve up to 1}^{\text{st}} \text{ crack Deflection}} \quad (2.4)$$

These dimensionless indices are beneficial in terms that they are not dependent on the specimen geometry. The toughness indices take into account the post peak behavior of the composites and incorporate all the toughening effects caused by the inclusions in the cement matrix. This standard also provides the residual strength factors $R_{5,10}$ and $R_{10,20}$ which are defined as the average strength retained in the matrix after the development of first crack as a percent of first crack strength. The expressions of the residual strength factors are presented below (Eq. 2.5 and 2.6):

$$R_{5,10} = 20 (I_{10} - I_5) \quad (2.5)$$

$$R_{10,20} = 10 (I_{20} - I_{10}) \quad (2.6)$$

The toughness indices $TI5$ and $TI10$ are defined as the dimensionless numbers obtained by dividing the area under the $F-\delta$ curve up to a deflection of 3.0 and 5.5 times the first-crack deflection respectively, by the area under the $F-\delta$ curve up to the first crack. The rationale to select the toughness indices for the energy absorption capability of cement composites is that the absolute values of toughness up to any specified deflection point depends entirely upon the geometrical variables associated to the specimens (i.e. sizes and shapes) and the testing arrangements (i.e. loading rate, span length). Therefore, the use of these indices caters for the above-mentioned variations.

2.5.2 Brittleness index

Cement composites are considered as brittle materials as they rupture at lower strains without going to plastic deformations. Brittleness may be regarded as the opposite of toughness. Wu keru and Zhou Jianhua (1987) suggested an index known as “Brittleness Index (BI)” for analyzing the brittleness of the composites. BI is

defined as the ratio of plastic strain energy of a material absorbed during a load cycle to the recovered elastic strain energy. The value of BI for the perfectly elastic materials is ‘infinity’ indicating that all the strain energy is recoverable while for perfectly elastic-plastic materials BI approaches to ‘zero’ showing that all the energy is stored in the material with zero recovery. The value of BI will be higher for the brittle material and lower for ductile materials (Topçu, 1997).

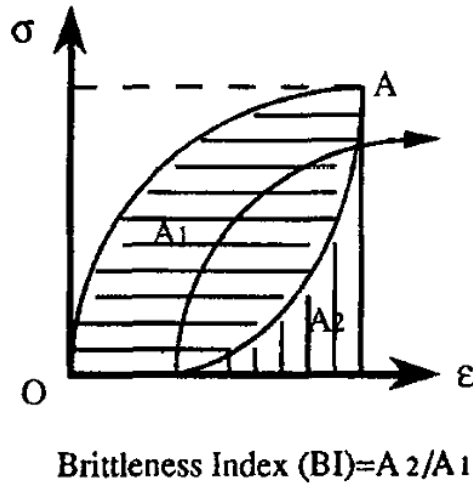


Figure 1.7: Description of brittness index (Topçu, 1997)

2.5.3 Characteristic length

Petersson(1981) and hillerborg(1985) presented the idea of characteristic length of a composite for the quantification of the ductility of composites. Characteristic length is defined as the ratio of material’s elastic modulus and fracture energy to the square of its tensile strength (Eq. 2.7) (Beygi, Kazemi, Nikbin, & Amiri, 2013; Korte, Boel, De Corte, & De Schutter, 2014).

$$l_{ch} = G_f E / f_t^2 \tag{2.7}$$

Where, G_f , E and f_t are the fracture energy, elastic modulus and tensile strength of the material. The higher values of the characteristic length indicate the higher

toughness of the material. Typical characteristics lengths for cement paste, mortar and concrete in the range of 5-15 mm, 100-200 mm and 200-400 mm, respectively (Brandt, 2009).

Chapter 3 Materials and methods

In the first part of the present chapter, all the materials used in the research work are briefly described and the preparation/synthesis of the micro sized, inert, carbonized materials are discussed in subsequent section. In the third part of the chapter, a short detail of the apparatus and equipment utilized for the research work is provided.

3.1 Materials

3.1.1 Cement

Type-1 ordinary Portland cement (OPC), commercially available under the brand name of Buzzi-Unicem S.p.A. was utilized throughout the research work. The OPC complies with the standard specification of UNI EN 197-1. The physical and chemical properties of OPC as per the manufacturer product datasheet are presented in Table 1.2& Table 1.3, respectively (Buzzi-Unicem S.p.A, 2014).

Table 1.2: Physical properties of ordinary Portland cement

Parameter	Test method	Value
Color	-	Light grey
Density	-	2,800 kg/m ³
Blaine specific surface	UNI EN 196-6	480 m ² /kg

Table 1.3: Chemical properties of ordinary Portland cement

Parameter	Test method	Value
Sulfates	UNI EN 196-2	3.5%
Chlorides	UNI EN 196-2	0.06%
Loss on ignition	UNI EN 196-2	5.0%
Insoluble residue	UNI EN 196-2	1.0%

3.1.2 Fine aggregates

Standardized sand was obtained from “Société Nouvelle du Littoral” for the composition of mortar specimens. It is a natural, siliceous sand having clean and isometric granules. The sand conforms to the standard specifications of EN 196-1 and ISO 679:2009 (Société Nouvelle du Littoral, 2014).

3.1.3 High range water reducing admixture (HRWRA)

Super-plasticizers or water-reducing admixtures are an essential component of self-consolidating cementitious systems. They ensure workability of the cement mixes even at a very low water to cement (w/c) ratio. In the present research work a HRWRA, bearing commercial name of “Mapei Dynamon SP1” was used. It is based on the second generation of modified acrylic polymers and conforms to the standard specification requirements of UNI EN 934-2:2012 (admixture for concrete, mortar and grout). Mapei Dynamon SP1 is an amber like liquid having density of 1.09 g/cm³ and solid content of 30.5% (Mapei S.p.A, 2014).

3.1.4 Raw materials for the synthesis of carbonized particles

In the present research work, the matrix structure of the cement composites was modified by the utilization of the micro sized, inert, carbonized particles. For the synthesis of the carbonized particles, three organic waste materials were selected keeping the considerations of eco-efficiency and the sustainability of the process. The selection of these materials was based upon their frequent availability, cheapness, easy processing and other environment related factors. Following is the list organic raw materials and their brief description:

- a. Bamboo
- b. Coconut shell
- c. Hemp hurds

Besides the above mentioned organic materials, another carbonaceous material named as “carbon soot” was also explored for the modification of the hardened state properties of the cementitious composites and the results were compared with the composites modified with micro sized inert carbonized particles.

3.1.4.1 Bamboo

Bamboo is found in abundance all over the world especially in Asia, South America and Africa (Choy, Barford, & McKay, 2005). It has very fast growth rate, as fast as 30 cm per day if the suitable conditions are met. It possesses good physical properties in terms of flexibility, strength and load bearing due to its fibrous nature.

It is widely used in construction as scaffolding due to its cheap availability, flexibility of cutting and strength. It is estimated that each year bamboo scaffolding produces over 50,000 tons of construction waste (Cheung, Lau, Leung, Ip, & McKay, 2012). The abundance of bamboo, its higher growth rate and high volume of bamboo waste production from construction industry makes it a potential candidate for the production of carbonaceous material.

Bamboo belongs to the family of large woody grasses and it has about 1250 known species. The heights of these species range from 10 cm to 40 m. Dwarf bamboo is the smallest specie having height as little as 10 cm whereas *dendrocalamus giganteus* is the tallest one with the height range of 40 m and 30 cm stem diameter. Most of the species are fast growing and have maturity age of about five years. Bamboo plant is very adaptable to various environmental conditions and it can be seen anywhere whether it is a plain, hilly region or high mountains. It grows approximately in all types of soils ranging from sand to clays.

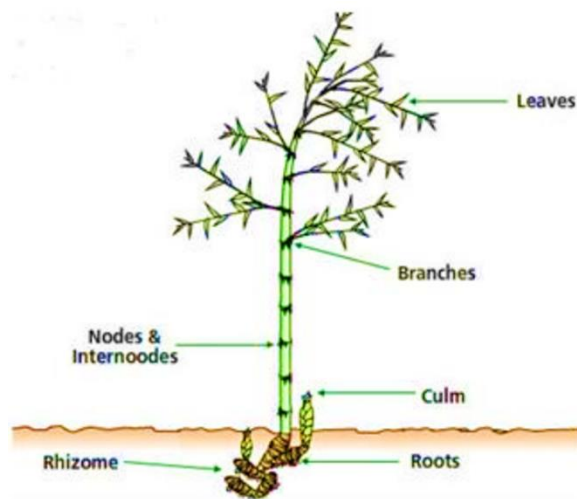


Figure 1.8: Typical structure of bamboo plant

Based on the structural properties, bamboo plant is divided into two major portions. Firstly the underground part named as “Rhizomes” and the remaining plant (above the ground) known as culm (as shown in Figure 1.8) (Sakaray, Togati, & Reddy, 2012). The culm or stem of the bamboo is of major importance. The stems do not have bark but possess a smooth and hard skin on them. The bamboo stem is divided

into small portions known as internodes. The internodes are connected to each other at the nodal points. At the nodes, the fibers are more compacted than internodes and show higher mechanical properties. The branches and leaves also emit from the nodal points only. Bamboo stems are fibrous in nature having texture and microstructure much similar to wood, but the arrangement of cells in the cross section is opposite to that of wood i.e. in plants, the central portion is strongest and the strength reduces going away from the center whereas in bamboo the outer part of the stem is the strongest one. This cell arrangement makes the bamboo a very stable material for bearing flexural stresses. The tube like structure ensures the presence of strong material at the location of highest static stress.

The literature survey shows that approximately all species of bamboo exhibit similar mechanical properties. The elastic modulus of bamboo is comparable to concrete and about 10 times lesser as compared to steel. In compression, dry and seasoned bamboo is twice strong to that of concrete. In tensile loading, it shows remarkably high load carrying capacity due to its fibrous nature and tube like structure. Bamboo has 180-200 MPa tensile strength, which is around 70% of the steel. Superior mechanical properties make the bamboo an interesting natural material for the construction industry.

The chemical composition of bamboo is much similar to the wood except higher silica content. The chemical composition of bamboo may be divided in to three main groups named as lignin, cellulose and hemicellulose. Lignin is an intrinsic component of all vascular plants, found in the cell walls, between the cells and even within the cells. The presence of lignin in the plants and vegetables makes them strong and crunchy. At molecular level, strong chemical bonds makes the lignin very resistant to degradation. It is composed of complex amorphous and three-dimensional compounds having phenylpropane structure (a benzene ring having three carbon atoms attached to it). Its molecular structures are so complex and length that sometimes their molecular weights may reach 15000 amu or more (Mccrady, 1991).

Cellulose is a homo-polymer of glucose having $\beta(1\rightarrow4)$ bonds whereas starch (another polymer of glucose) has $\alpha(1\rightarrow4)$ bond. Cellulose is a polymer that occurs most abundantly in nature. Cellulose and its derivatives have found their way in many applications due to their biocompatibility and degradability such as in producing films, plastics, composites, toothpastes, shampoos, suspension agents, coatings, drilling fluids and so on. Cellulose is a highly ordered linear homo-polymer structure formed by β -D-glucopyranose units. It contains both crystalline and amorphous parts. The repeating rings of the anhydroglucose are linked to each other through covalent bonding of oxygen. In plants, the cellulose is bonded to

hemicellulose and lignin through covalent bonding which makes a very complex structure. Cellulose consists of crystalline and amorphous regions. By treating it with strong acid, the amorphous regions degrade, thereby producing nanocrystalline cellulose, a novel material with many desirable properties (Peng, Dhar, Liu, & Tam, 2011).

Hemicelluloses, the third important constituent of the plants, are the heterogeneous polysaccharides just like cellulose. In nature, they also occur in abundance. Hemicellulose makes about 20-30% portion of the plants and typically 24.6% of bamboo (Adetoyese Olajire Oyedun, Gebreegziabher, & Hui, 2013). Hemicellulose plays its role in regulating the cellulose chains associations and influences the accumulation pattern of cellulose in fibrils (Bian et al., 2012). They also acts as supporting material for the cell walls just like cellulose. Hemicellulose can be extracted from wood by treating it with acetic acid or dilute H_2SO_4 but when it is removed through acidic treatment then the wood structure show kinks, terraces or steps (Bian et al., 2012). Hemicellulose is less stable thermodynamically and starts decomposing at 200°C and completes its decomposition around 260°C (Adetoyese Olajire Oyedun et al., 2013). The decomposition process of hemicellulose is exothermic similar to lignin whereas decomposition of cellulose is an endothermic process.

3.1.4.2 Coconut shell

The coconut plant belongs to the family of palm trees with heights ranging up to 30 m (“Coconut palm,” n.d.). Coconut is produced all over the world especially in the tropical regions of Asia, Africa and Latin America. FAO statistics shows that for the year 2012, the coconut plants covering area of 12.13 million hectares produced about 62.42 million ton of coconut fruit (“FAOSTAT Agriculture data,” 2012a).

Based on the structure of coconut fruit, it is generally divided in to three parts i.e. the innermost part or the coconut meat also known as copra, thick hard shell surrounding the coconut meat and the outermost layer of coconut coir. The copra is the most valuable part of the fruit and it is used in foods and production of coconut oil etc. The shell surrounding the copra is a waste material and it is generally used for burning and other such low-level applications. In the present research work, this hard shell was used as a source for the production of carbonized particles. The outermost part of the shell or coconut coir is the fiber like material that surrounds the hard shell having thickness up to 5 mm. The coconut coir is generally used in making filter’s pads, insulation materials, carpets, mats etc.

3.1.4.3 Hemp hurds

Hemp plant is a member of cannabis family of plants. It is a fast growing plant with a maturity age of 3 to 4 months. The plant usually grows in a single and slender stem of around 20 mm thickness and heights ranging up to 5 meters (Olsen, 2004). History of hemp cultivation and use dates back to twelve thousands years. In the 16th century, hemp was considered as a necessary crop for the production of cloth, food, oil and ropes (Luginbuhl, 2001). In the beginning of nineteenth century its importance was reduced due to the developments in cotton and synthetic fibers; however the interest of farmers has been revived by the use of hemp as insulation material, energy recovery and feedstock for paper (Finnan & Styles, 2013). Currently hemp is cultivated over an area of 41,246 hectare around the world producing 53,495 metric ton of hemp tow waste (“FAOSTAT Agriculture data,” 2012b). The structure of the hemp plant is composed of inner woody core with hollow inner space and the fibers that surrounds the woody core. These fibers are known as hemp or bast fibers. Hemp fibers are composed of disordered arrangement of cellulose fibrils that are held together by the complex organic matrix of hemicellulose, lignin and proteins (Stevulova, Kidalova, Junak, Cigasova, & Terpakova, 2012). The inner woody portion that is surrounded by the hemp fibers contains the pith and xylem vessels and is referred as hemp hurds (see Figure 1.9) (Olsen, 2004). The hemp hurds (HH) have wood like structure and makes about 70% of the stem’s mass (Beaugrand, Nottez, Konnerth, & Bourmaud, 2014)

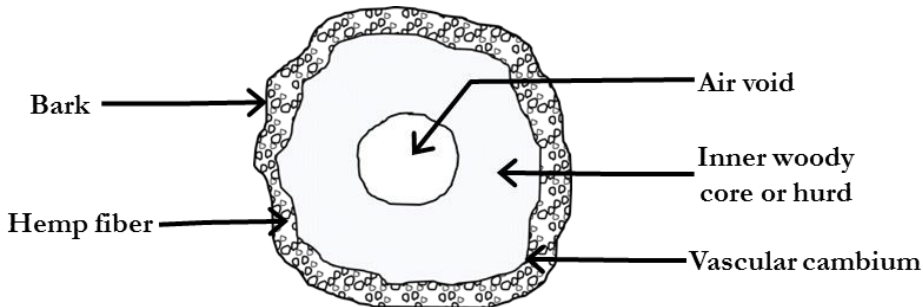


Figure 1.9: Transverse section of a hemp stem

Major portion of hemp hurds (HH) is generally used for inferior applications such as animal bedding etc. Being economically available, hemp hurds have been successfully tried with cement composites for producing light weight concrete or hempcrete, in epoxy composites and in magnesium oxide composites for producing

thermal insulation panels (Sassoni, Manzi, Motori, Montecchi, & Canti, 2014). There is nothing in the literature so far concerning its use in carbonized form in self-compacting cementitious systems. In the current study, hemp hurds have been investigated in a novel way to enhance the mechanical performance and fracture properties of self-compacting cementitious composites.

3.1.4.4 Carbon soot

Soot is an impure form of carbon particles that are produced by the incomplete combustion of hydrocarbons. Soot is generally produced from gas-phase combustion process but it may contain the pyrolyzed fuel particles such as coal, charred wood, petroleum, and so on (Nowack & Bucheli, 2007). Buseck et.al (Buseck, Adachi, Gelencsér, Tompa, & Pósfai, 2012) defines soot as a carbon rich solid material that condenses from the vapor phase during the combustion process. He proposed the term of “ns-soot” (nano-sphere soot) for soot particles to distinguish them from carbon black. The ns-soot particles have onion or grape like shapers having typical diameter between 10-100 nm. The onion like structure of soot particles is buildup from multilayers of graphite with interlayer spacing of 0.354 nm (Sawant, Somani, Panda, & Bajaj, 2013).

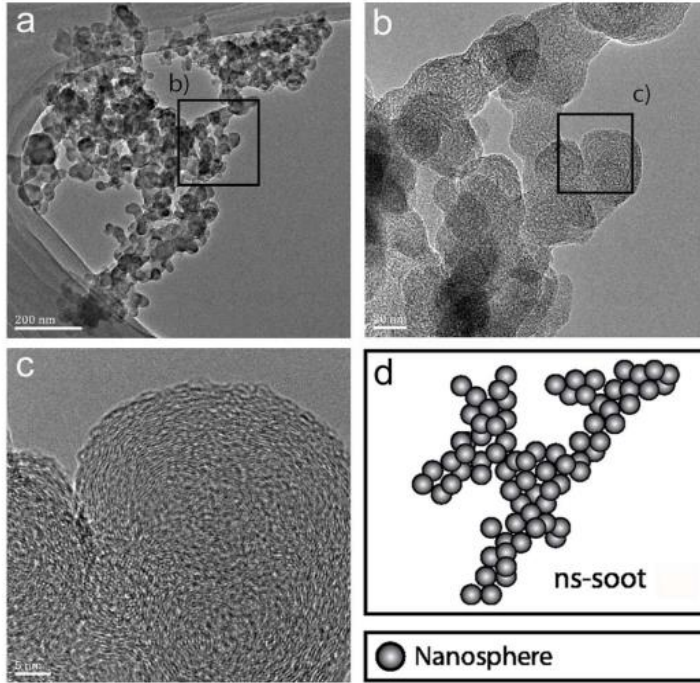


Figure 1.10: TEM and schematic images of soot and carbon nano-spheres. (a) An ns-soot particle from diesel particulate matter. (b) Enlarged image of (a). (c) High-resolution image of ns-soot particle from (b). (d) Schematic image of carbonaceous nano-spheres aggregated to form ns-soot. (Buseck et al., 2012)

The contribution of carbon soot to global warming is much higher than any other solid waste. In a comprehensive assessment on the environmental impact, carbon soot is on second number after the CO_2 in terms of its global warming impact on the current climate. Diesel emissions and agricultural waste fires are major sources of carbon soot production in the world. In the developing world, where the diesel consumption is a bit lesser, the carbon soot comes from other sources such as burning of wood and biomass for cooking and heating. Therefore, it is very important to control the production of carbon soot and its dispersion in the atmosphere for preserving the climate.

The carbon soot is a waste material that affects the environment. It is generated in much higher quantities due to the burning of fuel in industries and vehicles. Literature shows that its size is in nano range and structure is much similar to the

fullerene. This type of waste material may be added into the cementitious composites to enhance their mechanical properties such as their compressive strength, flexural strength, fracture energy and durability.

3.2 Processing of raw materials

In this phase of research, a detailed processing methodology was developed for the preparation of micro sized, inert, carbonized particles from the raw organic materials. Following is the brief description of the pyrolysis technique and grinding methods used for the synthesis of micro sized particles.

3.2.1 Pyrolysis of raw materials

Pyrolysis is a process of thermochemical decomposition of materials at elevated temperatures generally in the inert atmosphere (argon or nitrogen etc.) or in the absence of oxygen. The word pyrolysis is composed of two Greek elements “pyro” and “lysis” which mean “fire” and “separating”, respectively. Pyrolysis involves the simultaneous changes in chemical composition and the physical nature of the materials. It is an irreversible process and the changes (physical or chemical) occurred in the material are of permanent nature. The pyrolysis of organic materials such as wood generally begins around 200°C and major mass loss occurs up to 600°C. Pyrolysis is an overall endothermic process, which produces solid charcoal and flammable gases. The mixture of flammable gases is generally composed of carbon di oxide (CO₂), carbon mono oxide (CO), methane (CH₄), ethane (CH₂) and water vapors.

Carbonization or pyrolysis process of the bamboo, coconut shell and hemp hurds was carried out in a small quartz reactor under inert atmosphere (Figure 1.11). The inert atmosphere was achieved with the help of constant flow of 99.99% pure argon gas under a pressure of 0.2 bar. The furnace-heating ramp was adjusted at 1°C/sec until temperature reached 850°C and then the temperature was maintained there for 1 h.



Figure 1.11: Experimental setup for the pyrolysis of organic raw materials

After the completion of 1 h, the pyrolysis setup was allowed to cool under the constant flow of argon gas. The cooled down carbonized materials were retrieved from the quartz reactor and stored in airtight containers until further processing.

The carbonized materials obtained from bamboo and coconut shell were given annealing treatment to see the effect of this process on the internal structure and purity of these materials. Annealing is defined as a process of heat treatment, which may alter some physical and chemical properties of the materials. The annealing process refine, homogenizes and purifies the internal structure of a material. For annealing treatment, the carbonized materials were heated in the above shown setup with the temperature ramp of $1^{\circ}\text{C}/\text{sec}$ up to 850°C . Then the temperature was maintained at 850°C for 2 h, afterwards the materials were allowed to cool. The annealing process was also carried out under constant flow of argon.

3.2.1.1 Pyrolysis of bamboo

The bamboo utilized in the present research work for the preparation of carbonized particles was obtained from the Piedmont region of Italy. The hard dry bamboo stems were chopped down to small pieces of 2-3 cm in length and thickness of 2-3 mm. This chopping was done to ensure higher surface area exposure in subsequent operations. The small pieces of bamboo were washed with water and dried in oven at $105\pm 5^{\circ}\text{C}$ for 48 h.

Before pyrolysis and annealing, a chemical treatment was applied to bamboo. The chemical treatment was carried out to obtain more pure form of carbonized particles from the bamboo after pyrolysis. The small pieces of bamboo were soaked in 0.25M (1% w/v) aqueous solution of sodium hydroxide (NaOH) for 10 days in atmospheric conditions for chemical treatment. After 10 days, the bamboo pieces were washed with distilled water and dried in oven for 48 h at $105\pm 5^\circ\text{C}$. Literature indicates that the chemical treatment of organic materials partially disintegrate their organic structure by weakening the linkages between lignin, hemicellulose and cellulose.

The bamboo pieces were pyrolyzed by using the quartz reactor under inert atmosphere as explained in section 3.2.1. The as obtained bamboo after carbonization/pyrolysis was abbreviated as PB (pyrolyzed bamboo). Some quantity of PB was further annealed by following the above mentioned annealing process and the material obtained after the annealing was abbreviated as PBA (Pyrolyzed bamboo and annealed). Similarly, the chemically treated bamboo pieces were pyrolyzed and abbreviated as CPB (chemically treated pyrolyzed bamboo). The CPB material after annealing was named as CPBA (chemically treated pyrolyzed bamboo and annealed).

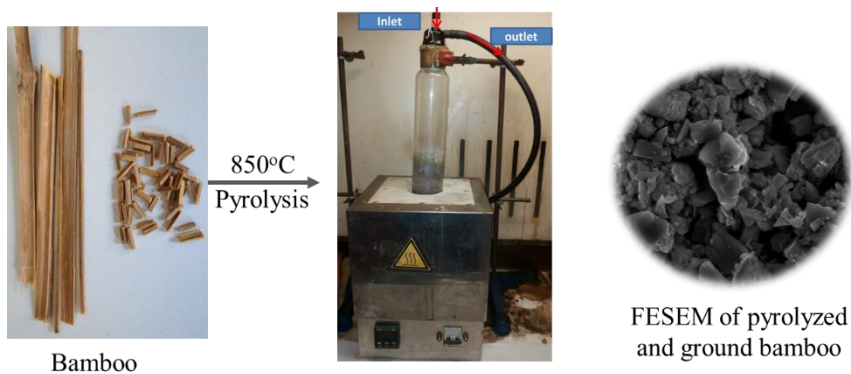


Figure 1.12: Schematic overview of pyrolysis process of bamboo

3.2.1.2 Pyrolysis of coconut shell

The as obtained coconut shells were broken in to small pieces for ease in handling and further processing. The broken pieces of coconut shell were washed with distilled water and dried in oven for 48 h at $105\pm 5^\circ\text{C}$. The dried pieces of coconut

shell were carbonized in the quartz reactor under inert atmosphere at 850°C for 1 h as explained above. The pyrolyzed coconut shell was named as PC (pyrolyzed coconut shell). Some quantity of PC was further annealed and designated as PCA (pyrolyzed coconut shell and annealed).

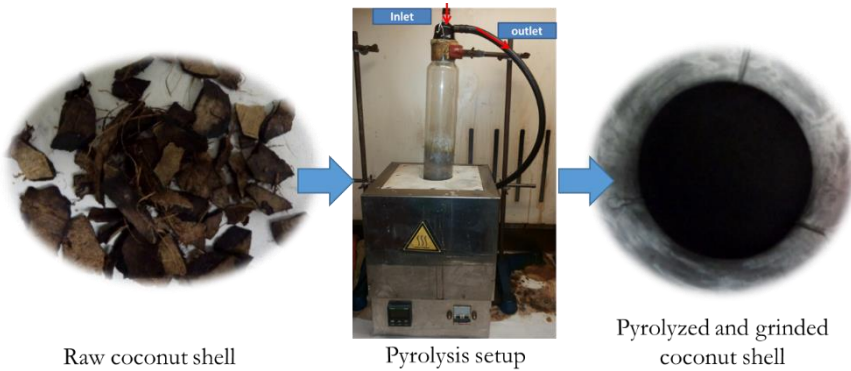


Figure 1.13: Schematic overview of pyrolysis process of coconut shell

3.2.1.3 Pyrolysis of hemp hurds

The size of as obtained hemp hurds was around 5-6 mm long and 2-3 mm thick. The as obtained hemp hurds were pyrolyzed in the quartz reactor at 850°C under constant flow of argon gas, rest of the details are similar to the pyrolysis of bamboo and coconut shell. The carbonized hemp hurds was designated HH (hemp hurds pyrolyzed).

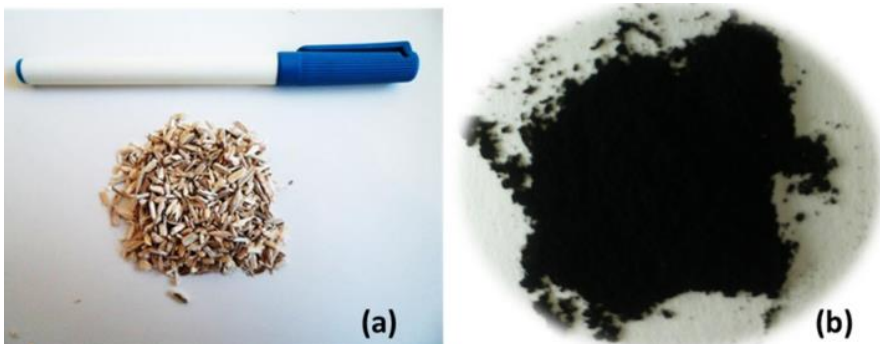


Figure 1.14: (a) As obtained hemp hurds, (b) Carbonized and ground hemp hurds

3.2.2 Grinding of pyrolyzed materials

The pyrolyzed materials were grinded to fine powder by following a sequence of manual grinded, ball milling and attrition milling. Laboratory scale mortar and pestle was used for the manual grinding of the carbonized materials. The manually grinded carbonized materials were passed through ASTM standard sieve no. 120 (having 125 μm aperture size). The sieved powder materials were then ball milled in small containers by using 10 mm diameter alumina balls. The particle size analysis of the carbonized materials was monitored after every 12 h of grinding with the help of laser granulometer. It was observed that 120 h of ball milling was reduced the size of the carbonized particles around 13-15 μm .

After ball milling the particle size of the carbonized materials was further reduced with the help of attrition milling for 1 h by using 2 mm alumina balls and water as grinding media. The attrition milling of the carbonized particles have reduced their d_{50} size in the range of 1-2 μm . After the completion of grinding, the carbonized powders were dried in oven at $50\pm 5^\circ\text{C}$ and stored in airtight containers.



Figure 1.15: Grinding apparatus (a) mortar and pestle, (b) ball mill, (c) attrition mill

3.3 Preparation of cement composites

3.3.1 Water demand and setting time of cement

The water demand of cement is defined as the quantity of water required to form a paste of standard consistency. The standard consistency is measured with Vicat apparatus by using 10 mm diameter plunger penetrating into the paste under the self-weight of 300 g through a distance of 30 mm. The water demand was measured according to ASTM C187, which came out to be 35%. The initial and final setting times were also determined according to ASTM C191 by using Vicat needle apparatus. The initial and final setting times were recorded as 190 min and 212 min respectively.

3.3.2 Super-plasticizer demand

The super-plasticizer demand is the quantity of super-plasticizer required to impart flow ability to the cement paste so that it can flow through a distance of 31 ± 2 cm by using Hagerman cone. After several trial mixes, the super-plasticizer demand was determined as 1.5% and 1.8% by the mass of cement for cement paste and mortar composites respectively.

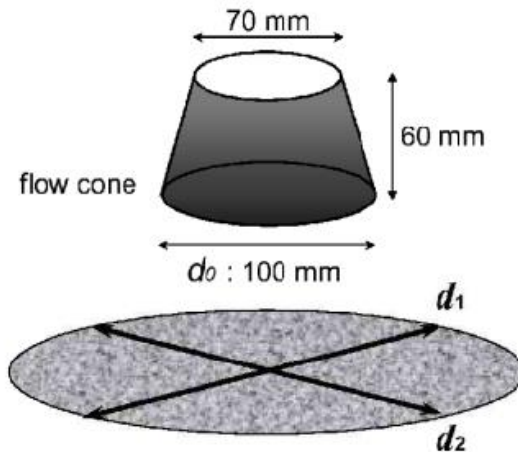


Figure 1.16: Typical dimensions of mini slump cone (Hagerman's cone)

3.3.3 Mix design of cement paste and mortar composites

The proportioning of all the self-consolidating paste (SCP) and self-consolidating mortar (SCM) systems was carried out to get the target flow of 31 ± 2 cm by Hagerman cone (mini slump cone, Figure 1.16). The flow measurements were taken after 30 sec of complete mixing. The time was fixed to eliminate the effect of workability loss with time. Mix proportion of SCP and SCM are shown below.

Table 1.4: Mix proportioning for paste and mortar systems

Constituent	Paste	Mortar
W/C ratio	0.35	0.35
Admixture	1.5%	1.8%
Cement : Sand	---	1:1.5

3.3.4 Cement paste sample preparation

The mixing procedure of cementitious composites is very crucial for their performance in fresh as well in the hardened state. A consistent mixing regime was followed for the preparation of all the cement composite that is described below:

Initially the required amount of carbonized particles and admixture was added in the measured quantity of water and the resulted solution was sonicated for 15 min. The sonication process resulted in the thorough dispersion of carbonized particles in the solution. Then the solution was transferred in to the mixing bowl of “Janke and Kunkel” homogenizer. The homogenizer was operated at 440 rpm for 2 min and during the first min of operation, the cement was gradually added in to the solution. After that the mixing speed of homogenizer was increased to 630 rpm and mixing was continued for the next 2 min, thus making the total mixing time of 4 min. Literature suggests that the mixing time of cement composites should be more than 3 min for the fully activation of the added super-plasticizer.

The mixing process produced a free flowing and self-compacting cement composite that was filled in to the acrylic molds of having dimensions of $20\times 20\times 75$ mm³. The molds were then placed in to the airtight plastic containers having approximately 90% humidity level at room temperature for 24 h. After the completion of 24 h, the prism samples were removed from the molds and immersed in water for curing.

The details of the paste samples composition are as follows:

Table 1.5: Composition of cement paste composites with carbonized bamboo particles*

Notation	Carbonized Bamboo		Notation	Carbonized Bamboo	
	%	mg		%	mg
CEM	0	0	-	-	-
CEM+0.05%PB	0.050	80	CEM+0.05%CPB	0.050	80
CEM+0.08%PB	0.080	128	CEM+0.08%CPB	0.080	128
CEM+0.20%PB	0.200	320	CEM+0.20%CPB	0.200	320
CEM+0.05%PBA	0.050	80	CEM+0.05%CPBA	0.050	80
CEM+0.08%PBA	0.080	128	CEM+0.08%CPBA	0.080	128
CEM+0.20%PBA	0.200	320	CEM+0.20%CPBA	0.200	320

*For each mix 160 g cement, 56 g water and 2.4 g HRWRA was used.

Table 1.6: Composition of cement paste composites with carbonized coconut shell particles*

Notation	Carbonized Coconut shell		Notation	Carbonized Coconut shell	
	%	mg		%	mg
CEM	0	0	-	-	-
CEM+0.05%PC	0.050	107	CEM+0.05%PCA	0.050	107
CEM+0.08%PC	0.080	171.2	CEM+0.08%PCA	0.080	171.2
CEM+0.20%PC	0.200	428	CEM+0.20%PCA	0.200	428

*For each mix 214 g cement, 74.9 g water and 3.21 g HRWRA was used.

Table 1.7: Composition of cement paste composites with carbonized hemp hurds particles*

Notation	Carbonized Hemp hurds	
	%	mg
CEM	0	0
CEM+0.05%HH	0.050	107
CEM+0.08%HH	0.080	171.2
CEM+0.20%HH	0.200	428
CEM+1.00%HH	1.000	2140
CEM+3.00%HH	3.000	6420

*For each mix 214 g cement, 74.9 g water and 3.21 g HRWRA was used.

Table 1.8: Composition of cement paste composites with carbon soot particles*

Notation	Carbon soot	
	%	mg
CEM	0	0
CEM+0.05%CS	0.050	107
CEM+0.08%CS	0.080	171.2
CEM+0.20%CS	0.200	428
CEM+1.00%CS	1.000	2140

*For each mix 214 g cement, 74.9 g water and 3.21 g HRWRA was used.

The results of the cementitious mixes indicated that overall improved performance might be obtained by incorporating 0.08% inert carbonized or carbon soot particles. It was also observed that the carbon soot particles results in substantial improvement in the modulus of rupture whereas other inert carbonized particles majorly improve the fracture toughness of the cement composites. Therefore, an optimization scheme was adopted to obtain improvement in modulus of rupture as well as in fracture toughness of cement composite. In that optimization process following mix proportions were selected and further analyzed for their mechanical properties.

Table 1.9: Composition of cement paste composites with carbon soot and other carbonized particles*

Notation	Carbon soot		Carbonized particles		
	%	mg	Type	%	mg
CEM	0	0	-	-	-
CEM+0.08%CS+0.08%PB	0.080	171.2	Carbonized bamboo	0.08	171.2
CEM+0.08%CS+0.08%PC	0.080	171.2	Carbonized coconut shell	0.08	171.2
CEM+0.08%CS+0.08%HH	0.080	171.2	Carbonized hemp hurds	0.08	171.2

*For each mix 214 g cement, 74.9 g water and 3.21 g HRWRA was used.

3.3.5 Mortar sample preparation

In the second phase of experiments, the influence of the micro carbonized particles inclusions on the performance of cement mortar composites was investigated. Mortar specimens were prepared with each carbonized material at their optimum

percentage inclusion as observed in the testing of paste specimens. The composition details of the mortar samples are given below:

Table 1.10: Composition details of cement mortar composites with various carbonized particles*

Notation	Carbonized material		
	Type	%	mg
M	-	0	0
M+0.08%PB	Carbonized bamboo	0.080	560
M+0.08%PC	Carbonized coconut shell	0.080	560
M+0.08%HH	Carbonized hemp hurds	0.080	560
M+1.00%CS	Carbon soot	1.000	7000

*For each mix 700 g cement, 1050 g sand, 245 g water and 12.6 g HRWRA was used.

For the preparation of the mortar specimens, initially the measured amount of sand and cement were fed in to the mixing bowl of Hobart mixer and mixed thoroughly. The solution of water, admixture and carbonized material was prepared and sonicated for 15 min. After that, the solution was fed in to the mixing bowl and slow mixing was done for 1 min. Then the mixer was stopped for 30 sec and the walls of the mixing bowl were cleaned with the help of spatula. Thereafter fast mixing was done for 2 min, thus making the total mixing time of 3 min. The mixture was then filled in the steel molds of 40x40x160 mm³. The steel molds were wrapped with polythene sheet and kept at room temperature. The dried samples were removed from molds after 24 h and cured in water for 28 days.

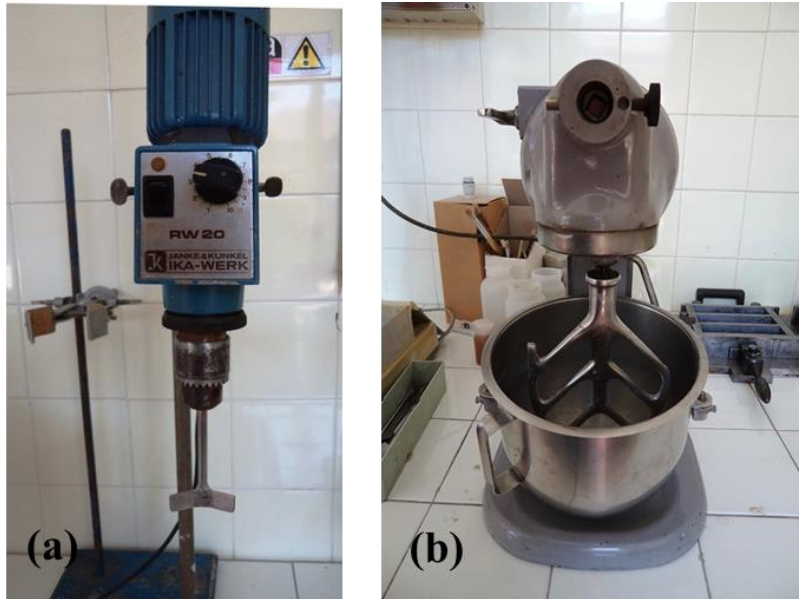


Figure 1.17: Janke & Kunkel homogenizer and (b) Hobart mixer

3.4 Material's characterization

In the present research, the materials characterization was carried out in four phases. In the first phase of research, the raw organic materials were analyzed in thermogravimetric analyzer (TGA) for determining their pyrolysis characteristics. The TGA characterization of the organic materials helped in the development of the pyrolysis methodology for the synthesis of carbonized materials. In the second phase, the synthesized carbonized materials were characterized with the help of field emission scanning electron microscope (FESEM), energy dispersive x-ray (EDX) analysis and x-ray diffraction (XRD). The third phase of characterization comprised of the mechanical characteristics of the cement paste and mortar composites. In the last phase, the cement composite samples were analyzed for their microstructure and crack growth characteristics.

3.4.1 Thermogravimetric analysis

Thermo-gravimetric analysis is a technique to study the thermal degradation kinetics of the materials. The organic raw materials were analyzed by TGA and their thermal disintegration behaviors were studied. TGA was performed using “Mettler TGA instrument model 851” in the temperature range of 25-1000°C with a heating ramp of 10°C/min. The analysis were performed under two different environments; inert atmosphere by using argon flow of 30 ml/min and oxygen rich atmosphere by using 99.99% dry air flow at 30 ml/min.

3.4.2 Carbonized material characterization

3.4.2.1 FESEM analysis

The carbonized and ground materials were characterized by “Zeiss Supra-40” field emission scanning electron microscopy (FESEM) equipped with energy dispersive x-ray spectroscopy (EDX) for their morphology, surface texture, particle sizes, shapes and elemental composition.

3.4.2.2 Raman analysis

The carbonized materials after grinding were analyzed for Raman spectroscopy by using Renishaw Micro-Raman scope operated at the excitation wavelength of 514.5 nm. The Raman analysis provides information about the degree of graphitization of the materials. The results of Raman analysis are reported in subsequent chapter. In the Raman spectra, two distinct peaks were observed at Raman shift of 1350 and 1600 cm^{-1} . These peaks are related to the D-band and G-band, respectively. D-band in the spectra indicates the presence of some disorder or defects in the graphitic structure of the material while G-band is a measure of degree of graphitization of the structure. The ratio of these peaks (I_D/I_G) is usually referred as the quality of the material (Dresselhaus, Dresselhaus, Saito, & Jorio, 2005; Malard, Pimenta, Dresselhaus, & Dresselhaus, 2009; Park et al., 2009).

3.4.2.3 Dispersion of carbonized particles in water

The major issue arises in the utilization of micro or nano sized materials and fibers in the cement and concrete composites is their thorough and uniform dispersion in the matrix. The dispersion of the micro sized inert carbonized particles in water was studied by visual analysis of the solutions. For the subject analysis, the solutions of water, HRWRA and carbonized particles were prepared by using 56 g water, 2.4 g HRWRA and 320 mg carbonized materials. The standard mixing procedure was adopted for dispersing the carbonized particles in the water and after the dispersion;

the solutions were kept in test tubes and visually observed after 1 h and 24 h of dispersion.

3.4.2.4 XRD analysis

The technique of X-ray diffraction measurement is a qualitative method of analyzing the internal structure of a material. The carbonized materials were analyzed by this technique through an angle of 5-80 degrees.

3.4.3 Mechanical characterization of cement composites

3.4.3.1 Three point flexure test

Prism shaped cement composite specimens were tested for their flexural strengths according to ASTM C348 (standard test method for flexural strength of hydraulic cement mortars) with a single column displacement controlled flexural testing machine (Zwick Line-Z010) with load cell capacity of 1.0 kN. The Crack Mouth Opening Displacement (CMOD) mode was used and the displacement rate of 0.003 mm/min was adopted. Prior to the flexural testing, 6 mm deep U shaped notches were made in the specimens with Remet type TR100S abrasive cutter having 2 mm thick diamond cut-off wheel. The mortar prism specimens of 40x40x160 mm³ size were also tested in three point bending. Prior to testing U shaped notches of 3 mm wide and 12 mm deep were made in all the specimens and were testing in CMOD control mode.

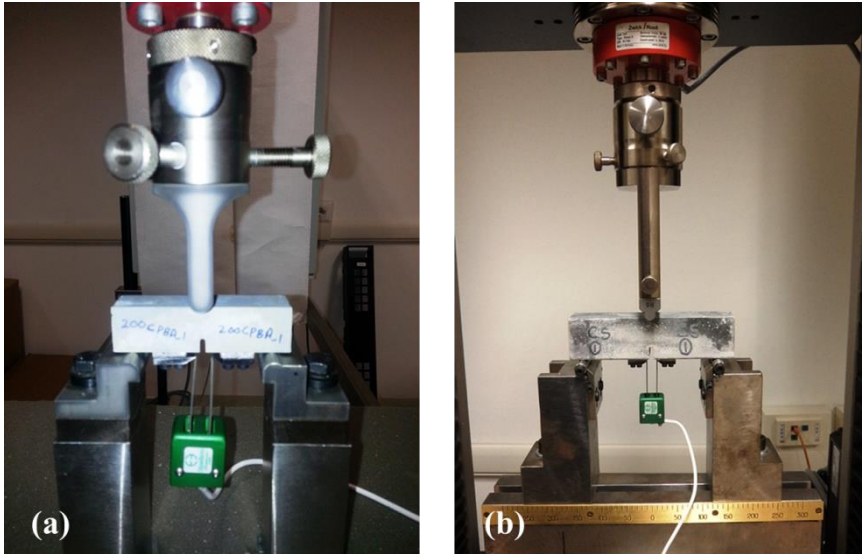


Figure 1.18: Three point flexure tests of (a) paste and (b) mortar composites

3.4.3.2 Compression test of specimens

After the flexural testing, the portions of broken prisms were tested in compression according to ASTM C349 (standard test method for compressive strength of hydraulic cement mortars) with displacement controlled compression testing machine (Zwick Line-Z010) with load cell capacity of 100 kN. The displacement rate was kept at 0.50 mm/min and 0.80 mm/min for loading and unloading, respectively.



Figure 1.19: Compression test setup of cement paste composites

3.4.4 Microstructural characterization of cement composites

The microstructure of the cement composites was analyzed with the help of FESEM. The FESEM analysis revealed information about the dispersion of the micro sized, inert, carbonized particles in the cement matrix and the influence of inert particles inclusion in the cement matrix on the crack growth behavior and fracture pattern.

Chapter 4 Experimental results

In the present chapter, the results of various tests performed related to the synthesis, grinding and characterization of the micro sized, inert, carbonized particles are presented. The results related to the mechanical characterization of the cement composites are also presented in this chapter.

4.1 Tests on raw materials

The first part of the research was related to the synthesis and characterization of the micro sized, inert carbonized particles from organic/agricultural waste, which were utilized in the mix design of the cementitious composites possessing enhanced ductility and strength. The pyrolysis mechanism of the raw materials was studied by Thermo-Gravimetric/ Differential Thermo-Gravimetric analysis (TG/DTG) technique and afterwards the size, shape and compositional analysis were carried out. The entire test results related to this activity are presented in this section.

4.1.1 Thermo-Gravimetric analysis

The thermo gravimetric analysis of the raw materials was carried out and their mass loss curves are presented in Figure 1.20. The results indicate that the weight loss of the organic raw materials may be divided in to three temperature ranges (Table 1.11).

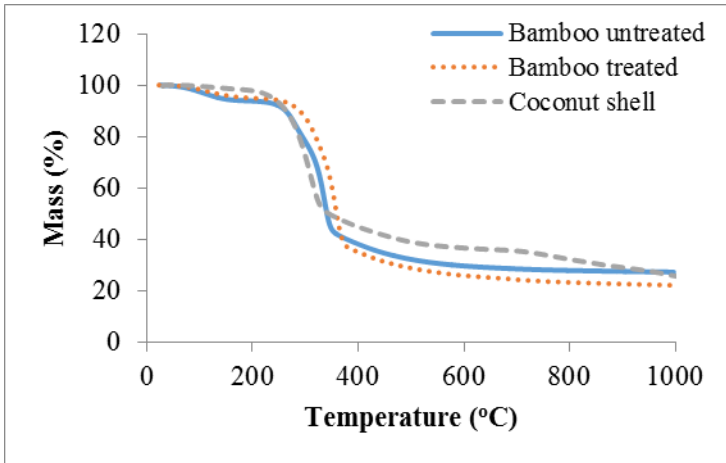


Figure 1.20: TGA analysis of raw materials in Argon

Table 1.11: Mass loss behavior of raw material in Argon

Pyrolysis characteristics	First step			Second step		
	Start (°C)	End (°C)	Mass loss (%)	Start (°C)	End (°C)	Mass loss (%)
As obtained bamboo	25	220	6.44	220	375	53.12
Chemically treated bamboo	25	220	5.29	220	375	57.04
Coconut shell	25	220	3.14	220	375	49.82

Pyrolysis characteristics	Third step			Residue (%)
	Start (°C)	End (°C)	Mass loss (%)	
As obtained bamboo	375	1000	13.11	27.33
Chemically treated bamboo	375	1000	15.68	22.42
Coconut shell	375	1000	22.22	24.82

The first temperature range as shown in Table 4.1, is in between 25°C and 220°C and is related to the evaporation of the moisture from the organic material (Adetoyese O Oyedun, Lam, Gebreegziabher, & Hui, 2012). The second and major weight loss was observed in the temperature range of 220°C to 375°C due to the simultaneous decomposition of hemicellulose and cellulose, during this temperature

range lignin also partially decomposes (Lopez-Velazquez, Santes, Balmaseda, & Torres-Garcia, 2013). The third weight loss region is in the temperature range of 375°C to 1000°C, this is the most prolonged zone responsible for the decomposition of lignin (Jiang et al., 2012).

The yield of carbonized material obtained from untreated bamboo, treated bamboo and coconut was 27.3, 22.4 and 24.8% respectively. The thermal decomposition of chemically treated bamboo showed higher weight losses in second and third temperature ranges as of untreated bamboo. This phenomena is attributed to the partial degradation of cellulose, lignin and other organic impurities by the chemical treatment process (Awwad et al., 2012).

The carbonized powders were also analyzed by TGA under the constant flow of air. This analysis was carried out to qualitatively investigate the purity of carbonized materials. The analysis results for bamboo and coconut shell are reported in Figure 1.21. It was observed that after the oxidation of the samples 1.48, 7.66 and 1.92% residue were obtained for untreated bamboo, treated bamboo and coconut shell.

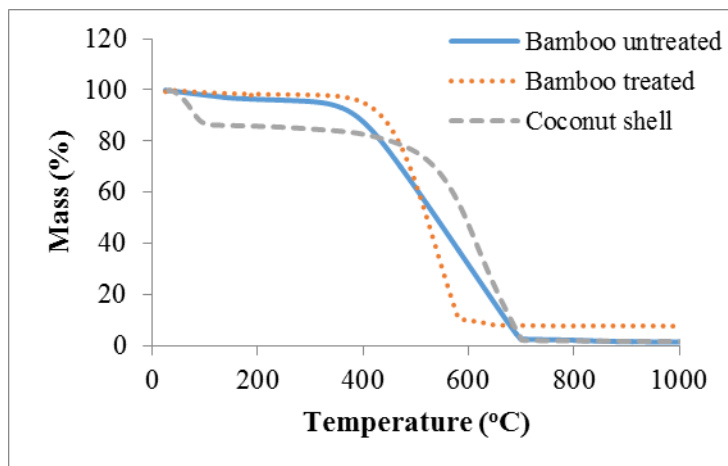


Figure 1.21: TGA analysis of carbonized materials in air

The individual plots of TGA accompanied with DTG of the raw and carbonized organic materials in argon and in air, respectively are presented in Figure 4.3, 4.4 & 4.5. The three characteristic ranges of material degradation are evident from these plots.

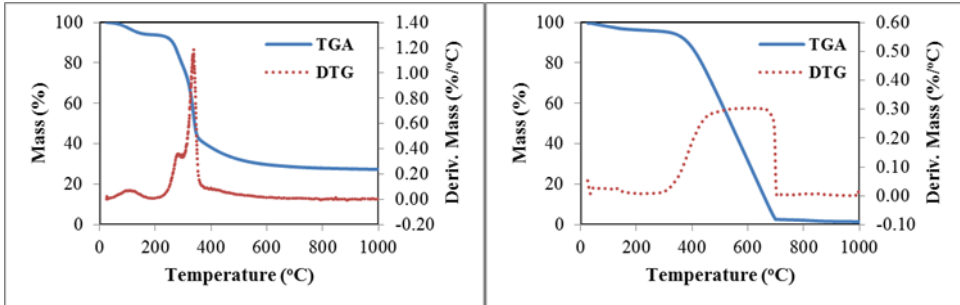


Figure 1.22: TGA & DTG curves of raw bamboo in argon (left) and carbonized bamboo in air (right)

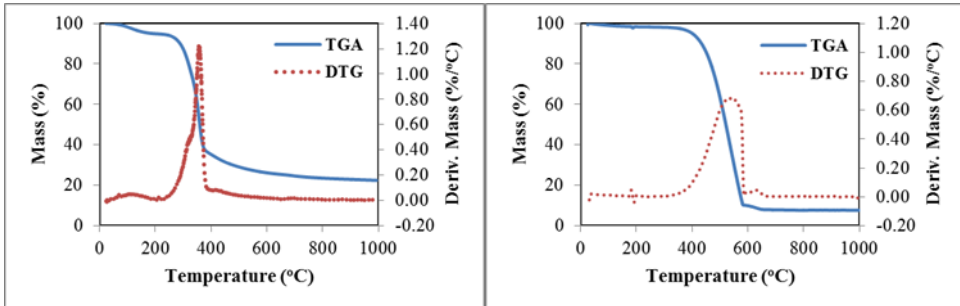


Figure 1.23: TGA & DTG curves of chemically treated bamboo in argon (left) and chemically treated and carbonized bamboo in air (right)

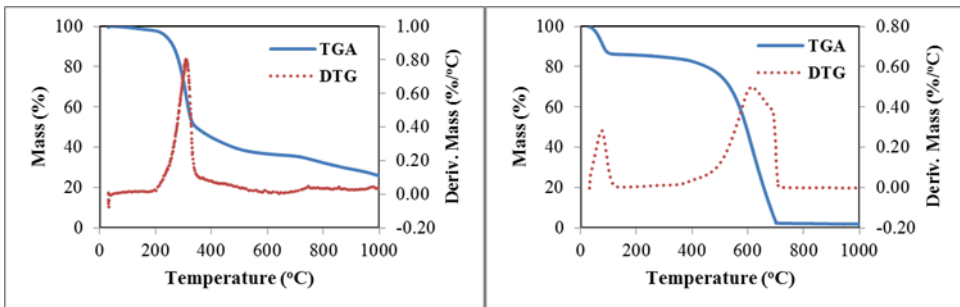


Figure 1.24: TGA & DTG curves of coconut shell in argon (left) and carbonized coconut shell in air (right)

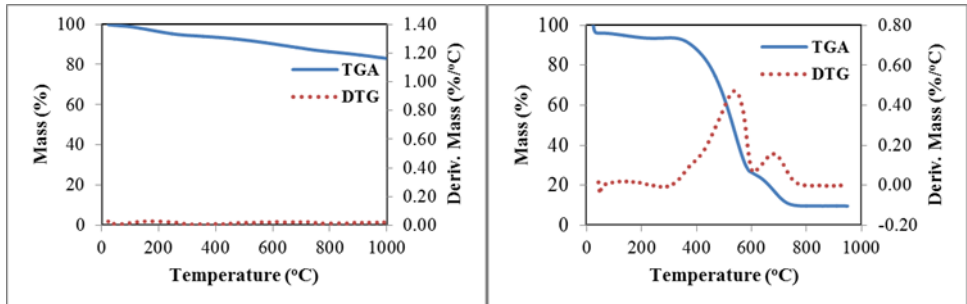


Figure 1.25: TGA & DTG curves of carbon soot in argon (left) and in air (right)

The carbon soot that is coming from an inorganic source was also analyzed in TGA in argon environment and oxidative environment. The Figure 4.6 (left) clearly indicate that the carbon soot particles are thermally very stable. Whereas in oxidative environment almost all the carbon soot was converted in to oxides indicating purity of the sample.

4.1.2 Raman analysis

The Raman spectra for the carbonized materials are reported in Figure 1.26. In the Raman spectra first distinct peaks of disorder band (D-band) was observed at 1350 cm^{-1} and second peak related to graphitic band (G-band) at 1600 cm^{-1} . The intensity peaks ratios (I_D/I_G) of the materials are reported in Table 1.12. The peak ratio is lowest for the carbonized hemp powder indicating lower defects in its structure whereas the highest peak ratios were observed for carbonized coconut shell and carbon soot.

Table 1.12: Intensity peak ratios of D and G bands of the carbonized materials and carbon soot in Raman spectrum

Material	I_D	I_G	I_D/I_G ratio
Bamboo	760.12	979.97	0.7756
Coconut	1216.44	1435.88	0.8471
Hemp	1557.96	2345.35	0.6642
Carbon soot	492.82	526.72	0.9356

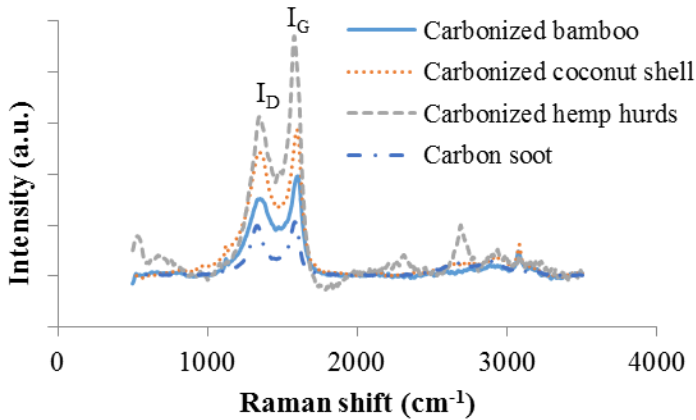


Figure 1.26: Raman spectrum of carbonized materials

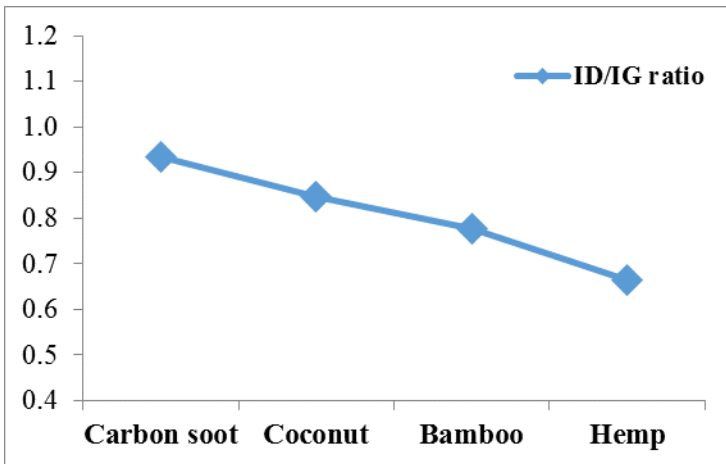


Figure 1.27: I_D/I_G variation for carbonized materials

4.1.3 FESEM analysis

The FESEM observations of the powder samples were carried out to observe the particle sizes, shapes, and morphology. Various images were taken at different resolutions, only few of them are reported here.

FESEM image of a small piece of carbonized bamboo after the TGA analysis in argon is shown in Figure 1.28. The observation revealed that along the length of the stem small circular channels exist having diameters in the range of 2.0 μm to 8.0 μm . This indicates that the carbonized bamboo contains a large number of continuous voids in the shape of narrow circular channels.

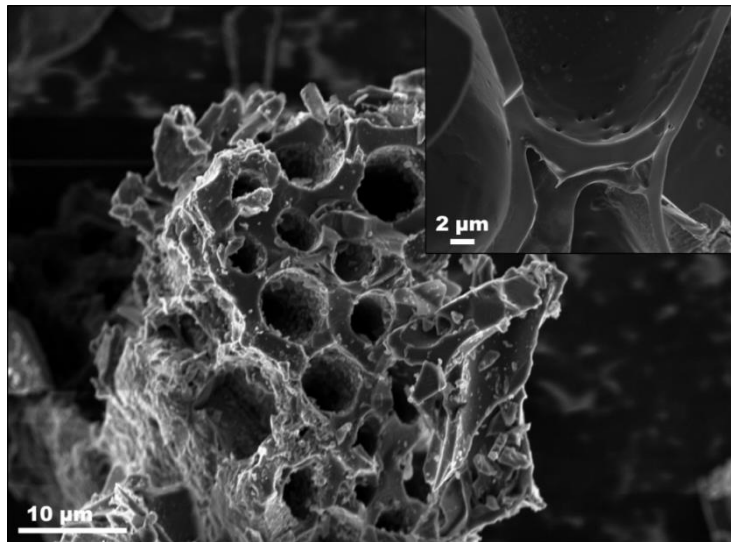


Figure 1.28: FESEM of a small bamboo piece after TGA

The carbonized bamboo particles were grinded by following a sequence of operations, starting from hand grinding, ball milling to attrition milling. The FESEM observations and laser particle size analysis were carried out after each grinding step. Following is the image of grinded carbonized bamboo particles (Figure 1.29). The grinding resulted in substantial reduction of particle size and produced small fragments ranging from 100 nm to 2.0 μm .

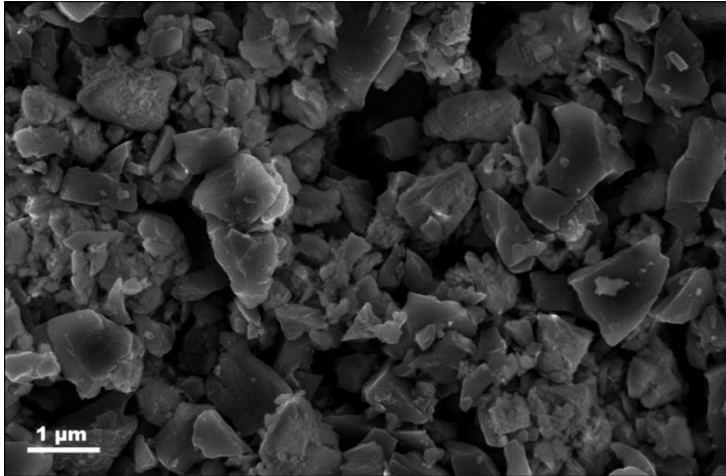


Figure 1.29: FESEM of carbonization and ground bamboo particles

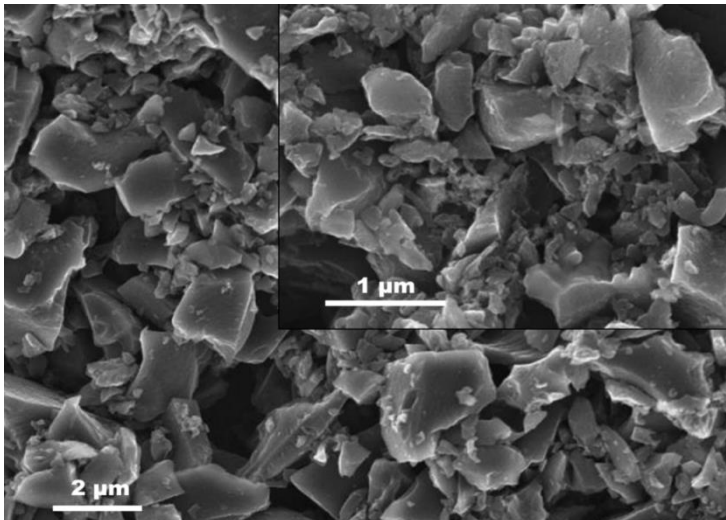


Figure 1.30: FESEM of carbonized and ground coconut shell particles

The same procedure of carbonization and grinding was used for the synthesis of micro sized, inert particles from coconut shell and hemp hurds. The FESEM images

for coconut shell and hemp hurds are reported in Figure 1.30 and Figure 1.31, respectively.

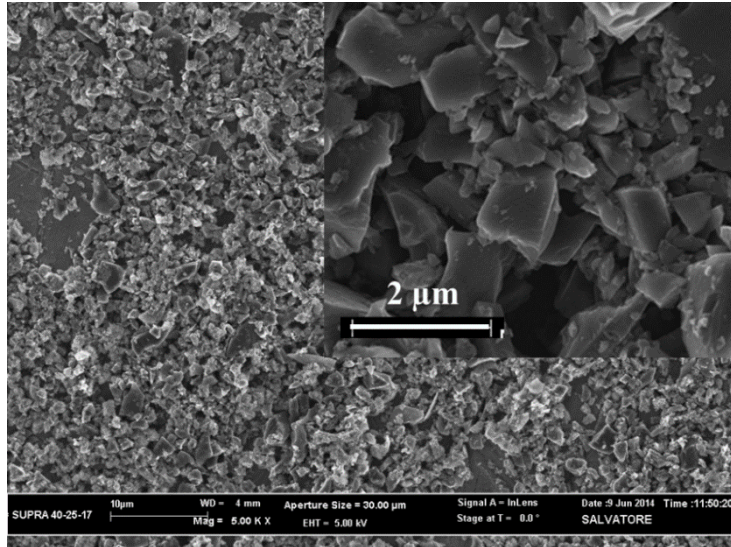


Figure 1.31: FESEM of carbonized and ground hemp hurds

Carbon soot is a waste product of fuel burning process and it does not require any pre-processing before its utilization in the cement matrix. The FESEM monograph of as obtained carbon soot are presented below (Figure 1.32). The average particle size of carbon soot was not possible to be determined by laser granulometer, therefore based on the FESEM observations it was evaluated that its average particle size is well below 50 nm.

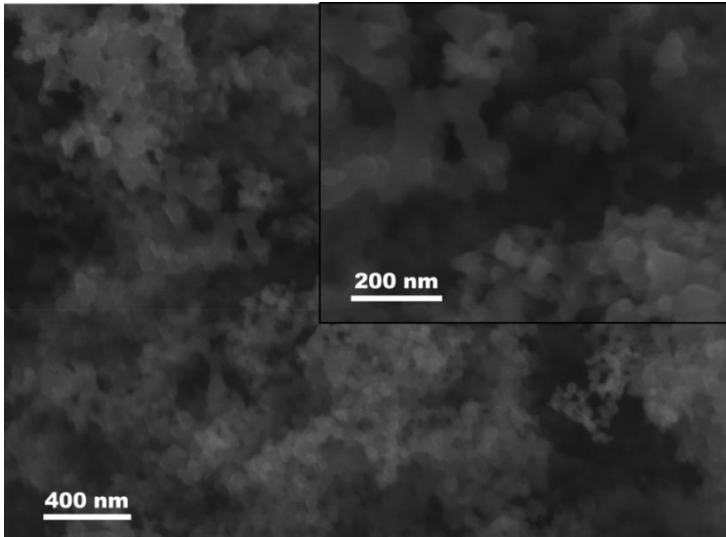


Figure 1.32: FESEM of carbon soot particles

4.1.4 EDX analysis

The carbonized and grinded bamboo, coconut shell, hemp hurds and carbon soot particles were analyzed by energy-dispersive x-ray (EDX) spectroscopy for their elemental composition. The composition details are reported in Table 1.13 and Table 1.14.

Table 1.13: Elemental composition of carbonized bamboo particles

Property	PB	PBA	CPB	CPBA
Carbon (C) %	59.01	82.34	76.58	82.45
Oxygen (O) %	38.41	15.46	21.88	14.25
Silica (Si) %	1.78	1.18	0.81	0.67
Calcium (Ca) %	0.79	1.00	0.73	1.08
Avg. particle size (d ₅₀) µm	1.22	1.66	1.58	1.43

Table 1.14: Elemental composition of carbonized coconut shell, hemp hurds and carbon soot particles

Property	PC	HH	CS
Carbon (C) %	87.29	43.90	92.00
Oxygen (O) %	12.26	44.42	8.00
Silica (Si) %	--	8.20	--
Calcium (Ca) %	--	2.04	--
Avg. particle size (d ₅₀) µm	1.72	1.54	Below 50 nm

4.1.5 Dispersion analysis of carbonized materials in water

The dispersion of the carbonized particles in water was observed visually after 1 and 24 h after mixing. Standard procedure for mixing was adopted so that the results can be correlated. The typical observation of carbonized bamboo particles dispersed in water are shown in Figure 1.33. From the observations it was certain that the particles disperse very well in water and this may guarantee their effective dispersion in the cement matrix.

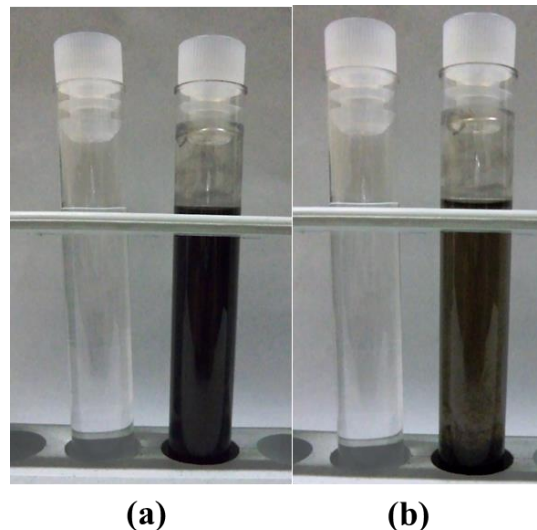


Figure 1.33: Water suspension containing carbonized bamboo particles (a) After 1 h of mixing, (b) After 24 h of mixing

4.2 Mechanical characterization of SCP composites

The self-consolidating cement paste (SCP) composites were characterized for their mechanical performance by carrying out three point bending and compression tests. The details about the mechanical tests are presented in this section.

4.2.1 SCP containing micro carbonized bamboo particles

4.2.1.1 Three point bending tests

The deformation behavior of cement composites due to applied stresses can be studied either by conventional stress-strain (σ - ϵ) curve or by load-deformation (F - δ) relationship, which is also known as tension softening curve (Bhatti, Kishi, Mikami, & Ando, 2009). The tension softening curves provide the relationship between the stresses acting across the cracked plane and the separation between them. The total energy absorbed by the material while undergoing deformation can be described by the area under the tension-softening curve. Typical load-deformation (F - δ) curve for the specimens tested is presented in Figure 1.34.

The three point bending tests were performed in CMOD controlled mode by using “Zwick Line (Z010)” flexural testing machine. The rate of CMOD was kept at 0.003 mm/min for all the test specimens. The CMOD values and the corresponding central point loads were digitally recorded with the help of “TestXpert II” software.

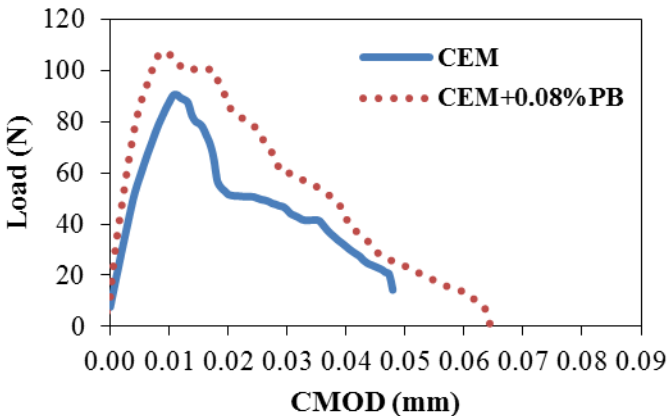


Figure 1.34: Typical load-CMOD curves for cement composites with and without carbonized bamboo particles

The load-CMOD curves for various types of carbonized bamboo particles represented the improved behavior of cement paste composites in terms of fracture energy and ductility.

4.2.1.2 Evaluation of flexural test results

The fracture energy parameters were employed and toughness indices were evaluated as per ASTM C1018 (ASTM, 1997) to assess the effects of carbonized particles inclusion on the energy absorption capability of cement composites. The results of the toughness indices and fracture energy analysis are presented in following figures.

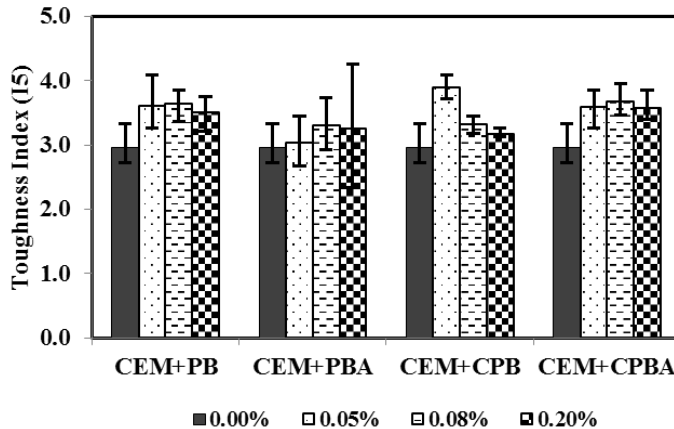


Figure 1.35: Comparison of toughness index I5 for the cement paste composites containing carbonized bamboo particles

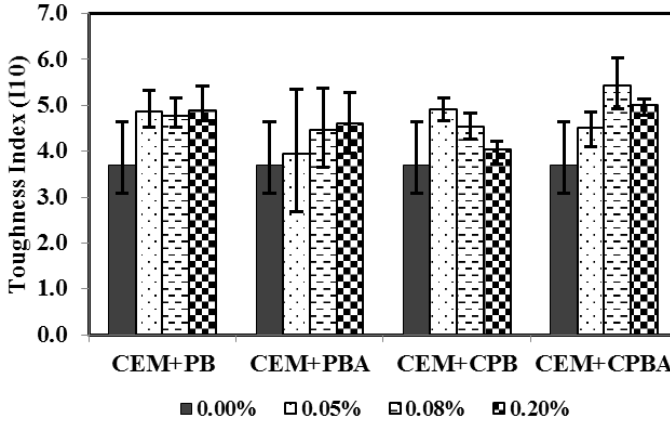


Figure 1.36: Comparison of toughness index I10 for the cement paste composites containing carbonized bamboo particles

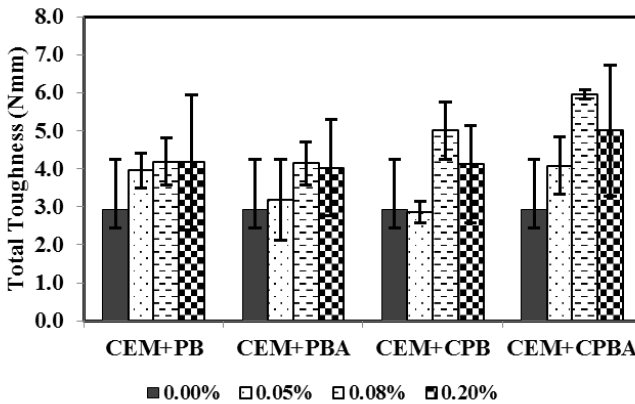


Figure 1.37: Comparison of total toughness of cement paste composites containing carbonized bamboo particles

The average modulus of rupture was calculated from the test results for each set of sample by using Equation 4.1 and reported in Figure 1.38.

$$\sigma_{\max} = \frac{3}{2} \frac{F_{\max}^2 l}{wh^2} \tag{4.1}$$

Where, “F” is the maximum force in the load deflection curve, “l” is the span length, “w” is the specimen width and “h” is the specimen height.

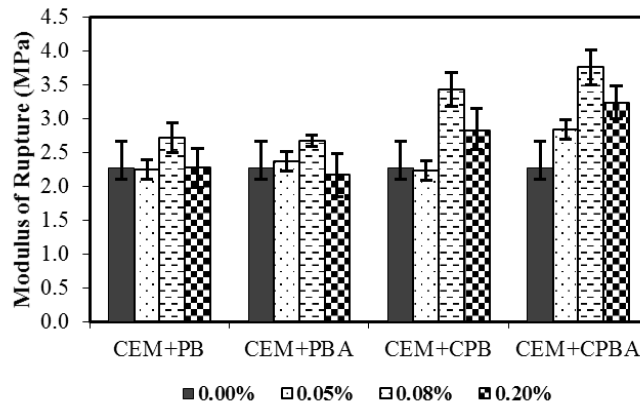


Figure 1.38: Comparison of flexural strength of cement paste composites containing carbonized bamboo particles



Figure 1.39: Typical fracture surfaces of the cement paste after third-point bending test

4.2.1.3 Compression tests

The compressive strength results of the cement composites are presented in Figure 1.40. The results show first increasing and then decreasing trend in the compressive strength of the cement composites. The maximum enhancement was observed at 0.08% inclusion in all types of carbonized particles.

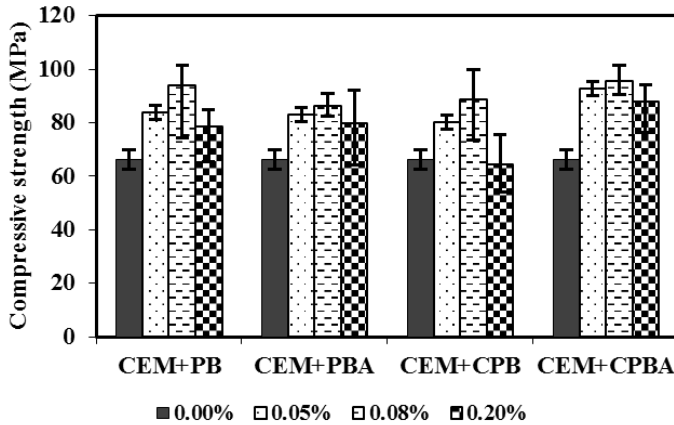


Figure 1.40: Compressive strength comparison of cement composites containing carbonized bamboo particles

4.2.1.4 FESEM of SCPs

The FESEM observations of small chunks of cement composite samples were carried out. Few snaps are presented below.

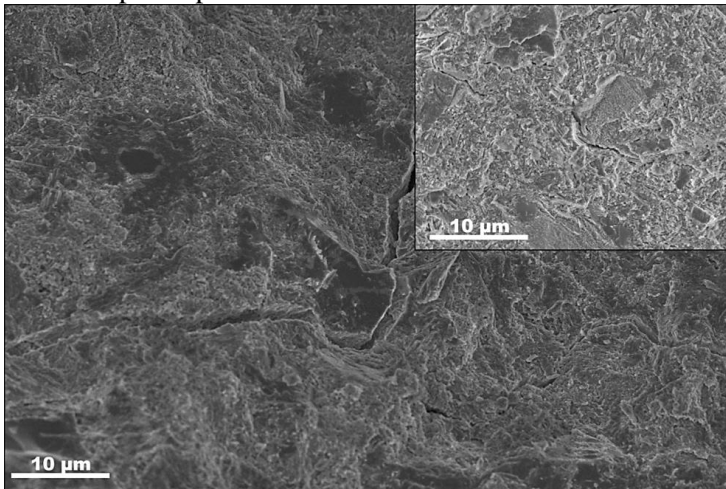


Figure 1.41: FESEM of cement composite sample containing carbonized particles

4.2.2 SCPs containing carbonized coconut shell particles

4.2.2.1 Three point bending tests

The cement composites prepared with carbonized coconut shell were tested in third-point bending tests. The typical behavior of flexural tests is reported in Figure 1.42. The tests revealed that the coconut shell particles inclusions enhanced the toughness properties of the cement composite and a decrease in the elastic modulus was observed.

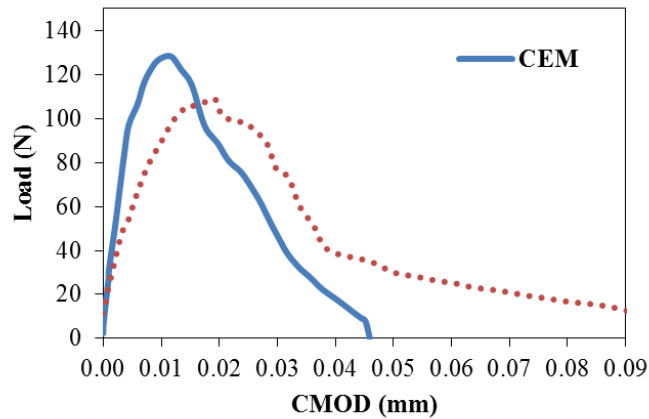


Figure 1.42: Typical load-CMOD curves for cement composites with and without carbonized coconut shell particles

4.2.2.2 Evaluation of flexural tests

The increase in toughness of the cement composite was evaluated by using the concept of toughness indices. The results of the toughness indices I_5 and I_{10} are reported in Figure 1.43 and Figure 1.44, respectively.

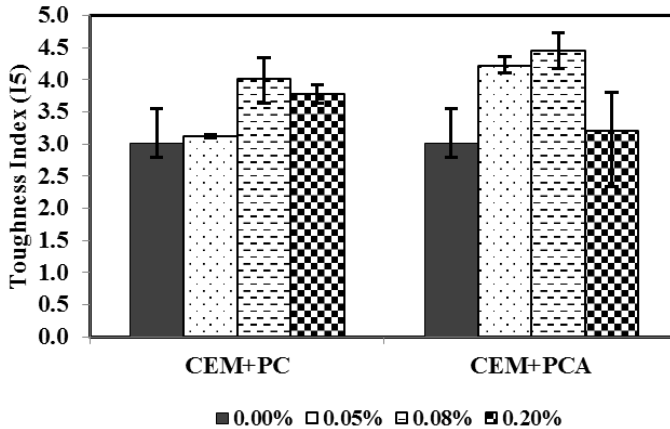


Figure 1.43: Comparison of toughness index I5 for the cement paste composites containing carbonized coconut shell particles

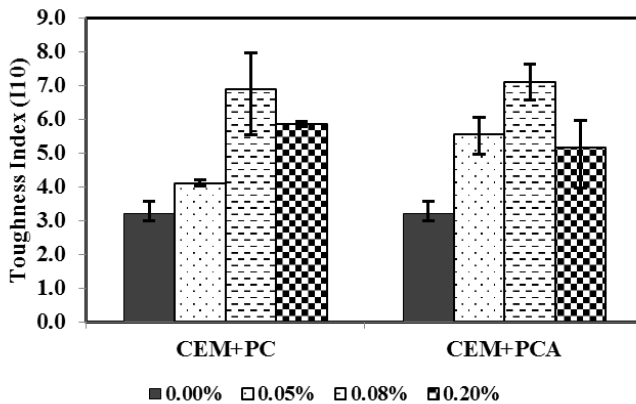


Figure 1.44: Comparison of toughness index I10 for the cement paste composites containing carbonized coconut shell particles

The cement composites represented enhancement in the total toughness due to the inclusion of the micro sized, inert carbonized particles in the cement mix. The comparative result of total toughness of cement composites is presented in Figure 1.45. The influence of carbonized particles inclusion on the modulus of rupture is presented in Figure 1.46. The results show that unlike carbonized bamboo particle,

carbonized coconut shell particles inclusion reduced the modulus of rupture of the resulting cement composites.

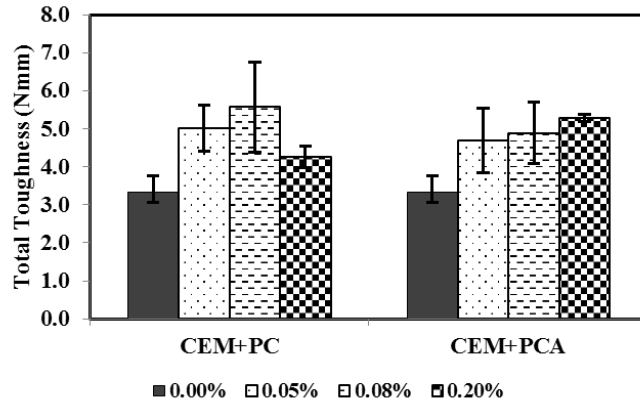


Figure 1.45: Comparison of total toughness of cement paste composites containing carbonized coconut shell particles

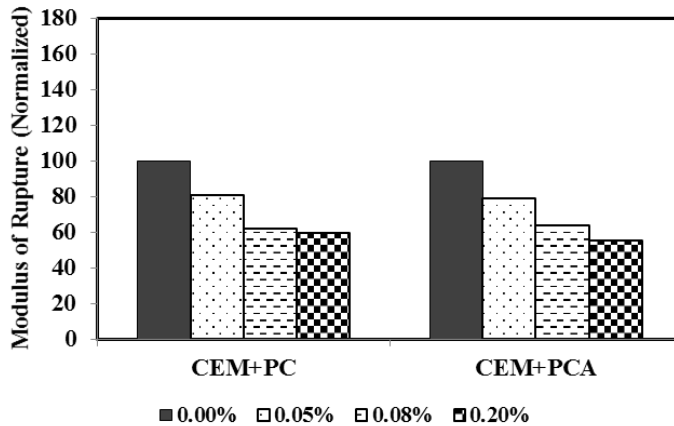


Figure 1.46: Comparison of flexural strength of cement paste composites containing carbonized coconut shell particles



Figure 1.47: Typical fracture surfaces of the cement paste containing carbonized coconut shell after third-point bending test

4.2.2.3 Compression tests

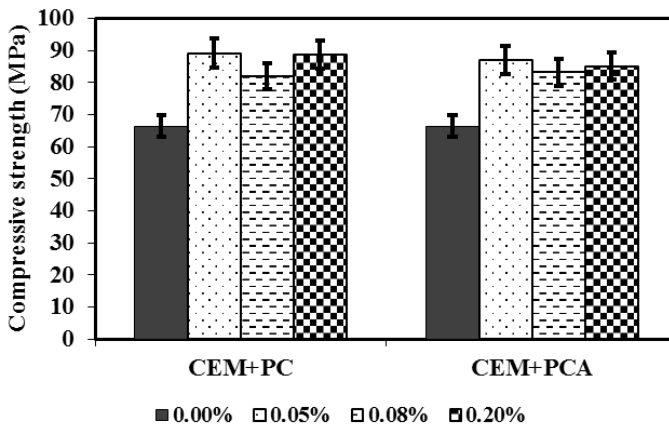


Figure 1.48: Compressive strength comparison of cement composites containing carbonized coconut shell particles

4.2.2.4 FESEM of SCPs

The FESEM observations of the fracture surfaces of cement composites containing micro sized, inert, coconut shell particles are reported in Figure 1.49. The

observation revealed that the inert micro particles acted as an obstacle in the crack growth path, therefore the growing cracks have to deflect and contour around the inclusion. The most interesting thing about this modified cracking mechanism is that all the phenomenon of crack pinning, trapping, deflection and contouring is happening at the micro level, thus resulting in substantially improved performance in terms of energy absorption capacity.

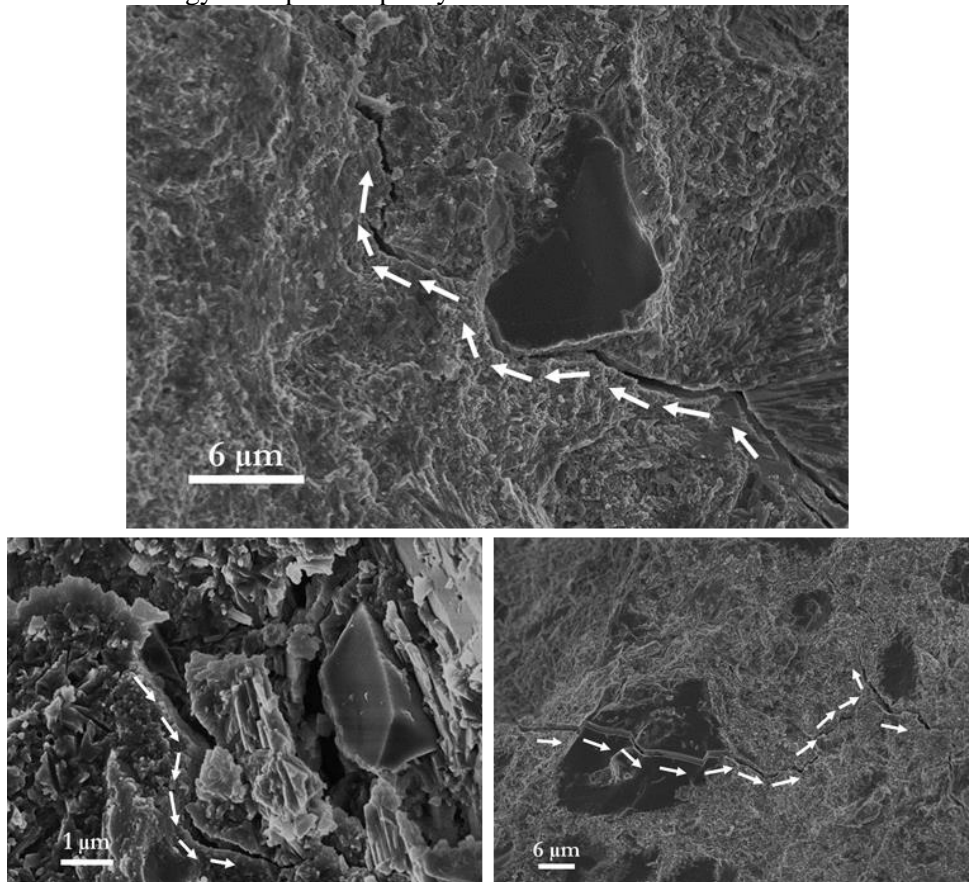


Figure 1.49: FESEM of cement composite sample containing carbonized 0.2% coconut particles

4.2.3 SCPs containing micro carbonized hemp hurds particles

4.2.3.1 Three point bending tests

The notched specimen of cement composites containing carbonized hemp hurds were tested in three point bending. For each composition a set of minimum three specimens were tested and their average modulus of rupture and toughness indices were evaluated.

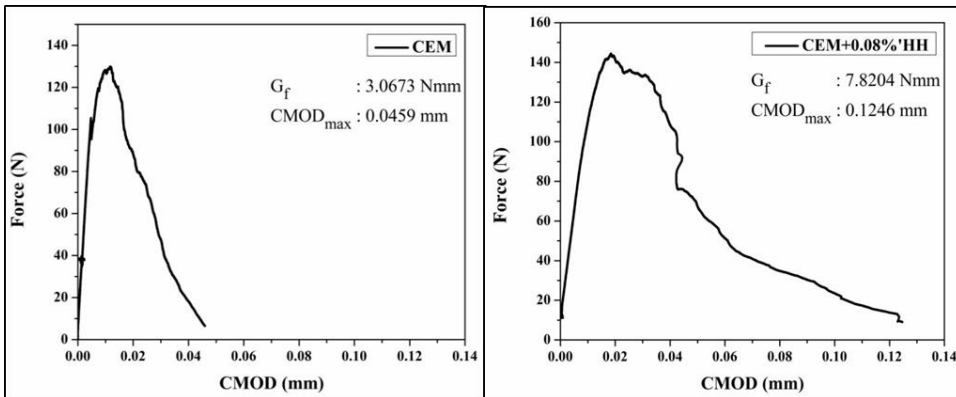


Figure 1.50: Typical load-CMOD curve of control mix and cement composite with 0.08% hemp hurds

The three-point bending tests of cement composites containing inert carbonized particles inclusions showed that the post peak performance has been improved substantially. The increase in the post peak behavior resulted in approximately more than 100% increase in the fracture energy capacity of the cementitious composites.

4.2.3.2 Evaluation of flexural tests

The flexural behavior was studied by applying the concept of the toughness indices to the cementitious composites. The results of the toughness indices are presented in Figures 4.32 and 4.33.

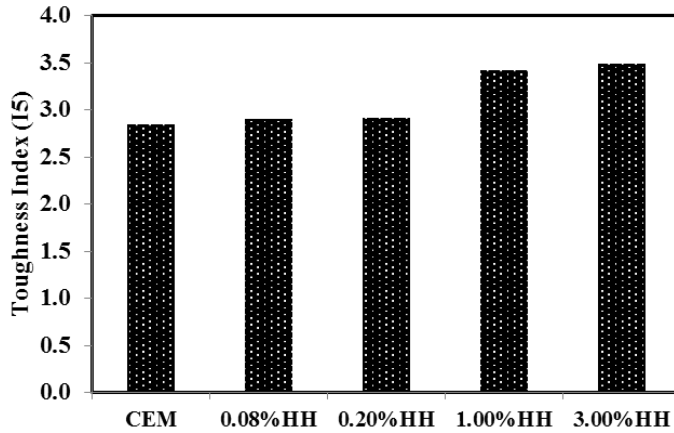


Figure 1.51: Comparison of toughness index I5 for the cement paste composites containing carbonized hemp hurds particles

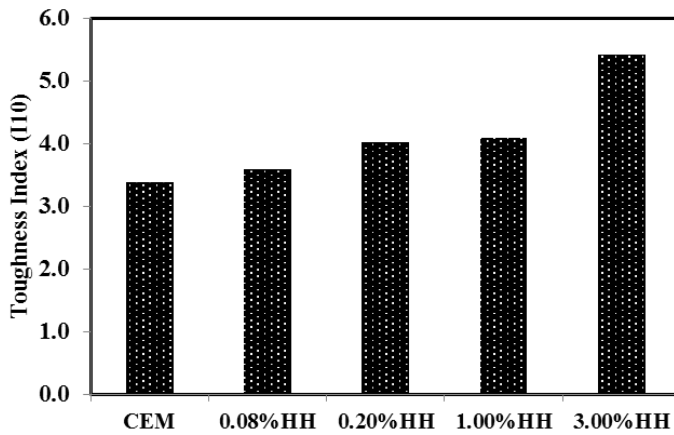


Figure 1.52: Comparison of toughness index I10 for the cement paste composites containing carbonized hemp hurds particles

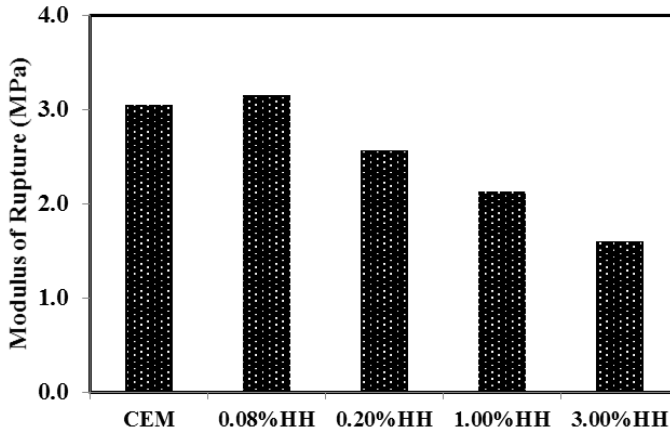


Figure 1.53: Comparison of flexural strength of cement paste composites containing carbonized hemp hurd particles



Figure 1.54: Typical fracture surfaces of the cement composites after third-point bending test (a) control mix, (b) CEM+0.08HH

4.2.3.3 Compression tests

The results of the compression tests performed on the prisms of the cement composite samples which were broken in three-point bending test are reported in Figure 4.36.

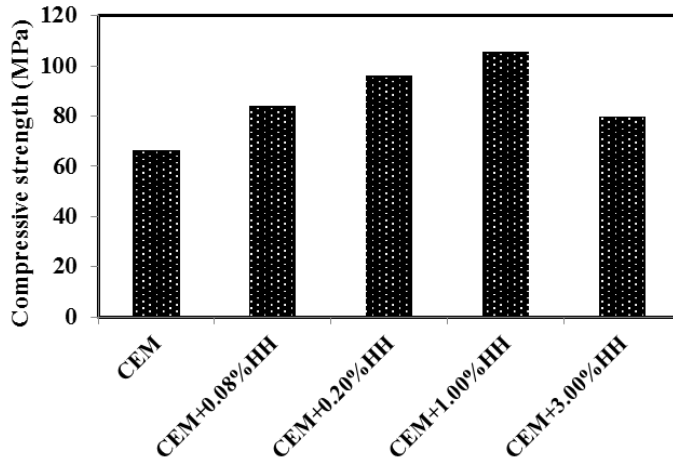


Figure 1.55: Compressive strength comparison of cement composites containing carbonized hemp hurd particles

4.2.3.4 FESEM of SCPs

The FESEM micrographs of the cement composite specimen are presented in Figure 4.37. The micrograph indicate that the cracks growth are affected by the inclusion of the micro carbonized particles. The growing cracks generally divert their path when they come in contact with the inert carbonized particles thus resulting in the increased fracture energy of the cement composites.

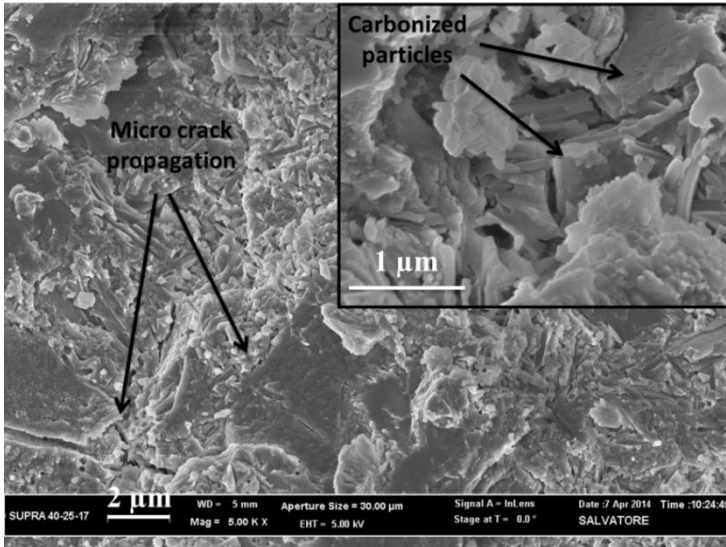


Figure 1.56: FESEM of cement composite sample containing carbonized hemp hurd particles

4.2.5 SCPs containing carbon soot particles

4.2.5.1 Three point bending tests

Carbon soot cement composite were prepared by using four different percent additions (i.e. 0.05, 0.08, 0.2 and 1.0% by the weight of cement) of carbon soot particles. The carbon soot particles are very small in size (i.e. well below than 50 nm) and correspondingly possess very large surface area. Therefore, the addition of carbon soot in higher amounts (for example 1% or more) considerably reduces the flow-ability of the cement composite in fresh state. The flexural test of the composite specimen indicated substantial increase in the flexural strength while reducing the ultimate deformation capacity. The toughness indices were evaluated from the flexural tests and reported in following figures.

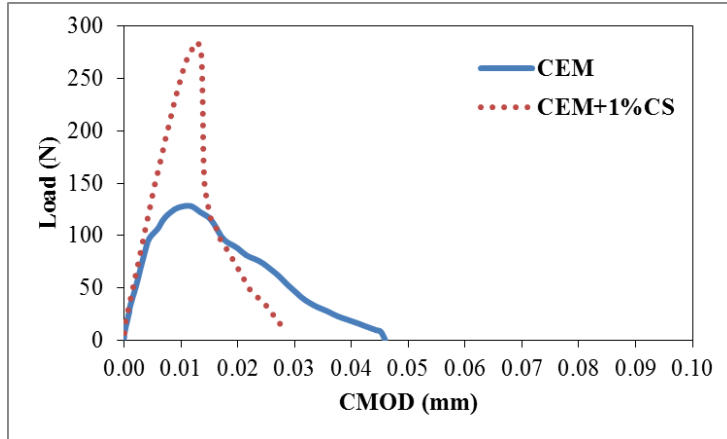


Figure 1.57: Typical load-CMOD curve of control mix and cement composite with 1.0% carbon soot

4.2.5.2 Evaluation of flexural test results

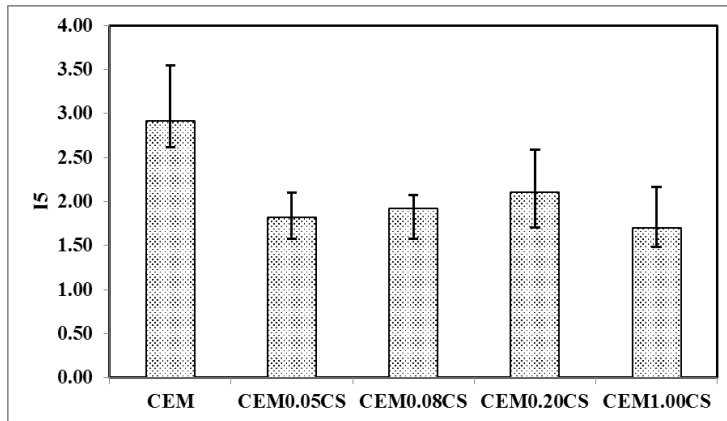


Figure 1.58: Comparison of toughness index I5 for the cement paste composites containing carbon soot particles

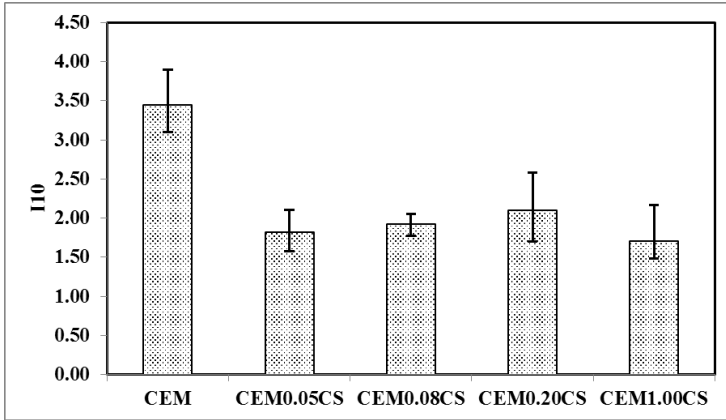


Figure 1.59: Comparison of toughness index I10 for the cement paste composites containing carbon soot particles

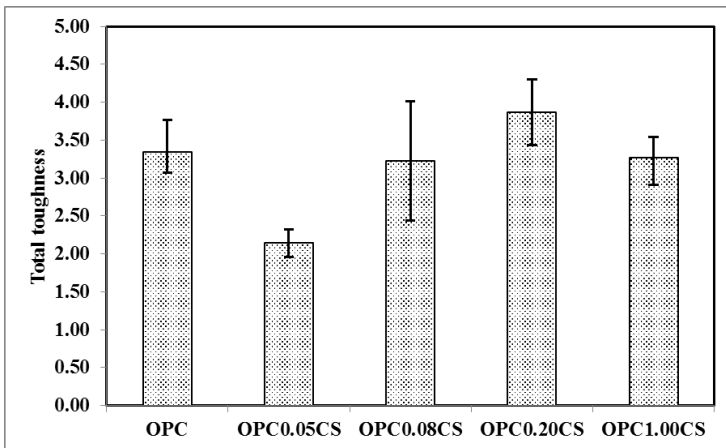


Figure 1.60: Comparison of total toughness of cement paste composites containing carbon soot particles

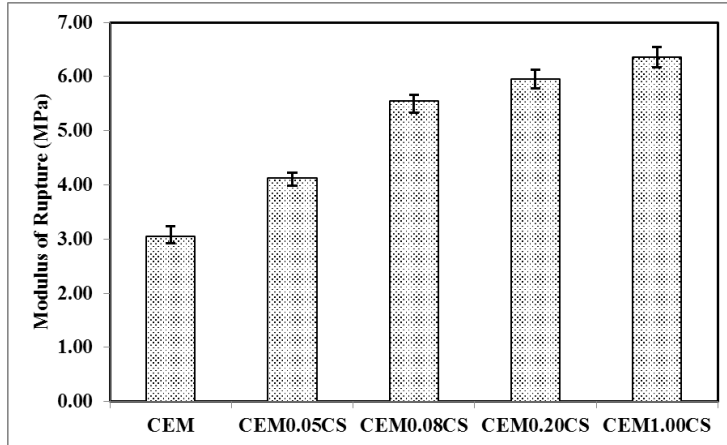


Figure 1.61: Comparison of flexural strength of cement paste composites containing carbon soot particles

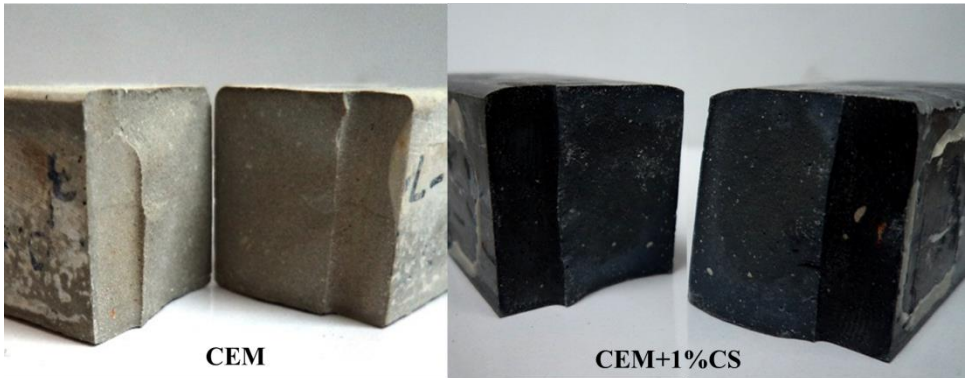


Figure 1.62: Typical fracture surfaces of the cement paste containing carbon soot particles after third-point bending test

4.2.6 SCPs containing micro carbonized particles and carbon soot

The cement composite specimen were prepared by using a combination of micro carbonized particles and carbon soot particles. The main purpose behind this series of tests was to obtain the optimum results in terms of fracture energy and modulus of rupture.

4.2.6.1 Three point bending test

The notched cement composite specimens containing carbonized particles and carbon soot were tested in three point bending test. Typical load-CMOD curves for the specimen are presented below. The plot indicate that the modulus of rupture as well as the ultimate CMOD have been enhanced substantially.

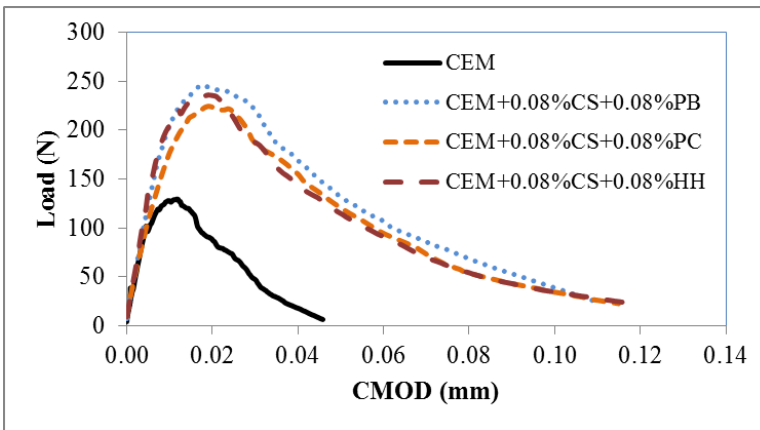


Figure 1.63: Typical load-CMOD curve of control mix and cement composites containing carbon soot and inert carbonized particles

4.2.6.2 Evaluation of flexural test results

The flexural results of cement composites were evaluated for toughness indices to assess their ductility and fracture energy absorption capacity. The results of the toughness indices I_5 and I_{10} are reported below.

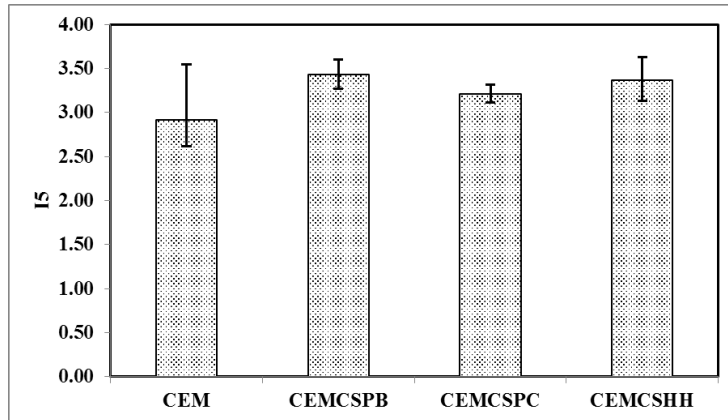


Figure 1.64: Comparison of toughness index I5 for the cement paste composites containing carbon soot and inert carbonized particles

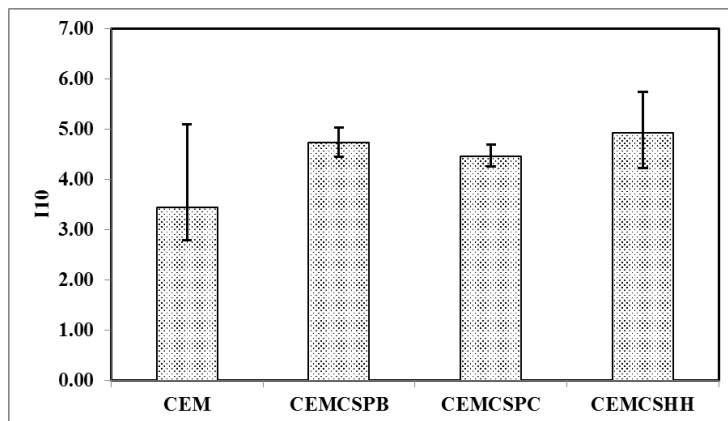


Figure 1.65: Comparison of toughness index I10 for the cement paste composites containing carbon soot and inert carbonized particles

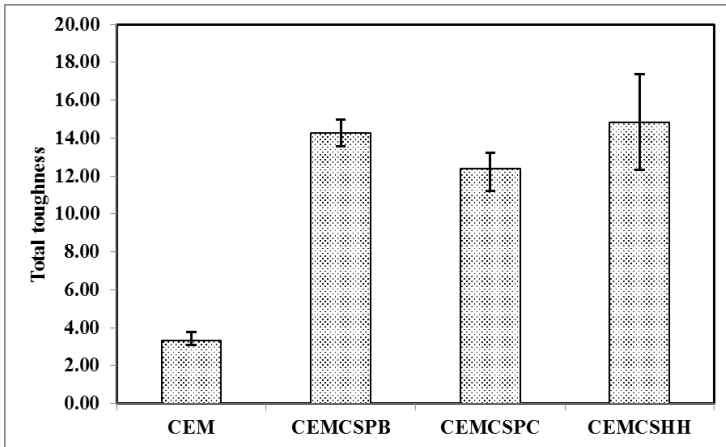


Figure 1.66: Comparison of total toughness of the cement paste composites containing carbon soot and inert carbonized particles

4.3 Tests on SCMs

4.3.1 Third-point bending tests

The mortar samples having size of 40x40x160 mm³ were tested in third-point flexure and the effect of carbonized particles addition was studied. The load-CMOD curves for the mortar specimens are reported in Figure 1.67 and Figure 1.68. The crack mouth opening rate was fixed at 0.005 mm/min so that the maximum load is reached within 5 minutes.

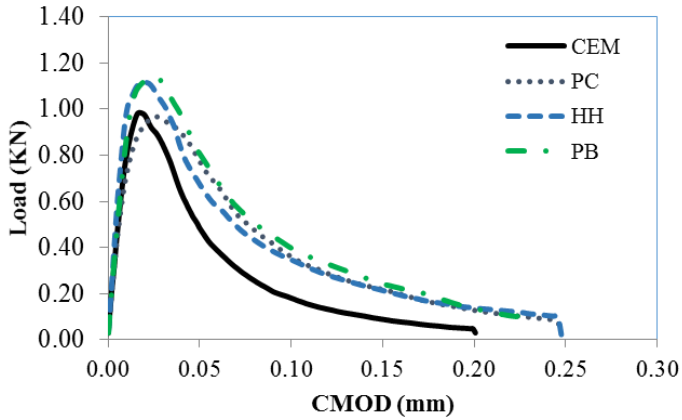


Figure 1.67: Typical load-CMOD relation of cement mortar composites containing various types of carbonized particles

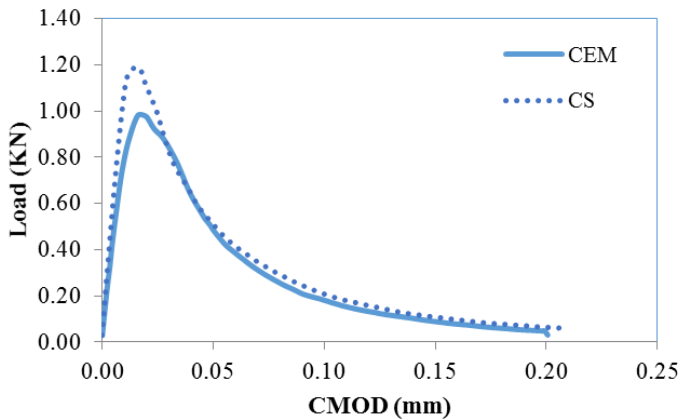


Figure 1.68: Load-CMOD curve for the cement composite containing carbon soot particles

4.3.2 Evaluation of flexural test results

The response of third-point bending tests were evaluated and compared to the control mix. The toughness indices I5, I10 and I20 were calculated.

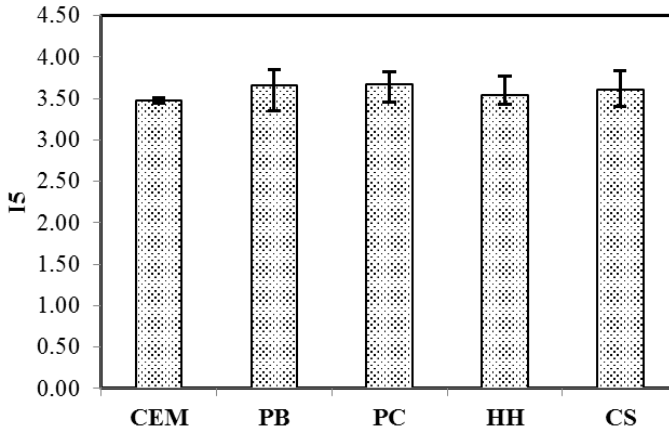


Figure 1.69: Comparison of toughness index I5 of mortar composites

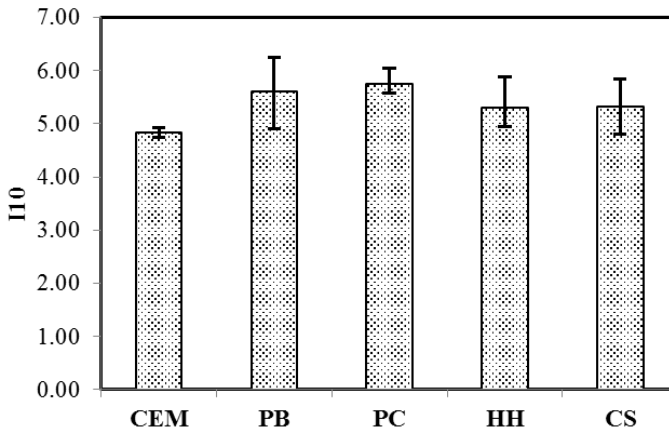


Figure 1.70: Comparison of toughness index I10 of mortar composites

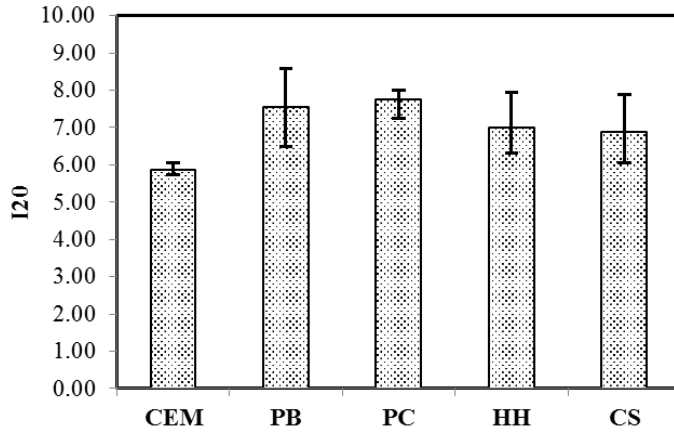


Figure 1.71: Comparison of toughness index I20 of mortar composites

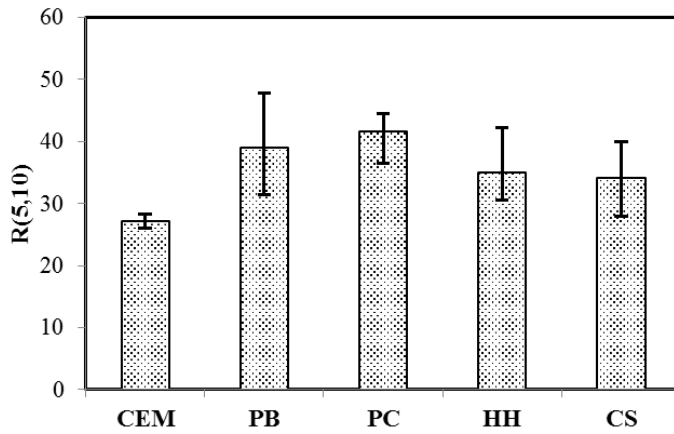


Figure 1.72: Comparison of residual toughness R(5,10) of cement mortar composites

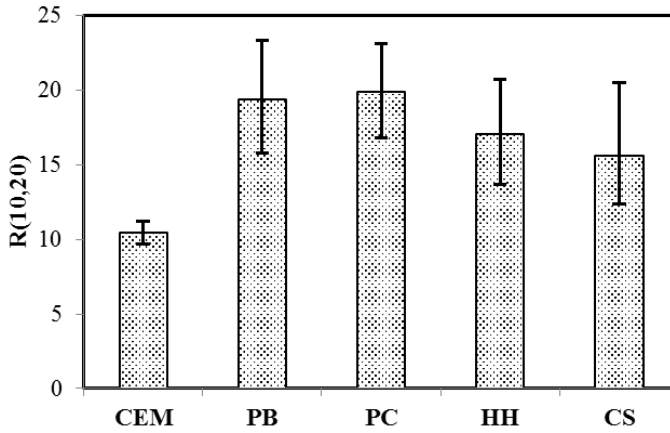


Figure 1.73: Comparison of residual toughness $R(10,20)$ of cement mortar composites

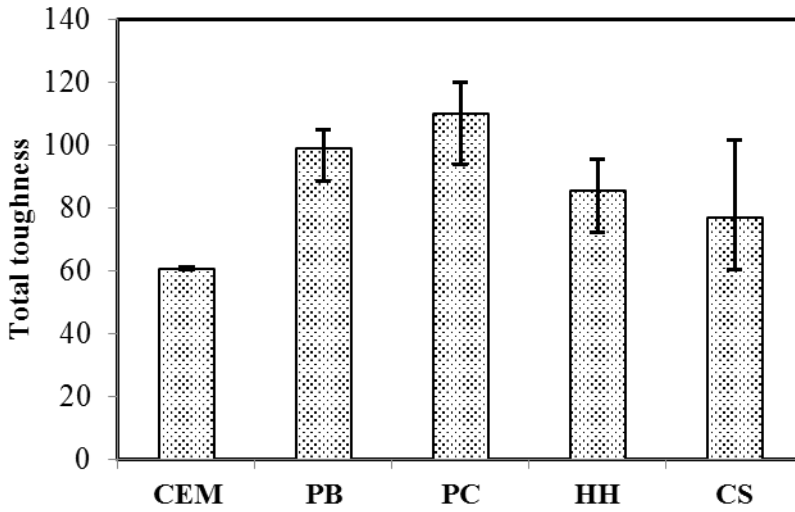


Figure 1.74: Total toughness of cement mortar composites

4.3.3 Modulus of rupture of mortar composites

The modulus of rupture was evaluated for all the cement mortar composites and results are reported in Figure 1.75.

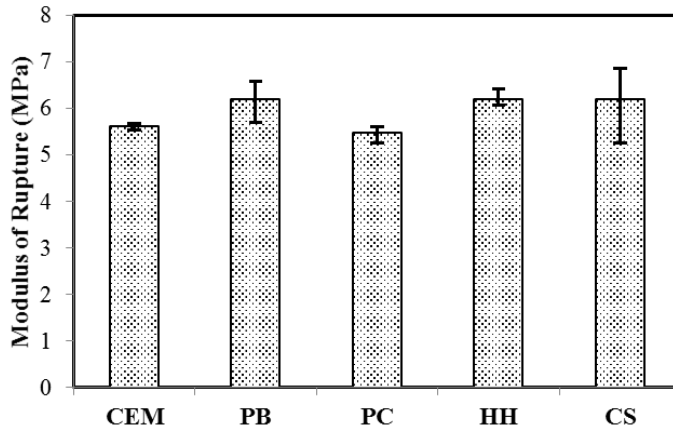


Figure 1.75: Modulus of rupture of cement mortar composites

Chapter 5 Discussion on results

The discussion on the result is presented in this chapter. It comprises of three parts based upon the types of experimental activity. In the first part, the results regarding the materials preparation of carbonaceous materials are discussed which includes the pyrolysis mechanisms and microstructures of the organic waste materials. Later in the chapter, the mechanical results of the cement composites are discussed based on the microstructure of the cement composites. In the third and last part of the chapter detailed description about the behavior of cement composites in pre peak and post peak performance is given.

5.1 Discussion on carbonized inert particles

5.1.1 Pyrolysis kinetics of materials

In the process of thermal degradation of organic materials, it is important to understand the pyrolysis process and the products obtained from the reactions. The process of pyrolysis strongly affects the quality of carbonized material as well as the products obtained from the process (Tsamba, Yang, & Blasiak, 2006). The thermal degradation behavior of bamboo and coconut shell were analyze with TGA technique from 25°C to 1000°C. The analysis indicated that the initial mass loss that is about 3.14 to 6.44 % of original mass for coconut shell and bamboo respectively is due to the physically adsorbed moisture in the feedstock. The second major mass loss happened from 220°C to 375°C is due to the simultaneously decomposition of the hemicellulose, cellulose and lignin. This mass loss behavior is common for all the woody materials (Byrne & Nagle, 1997). The last part of decomposition is related only to the lignin and the trend showed that almost the decomposition of the materials completes around 800°C (Adetoyese O Oyedun et al., 2012). Therefore, to optimize the process the pyrolysis temperature was kept at 850°C in the carbonization process of all the materials.

The chemical treatment of the bamboo with NaOH resulted in the partial degradation of the hemicellulose and cellulose structure prior to pyrolysis. This degradation effect can be observed by TGA curve as the material represented lower mass loss initially (i.e. in the temperature range of hemicellulose and cellulose decomposition.). In the latter phase when lignin starts to contribute, higher mass losses were observed.

The carbonized materials were analyzed by TGA in oxygen rich atmosphere to assess the purity of the samples. The analysis results showed that about 2% residues for untreated and carbonized bamboo and carbonized coconut shell were obtained indicating the purity of the carbonized materials. The DTG curves of the carbonized materials indicate that the oxidation was started at 400°C for untreated carbonized bamboo particles and represented a flat peak indicating the presence of small amounts of amorphous carbon particles along with crystalline carbon particles. The treated bamboo carbonized particles and coconut shell carbonized particles indicated crystalline behavior.

Carbon soot is a pure form of carbon obtained from the burning of fuel. The TGA analysis indicated that the soot is highly resistant to thermal degradation. A gradual mass loss of 16% was recorded from 25°C to 1000°C in argon atmosphere and 99% oxidation was observed while tested under air in the same temperature range.

5.1.2 Micro structure and composition

The FESEM observation showed that the particles obtained from the carbonization and grinding processes are highly angular with sharp edges. They show glossy look with smooth surfaces. The qualitative elemental analysis by EDX indicate that the chemical treatment of bamboo resulted in an 18% higher amount of fixed carbon form carbonization process as compared to the untreated one. Moreover, the annealing process led to a 6% increase of fixed carbon content, resulting in a more complete carbon conversion of the raw materials and to an equal amount of fixed carbon content for PBA and CPBA (Table 1.13). From the point of view of resulting carbon content, both routes (pyrolysis of bamboo as it is or after NaOH etching) are equivalent after annealing.

The elemental composition of coconut shell is a bit higher than the carbonized bamboo particles. This may be due to the higher amounts of lignin present in the coconut shell as indicated by the DTG curve of coconut shell. The EDX analysis results of carbonized hemp hurds indicated that the amount of fixed carbon is 44% which is low as compared to the other carbonized materials.

The Raman analysis results (Figure 1.27) indicate that although the amount of fixed carbon is low for carbonized hemp hurds but the material quality is better as compared to others. As the I_D/I_G ratio for hemp is 0.66 whereas for coconut shell it is about 0.84. The higher peak ratios indicate the inherent defects in the arrangement of carbon atoms. Considering the carbonized bamboo particles, the Raman intensity peak ratio is moderate as compared to coconut shell and hemp hurds and also the fixed carbon content is in the same pattern.

5.2 Mechanical results

5.2.1 Load-CMOD relation & modulus of rupture

The deformation behaviors of the cement composites were studied by using their load-CMOD relationships. Typical load-CMOD relationships for carbonized bamboo, coconut hemp and carbon soot are shown in Figure 1.34, Figure 1.42, Figure 1.50 and Figure 1.57, respectively. The load-CMOD relations showed that the initial cracks happens around 0.01 ± 0.002 mm CMOD for all the samples but the final split or the braking of the cement paste composites are delayed by the addition of inert carbonized particles. The enhancement in the maximum CMOD varies from sample to sample, with an average trend of 25% to 100% enhancement. In case of cement composites, containing carbon soot particles the initial crack CMOD is in of the same order of reference mix but the final split occurred much earlier as compared to the reference mix. This typical behavior indicates that the inclusion of carbon soot substantially increased the brittleness of the cement composites.

The influence of carbonized bamboo particles inclusions on the flexural strength of cement composites is presented in Figure 1.38. The results indicate that the flexural strength of cement composites enhances by the inclusion of inert carbonized bamboo particles. For all four types of carbonized bamboo particles inclusions, the flexural strength improves with the maximum increment occurring at 0.08% inclusion. The carbonized bamboo particles that were produced without chemical treatment showed a 20% increment in the flexural strength at 0.08% addition, while the chemically treated and carbonized bamboo particles resulted in 51% increment and it was further enhanced to 66% for annealed particles. These results may be explained on the basis of the increasing carbon content in the particles (Table 1.13): $PB < CPB < CPBA$. A lower carbon content leads to particles containing more defects and thus, having a lower mechanical resistance. The impact of carbonized coconut shell particles on the modulus of rupture of cement composites is reported in Figure 1.46. The results indicate that the flexural strength of cement composites containing

carbonized coconut shell particles has been reduced substantially. The 0.05% inclusion resulted in a reduction of 20% strength in flexure. The strength reduction behavior is common for both types of coconut shell particles. The elemental composition indicates that the fixed carbon content of coconut shell particles is higher than the carbonized bamboo particles but the flexural strength behavior observed is poor than the carbonized bamboo particles. Therefore, it may be concluded that the flexural strength improvement of the cement composites is not a direct function of fixed carbon content of the carbonized materials but also depends upon the other properties of the carbonized particles.

The cement composites with carbonized hemp hurds particles were tested in four different percentage additions i.e. 0.08, 0.2, 1.0 and 3.0%. The flexural test results indicated that the improvement was observed for 0.08% carbonaceous particles inclusion which is about 7%. Afterwards the flexural strength indicates a substantial decrease of about 45%. This indicates that the optimum percentage addition for bamboo and hemp hurds carbonized particles in terms of modulus of rupture is 0.08%.

Cement composites containing carbon soot particles substantially enhanced the modulus of rupture and made the composite more brittle. The test results show that the enhancement in the modulus of rupture is obtained with the increase in carbon soot content inclusion in the cement matrix i.e. with the inclusion of 0.05, 0.08, 0.2 and 1% carbon soot particles the enhancement observed was about 35%, 81%, 95% and 108%, respectively. The cement mixes with higher amount of carbon soot inclusion showed reduced workability in fresh state. The reduction in workability is attributed to the large surface area of the carbon soot particles. Similarly the enhanced strength may be attributed to the reduction in effective w/c as well as the availability of the large number of sites for the deposition of hydration products (Yahia, Tanimura, & Shimoyama, 2005).

In the last series of cementitious composites containing carbon soot and inert carbonized particles provided optimized performance in terms of strength and ductility. The analysis of the results reveals that the carbon soot particles played their role in improving the modulus of rupture of the cement composites while the inert carbonized particles played their role in the enhancement of the deformation capacity by modifying the crack growth pattern.

5.2.2 Crack surfaces and cement composites microstructure

The inert carbonized particles affect the cement matrix in two ways, one is that they provide the nucleation sites for the deposition of the calcium hydrated products and

results in stronger matrix (Lawrence, Cyr, & Ringot, 2003); the second factor, which is more pronounced is that the inert carbonized particles affects the growing crack path. In pure cement matrix after the initiation of the crack, it propagates rapidly resulting in sudden failure while in other case the cracks are trapped by the inert carbonized particles so the cracks have to divert their path involving more material in the failure process. Figure 1.39, Figure 1.47 and Figure 1.54 shows the typical fracture surfaces of cement composites with and without carbonized bamboo, coconut shell and hemp hurds particles inclusions, respectively. The diversion of cracks due the toughening mechanisms led by the inclusion of inert carbonaceous particles results in the development of three-dimensional fracture surface of the cement composites. The development of torturous crack surfaces indicates that more energy is required by the composite for the growth of cracks.

The FESEM observations of the cement composites revealed that the inert micro particles acted as an obstacle in the crack growth path, therefore the growing cracks have to deflect and contour around the inclusion. The most interesting thing about this modified cracking mechanism is that all the phenomenon of crack pinning, trapping, deflection and contouring is happening at the micro level, thus resulting in substantially improved performance in terms of energy absorption capacity.

5.2.3 Dispersion of carbonized inert particles

The dispersion of small sized inclusions in the host matrix is a well-known issue. The micro carbonized particles were first dispersed in water with the help of sonication and the solutions were observed visually for the dispersion of carbonized particles. In water, the carbonized material disperse very well and even after the 24 h of stand time few particles from the suspension settled down. The second step of the observation of particles dispersion in cement composite was carried out with the help of FESEM. The FESEM observations of small pieces of cement composite samples revealed that the carbonized particle dispersed well in the cement matrix. In the FESEM observations, it was also observed that the carbonized particles play an effective role in changing the crack path in cement matrix and cracks usually contours around the particles, resulting in tortures fracture surface. This improved randomness of the crack growth paths increases the energy required to break the specimen in two halves.

5.3 Evaluation of flexural test results

The effects of carbonized particles inclusion in the cement matrix were studied in detailed by considering the dimensionless toughness indices. The specimens containing untreated carbonized bamboo particles (PB) showed an increase in I_5 value with a maximum increment of 23% occurring at 0.08% addition of PB. In case of chemical treatment, the increment is 31% even for lesser addition of carbonized material. For chemically treated annealed and pyrolyzed bamboo, the maximum enhancement was observed at 0.08% addition like PB with a value of 24%. The toughness index I_{10} showed an increment of 31% and 32% for PB (untreated carbonized bamboo) and CPB (treated carbonized bamboo) at 0.05% inclusion, respectively. The result of total toughness indicates increments of 43, 41, 71 and 103% in the energy absorption capability of cement composites containing 0.08% of PB, PBA, CPB and CPBA, respectively. The total toughness results show that the trend of the total toughness enhancement is similar to the toughness indices. Initially the toughness increases and maximum is observed at 0.08% and decrease afterwards. The enhancement observed were 43%, 42%, 71% and 104% for PB, PBA, CPB and CPBA respectively.

The results of toughness indices I_5 and I_{10} are reported in Figure 1.43 and Figure 1.44. The toughness indices results showed that an inclusion of 0.05, 0.08 and 0.20% of carbonized coconut shell particles in the cement matrix enhanced the toughness index I_5 about 3, 33 and 25%, respectively. The trend is similar for the carbonized and annealed particles with an increment of 40, 47 and 3% for 0.05, 0.08 and 0.20% particles inclusion. Toughness index I_{10} for the cement composites containing carbonized coconut shell particles showed that maximum improvement occurs at 0.08% inclusion of micro particles with a magnitude of 115 and 119 % for PC and PCA, respectively. The total toughness was also increased due to the longer post peak response of the CEM+PC and CEM+PCA composites. The increased total toughness and toughness indices represent that the idea of using inert carbonized particles in the cement matrix for the enhancement of fracture energy and ductility is fruitful.

Evaluated toughness indices (I_5 & I_{10}) of the cement composites clearly demonstrate that the addition of HH (in micro-carbonized form) significantly increase the fracture toughness. The rate of increase in flexural toughness is non-linearly related to the added content of micro-carbonized HH. It is believed that presence of high number of irregular shaped carbonized particles control the cracks by increasing their lengths. This phenomenon considerably increases the energy

required for crack propagation and resultantly enhances the overall fracture toughness of cement composites.

Chapter 6 Conclusions

Based on the research conducted on the utilization of the micro carbonized particles for the development of innovative cement composites for the enhanced ductility, strength and reduced brittleness, following conclusions have been drawn.

- a. The investigation on the synthesis of the carbonized particles revealed that the annealing and chemical treatments improve the quality of the micro carbonized inert particles.
- b. The inert carbonized particles are capable of producing cement composites with improved fracture energy and toughness indices, creating a new family of cement composites.
- c. The performance of the cement composites containing carbonized inert particles greatly depends upon the organic source from which the carbonized particles are synthesized
- d. Carbonized inert particles produced from bamboo can enhance the flexural strength, toughness and the compressive strength of cement composites and also affect the fracture surface and enhance the post peak load carrying capacity
- e. Cement composites prepared with carbonized particles obtained from the carbonization of coconut shell represented enhanced fracture energy and post peak response but reduced the stiffness and modulus of rupture

- f. The micro carbonized particles prepared from hemp hurds were found quite effective in enhancing the fracture toughness, post peak response and compressive strength with a slight improvement in the modulus of rupture at 0.08% inclusion.
- g. The carbon soot inclusion resulted in substantial improvement in the modulus of rupture but as a side effect, the brittleness of the composite was also enhanced as observed from the comparison of toughness indices.
- h. The study reveal that the utilization of the combination of two or more inert particles in the cement mixes may provide optimum performance in terms of strength and ductility.
- i. The study shows that the micro sized carbonized inert particles disperse well uniformly in the cement matrix without making agglomerations thus resulting in more uniformed performance throughout the composite.

References

- Abd Elrahman, M., & Hillemeier, B. (2014). Combined effect of fine fly ash and packing density on the properties of high performance concrete: An experimental approach. *Construction and Building Materials*, 58, 225–233. <http://doi.org/10.1016/j.conbuildmat.2014.02.024>
- Ahmad, I., Yazdani, B., & Zhu, Y. (2015). Recent Advances on Carbon Nanotubes and Graphene Reinforced Ceramics Nanocomposites. *Nanomaterials*, 5, 90–114. <http://doi.org/10.3390/nano5010090>
- Ahmad, S., Khushnood, R. A., Jagdale, P., Tulliani, J., & Ferro, G. A. (2015). High performance self-consolidating cementitious composites by using micro carbonized bamboo particles. *Materials & Design*. <http://doi.org/10.1016/j.matdes.2015.03.048>
- Alkhateb, H., Al-Ostaz, A., Cheng, A. H.-D., & Li, X. (2013). Materials Genome for Graphene-Cement Nanocomposites. *Journal of Nanomechanics and Micromechanics*, 3(3), 67–77. [http://doi.org/10.1061/\(ASCE\)NM.2153-5477.0000055](http://doi.org/10.1061/(ASCE)NM.2153-5477.0000055)
- Aly, M., Hashmi, M. S. J., Olabi, A. G., Messeiry, M., & Hussain, A. I. (2011). Effect of nano clay particles on mechanical , thermal and physical behaviours of waste-glass cement mortars. *Materials Science & Engineering A*, 528(27), 7991–7998. <http://doi.org/10.1016/j.msea.2011.07.058>
- ASTM. (1997). *ASTM C1018-97 Standard test method for flexural toughness and first-crack strength of fiber reinforced concrete (using beam with third-point loading)*. *ASTM Standard*. <http://doi.org/10.1520/C1018-97>

- Awwad, E., Mabsout, M., Hamad, B., Farran, M. T., & Khatib, H. (2012). Studies on fiber-reinforced concrete using industrial hemp fibers. *Construction and Building Materials*, *35*, 710–717.
<http://doi.org/10.1016/j.conbuildmat.2012.04.119>
- Banthia, N., & Sheng, J. (1996). Fracture toughness of micro-fiber reinforced cement composites. *Cement and Concrete Composites*, *18*(4), 251–269.
[http://doi.org/10.1016/0958-9465\(95\)00030-5](http://doi.org/10.1016/0958-9465(95)00030-5)
- Bazant, Z. P., & Pfeiffer, P. A. (1987). Determination of fracture energy from size effect and brittleness number. *ACI Materials Journal*, *84*(6), 463–480.
<http://doi.org/10.14359/2526>
- Beaugrand, J., Nottez, M., Konnerth, J., & Bourmaud, A. (2014). Multi-scale analysis of the structure and mechanical performance of woody hemp core and the dependence on the sampling location. *Industrial Crops and Products*, *60*, 193–204. <http://doi.org/10.1016/j.indcrop.2014.06.019>
- Becker, T. L., Cannon, R. M., & Ritchie, R. O. (2002). *Statistical fracture modeling: Crack path and fracture criteria with application to homogeneous and functionally graded materials*. *Engineering Fracture Mechanics* (Vol. 69). [http://doi.org/10.1016/S0013-7944\(02\)00047-4](http://doi.org/10.1016/S0013-7944(02)00047-4)
- Beigi, M. H., Berenjian, J., Lotfi Omran, O., Sadeghi Nik, A., & Nikbin, I. M. (2013). An experimental survey on combined effects of fibers and nanosilica on the mechanical, rheological, and durability properties of self-compacting concrete. *Materials and Design*, *50*, 1019–1029.
<http://doi.org/10.1016/j.matdes.2013.03.046>
- Beygi, M. H. A., Kazemi, M. T., Nikbin, I. M., & Amiri, J. V. (2013). The effect of water to cement ratio on fracture parameters and brittleness of self-compacting concrete. *Materials & Design*, *50*, 267–276.
<http://doi.org/10.1016/j.matdes.2013.02.018>
- Bhatti, A. Q., Kishi, N., Mikami, H., & Ando, T. (2009). Elasto-plastic impact response analysis of shear-failure-type RC beams with shear rebars.

- Materials & Design*, 30(3), 502–510.
<http://doi.org/10.1016/j.matdes.2008.05.068>
- Bian, J., Peng, F., Peng, X., Peng, P., Xu, F., & Sun, R. (2012). Acetic acid enhanced purification of crude cellulose from sugarcane bagasse: Structural and morphological characterization. *BioResources*, 7(4), 4626–4639. Retrieved from <http://www.scopus.com/inward/record.url?eid=2-s2.0-84872793176&partnerID=tZOtx3y1>
- Brandt, A. M. (2009). *Cement based composites; Materials, mechanical properties and performance* (2nd ed.). Taylor & Francis.
- Buseck, P. R., Adachi, K., Gelencsér, A., Tompa, É., & Pósfai, M. (2012). Are black carbon and soot the same? *Atmospheric Chemistry and Physics Discussions*, 12(9), 24821–24846. <http://doi.org/10.5194/acpd-12-24821-2012>
- Buzzi-Unicem S.p.A. (2014). Buzzi Unicem. Retrieved July 15, 2014, from <http://www.buzziunicem.it/online/download.jsp?idDocument=2327&instance=1>
- Byrne, C. E., & Nagle, D. C. (1997). Carbonization of wood for advanced materials applications. *Carbon*, 35(2), 259–266. [http://doi.org/10.1016/S0008-6223\(96\)00136-4](http://doi.org/10.1016/S0008-6223(96)00136-4)
- Cao, M., Zhang, C., & Wei, J. (2013). Microscopic reinforcement for cement based composite materials. *Construction and Building Materials*, 40, 14–25. <http://doi.org/10.1016/j.conbuildmat.2012.10.012>
- Carneiro, J. A., Lima, P. R. L., Leite, M. B., & Toledo Filho, R. D. (2014). Compressive stress–strain behavior of steel fiber reinforced-recycled aggregate concrete. *Cement and Concrete Composites*, 46, 65–72. <http://doi.org/10.1016/j.cemconcomp.2013.11.006>
- Cheung, W. H., Lau, S. S. Y., Leung, S. Y., Ip, A. W. M., & McKay, G. (2012). Characteristics of Chemical Modified Activated Carbons from Bamboo

Scaffolding. *Chinese Journal of Chemical Engineering*, 20(3), 515–523.
[http://doi.org/10.1016/S1004-9541\(11\)60213-9](http://doi.org/10.1016/S1004-9541(11)60213-9)

Choi, W. C., Yun, H. Do, & Lee, J. Y. (2012). Mechanical properties of mortar containing bio-char from pyrolysis. *Maintenance Engineering Society of Korea Diagnosis Structures*, 16(3), 1–8.

Choy, K. K. H., Barford, J. P., & McKay, G. (2005). Production of activated carbon from bamboo scaffolding waste—process design, evaluation and sensitivity analysis. *Chemical Engineering Journal*, 109(1-3), 147–165.
<http://doi.org/10.1016/j.cej.2005.02.030>

Chung, D. D. L. (2000). Cement reinforced with short carbon fibers: a multifunctional material. *Composites Part B: Engineering*, 31, 511–526.

Coconut palm. (n.d.). Retrieved October 16, 2014, from
http://simple.wikipedia.org/wiki/Coconut_palm

Constantinides, G., & Ulm, F. J. (2004). The effect of two types of C-S-H on the elasticity of cement-based materials: Results from nanoindentation and micromechanical modeling. *Cement and Concrete Research*, 34(1), 67–80.
[http://doi.org/10.1016/S0008-8846\(03\)00230-8](http://doi.org/10.1016/S0008-8846(03)00230-8)

Domone, P. L. (2007). A review of the hardened mechanical properties of self-compacting concrete. *Cement and Concrete Composites*, 29(1), 1–12.
<http://doi.org/10.1016/j.cemconcomp.2006.07.010>

Dresselhaus, M. S., Dresselhaus, G., Saito, R., & Jorio, A. (2005). Raman spectroscopy of carbon nanotubes. *Physics Reports*, 409(2), 47–99.
<http://doi.org/10.1016/j.physrep.2004.10.006>

Einsfeld, R. a., & Velasco, M. S. L. (2006). Fracture parameters for high-performance concrete. *Cement and Concrete Research*, 36, 576–583.
<http://doi.org/10.1016/j.cemconres.2005.09.004>

FAOSTAT Agriculture data. (2012a). Retrieved October 16, 2014, from
http://faostat3.fao.org/faostat-gateway/go/to/browse/Q/*E

- FAOSTAT Agriculture data. (2012b). Retrieved July 12, 2014, from <http://faostat3.fao.org/faostat-gateway/go/to/download/Q/QC/E>
- Ferro, G. A., Ahmad, S., Khushnood, R. A., Restuccia, L., & Tulliani, J. M. (2014). Improvements in self-consolidating cementitious composites by using micro carbonized aggregates. *Fracture and Structural Integrity*, 30, 75–83. <http://doi.org/10.3221/IGF-ESIS.30.11>
- Ferro, G., Tulliani, J. M., Lopez, A., & Jagdale, P. (2015). New cementitious composite building material with enhanced toughness. *Theoretical and Applied Fracture Mechanics*. <http://doi.org/10.1016/j.tafmec.2015.01.005>
- Finnan, J., & Styles, D. (2013). Hemp: A more sustainable annual energy crop for climate and energy policy. *Energy Policy*, 58, 152–162. <http://doi.org/10.1016/j.enpol.2013.02.046>
- Freiman, S. W., & Mecholsky, J. J. (2012). *The fracture of brittle materials: Testing and analysis* (1st ed.). John Wiley & Sons, Inc.
- Gambhir, M. L. (2004). *Concrete technology* (3rd ed.). Tata McGraw-Hill publishing company.
- Grilo, J., Santos Silva, A., Faria, P., Gameiro, A., Veiga, R., & Velosa, A. (2014). Mechanical and mineralogical properties of natural hydraulic lime-metakaolin mortars in different curing conditions. *Construction and Building Materials*, 51, 287–294. <http://doi.org/10.1016/j.conbuildmat.2013.10.045>
- Hakamy, A., Shaikh, F., & Low, I. M. (2013). Microstructures and mechanical properties of hemp fabric reinforced organoclay–cement nanocomposites. *Construction and Building Materials*, 49, 298–307. <http://doi.org/10.1016/j.conbuildmat.2013.08.028>
- Hakamy, A., Shaikh, F. U. A., & Low, I. M. (2014). Characteristics of hemp fabric reinforced nanoclay–cement nanocomposites. *Cement and Concrete Composites*, 50, 27–35. <http://doi.org/10.1016/j.cemconcomp.2014.03.002>

- Hamzaoui, R., Guessasma, S., Mecheri, B., Eshtiaghi, A. M., & Bennabi, A. (2014). Microstructure and mechanical performance of modified mortar using hemp fibres and carbon nanotubes. *Materials & Design*, *56*, 60–68. <http://doi.org/10.1016/j.matdes.2013.10.084>
- Hillerborg, A. (1983). Analysis of one single crack. *Developments in Civil Engineering*, 223–249. Retrieved from <http://www.scopus.com/inward/record.url?eid=2-s2.0-0020979078&partnerID=tZOtx3y1>
- Hillerborg, A. (1985). The theoretical basis of a method to determine the fracture energy GF of concrete. *Materials and Structures*, *18*, 291–296. <http://doi.org/10.1007/BF02472919>
- Hu, C., Han, Y., Gao, Y., Zhang, Y., & Li, Z. (2014). Property investigation of calcium–silicate–hydrate (C–S–H) gel in cementitious composites. *Materials Characterization*, *95*, 129–139. <http://doi.org/10.1016/j.matchar.2014.06.012>
- Hu, C., & Li, Z. (2014). Micromechanical investigation of Portland cement paste. *Construction and Building Materials*, *71*, 44–52. <http://doi.org/10.1016/j.conbuildmat.2014.08.017>
- Jayapalan, A. R., Lee, B. Y., & Kurtis, K. E. (2013). Can nanotechnology be “green”? Comparing efficacy of nano and microparticles in cementitious materials. *Cement and Concrete Composites*, *36*, 16–24. <http://doi.org/10.1016/j.cemconcomp.2012.11.002>
- Jennings, H. M., Thomas, J. J., Gevrenov, J. S., Constantinides, G., & Ulm, F. J. (2007). A multi-technique investigation of the nanoporosity of cement paste. *Cement and Concrete Research*, *37*(3), 329–336. <http://doi.org/10.1016/j.cemconres.2006.03.021>
- Jenq, Y.-S., & Shah, S. P. (1991). Features of mechanics of quasi-brittle crack propagation in concrete. In Z. P. Bažant (Ed.), *Current trends in concrete fracture research* (pp. 103–120). Dordrecht: Springer Netherlands. <http://doi.org/10.1007/978-94-011-3638-9>

- Jiang, Z., Liu, Z., Fei, B., Cai, Z., Yu, Y., & Liu, X. (2012). The pyrolysis characteristics of moso bamboo. *Journal of Analytical and Applied Pyrolysis*, *94*, 48–52. <http://doi.org/10.1016/j.jaap.2011.10.010>
- Kawashima, S., Hou, P., Corr, D. J., & Shah, S. P. (2013). Modification of cement-based materials with nanoparticles. *Cement and Concrete Composites*, *36*, 8–15. <http://doi.org/10.1016/j.cemconcomp.2012.06.012>
- Khushnood, R. A., Rizwan, S. A., Memon, S. A., Tulliani, J., & Ferro, G. A. (2014). Experimental investigation on use of wheat straw ash and bentonite in self-compacting cementitious system. *Advances in Materials Science and Engineering*, *2014*, 1–11. <http://doi.org/10.1155/2014/832508>
- Kim, J. J., Foley, E. M., & Reda Taha, M. M. (2013). Nano-mechanical characterization of synthetic calcium–silicate–hydrate (C–S–H) with varying CaO/SiO₂ mixture ratios. *Cement and Concrete Composites*, *36*, 65–70. <http://doi.org/10.1016/j.cemconcomp.2012.10.001>
- Konsta-Gdoutos, M. S., Metaxa, Z. S., & Shah, S. P. (2010). Highly dispersed carbon nanotube reinforced cement based materials. *Cement and Concrete Research*, *40*(7), 1052–1059. <http://doi.org/10.1016/j.cemconres.2010.02.015>
- Korte, S., Boel, V., De Corte, W., & De Schutter, G. (2014). Static and fatigue fracture mechanics properties of self-compacting concrete using three-point bending tests and wedge-splitting tests. *Construction and Building Materials*, *57*, 1–8. <http://doi.org/10.1016/j.conbuildmat.2014.01.090>
- Kwan, A. K. H., Ng, P. L., & Huen, K. Y. (2014). Effects of fines content on packing density of fine aggregate in concrete. *Construction and Building Materials*, *61*, 270–277. <http://doi.org/10.1016/j.conbuildmat.2014.03.022>
- Kwan, A. K. H., & Yeung, J. S. K. (2014). Reducing cement paste volume for production of self-consolidating concrete by adding fillers. *HKIE Transactions*, *21*(2), 71–80. <http://doi.org/10.1080/1023697X.2014.909559>

- Lawrence, P., Cyr, M., & Ringot, E. (2003). Mineral admixtures in mortars: Effect of inert materials on short-term hydration. *Cement and Concrete Research*, 33(12), 1939–1947. [http://doi.org/10.1016/S0008-8846\(03\)00183-2](http://doi.org/10.1016/S0008-8846(03)00183-2)
- Li, V. C., & Maalej, M. (1996a). Toughening in cement based composites. Part I: Cement, mortar, and concrete. *Cement and Concrete Composites*, 18(4), 223–237. [http://doi.org/10.1016/0958-9465\(95\)00028-3](http://doi.org/10.1016/0958-9465(95)00028-3)
- Li, V. C., & Maalej, M. (1996b). Toughening in cement based composites. Part II: Fiber reinforced cementitious composites. *Cement and Concrete Composites*, 18(4), 239–249. [http://doi.org/10.1016/0958-9465\(95\)00029-1](http://doi.org/10.1016/0958-9465(95)00029-1)
- Li, Z., Kulkarni, S. M., & Shah, S. P. (1993). New test method for obtaining softening response of unnotched concrete specimen under uniaxial tension. *Experimental Mechanics*, 33(3), 181–188. <http://doi.org/10.1007/BF02322570>
- Lima, P. R. L., Toledo Filho, R. D., & Melo Filho, J. A. (2014). Compressive stress-strain behaviour of cement mortar-composites reinforced with short sisal fibre. *Materials Research*, 17(1), 38–46. <http://doi.org/10.1590/S1516-14392013005000181>
- Lin, C., Kayali, O., Morozov, E. V., & Sharp, D. J. (2014). Influence of fibre type on flexural behaviour of self-compacting fibre reinforced cementitious composites. *Cement and Concrete Composites*, 51, 27–37. <http://doi.org/10.1016/j.cemconcomp.2014.03.007>
- Lopez, A., Ferro, G., Jagadale, P., & Tulliani, J.-M. (2013). Influence of carbon nanotubes addition onto the mechanical properties of restoration mortars. In *Convegno Nazionale IGF XXII* (pp. 278–286). Rome, Italy.
- Lopez-Velazquez, M. A., Santes, V., Balmaseda, J., & Torres-Garcia, E. (2013). Pyrolysis of orange waste: A thermo-kinetic study. *Journal of Analytical and Applied Pyrolysis*, 99, 170–177. <http://doi.org/10.1016/j.jaap.2012.09.016>

- Luginbuhl, A. M. (2001). Industrial Hemp (*Cannabis sativa* L): The Geography of a Controversial Plant. *The California Geographer*, *41*, 1–14. Retrieved from <http://hdl.handle.net/10211.2/2738>
- Lv, S., Ma, Y., Qiu, C., Sun, T., Liu, J., & Zhou, Q. (2013). Effect of graphene oxide nanosheets of microstructure and mechanical properties of cement composites. *Construction and Building Materials*, *49*, 121–127. <http://doi.org/10.1016/j.conbuildmat.2013.08.022>
- Malard, L. M., Pimenta, M. A., Dresselhaus, G., & Dresselhaus, M. S. (2009). Raman spectroscopy in graphene. *Physics Reports*, *473*(5-6), 51–87. <http://doi.org/10.1016/j.physrep.2009.02.003>
- Mapei S.p.A. (2014). Mapei; Adhesives, sealants, chemical products for buildings. Retrieved from http://www.mapei.com/public/COM/products/671_dynamon_sp1_gb.pdf
- Martone, A., Formicola, C., Giordano, M., & Zarrelli, M. (2010). Reinforcement efficiency of multi-walled carbon nanotube/epoxy nano composites. *Composites Science and Technology*, *70*(7), 1154–1160. <http://doi.org/10.1016/j.compscitech.2010.03.001>
- Mccrady, E. (1991). The nature of lignin. *Alkaline Paper Advocate*, *4*(4), 2–5.
- Mehta, P. K., & Monteiro, P. J. M. (2006). *Concrete microstructure, properties and materials* (3rd ed.). McGraw-Hill.
- Memon, S. A., Arsalan, R., Khan, S., & Lo, T. Y. (2012). Utilization of Pakistani bentonite as partial replacement of cement in concrete. *Construction and Building Materials*, *30*, 237–242. <http://doi.org/10.1016/j.conbuildmat.2011.11.021>
- Metaxa, Z. S., Konsta-Gdoutos, M. S., & Shah, S. P. (2013). Carbon nanofiber cementitious composites: Effect of debulking procedure on dispersion and reinforcing efficiency. *Cement and Concrete Composites*, *36*, 25–32. <http://doi.org/10.1016/j.cemconcomp.2012.10.009>

- Mondal, P., Shah, S. P., & Marks, L. (2007). A reliable technique to determine the local mechanical properties at the nanoscale for cementitious materials. *Cement and Concrete Research*, 37(10), 1440–1444. <http://doi.org/10.1016/j.cemconres.2007.07.001>
- Mróz, K. P., & Mróz, Z. (2010). On crack path evolution rules. *Engineering Fracture Mechanics*, 77, 1781–1807. <http://doi.org/10.1016/j.engfracmech.2010.03.038>
- Mueller, F. V., Wallevik, O. H., & Khayat, K. H. (2014). Linking solid particle packing of Eco-SCC to material performance. *Cement and Concrete Composites*, 54, 117–125. <http://doi.org/10.1016/j.cemconcomp.2014.04.001>
- Musso, S., Tulliani, J.-M., Ferro, G., & Tagliaferro, A. (2009). Influence of carbon nanotubes structure on the mechanical behavior of cement composites. *Composites Science and Technology*, 69(11-12), 1985–1990. <http://doi.org/10.1016/j.compscitech.2009.05.002>
- Neville, A. ., & Brooks, J. . (2010). *Concrete technology* (2nd ed.). Prentice Hall.
- Nowack, B., & Bucheli, T. D. (2007). Occurrence, behavior and effects of nanoparticles in the environment. *Environmental Pollution*, 150(1), 5–22. <http://doi.org/10.1016/j.envpol.2007.06.006>
- Olsen, J. (2004). *Information paper on industrial hemp (industrial cannabis)*. Department of Primary Industries, Queensland. Retrieved from <http://web.archive.org/web/20080723143556/http://www2.dpi.qld.gov.au/hemp/16241.html>
- Onuaguluchi, O., Panesar, D. K., & Sain, M. (2014). Properties of nanofibre reinforced cement composites. *Construction and Building Materials*, 63, 119–124. <http://doi.org/10.1016/j.conbuildmat.2014.04.072>
- Oyedun, A. O., Gebreegziabher, T., & Hui, C. W. (2013). Mechanism and modelling of bamboo pyrolysis. *Fuel Processing Technology*, 106, 595–604. <http://doi.org/10.1016/j.fuproc.2012.09.031>

- Oyedun, A. O., Lam, K., Gebreegziabher, T., & Hui, C. (2012). Kinetic Modelling and Analysis of Waste Bamboo Pyrolysis. *Chemical Engineering Transactions*, 29, 697–702. <http://doi.org/10.3303/CET1229117>
- Park, J. S., Reina, A., Saito, R., Kong, J., Dresselhaus, G., & Dresselhaus, M. S. (2009). Raman spectra of single, double and triple layer graphene. *Carbon*, 47(5), 1303–1310. <http://doi.org/10.1016/j.carbon.2009.01.009>
- Peled, A., Castro, J., & Weiss, W. J. (2013). Atomic force and lateral force microscopy (AFM and LFM) examinations of cement and cement hydration products. *Cement and Concrete Composites*, 36, 48–55. <http://doi.org/10.1016/j.cemconcomp.2012.08.021>
- Peng, B. L., Dhar, N., Liu, H. L., & Tam, K. C. (2011). Chemistry and applications of nanocrystalline cellulose and its derivatives: A nanotechnology perspective. *The Canadian Journal of Chemical Engineering*, 89(5), 1191–1206. <http://doi.org/10.1002/cjce.20554>
- Pourjavadi, A., Fakoopoor, S. M., Khaloo, A., & Hosseini, P. (2012). Improving the performance of cement-based composites containing superabsorbent polymers by utilization of nano-SiO₂ particles. *Materials & Design*, 42, 94–101. <http://doi.org/10.1016/j.matdes.2012.05.030>
- Quercia, G., Spiesz, P., Hüsken, G., & Brouwers, H. J. H. (2014). SCC modification by use of amorphous nano-silica. *Cement and Concrete Composites*, 45, 69–81. <http://doi.org/10.1016/j.cemconcomp.2013.09.001>
- Rahman, M. K., Baluch, M. H., & Malik, M. A. (2014). Thixotropic behavior of self compacting concrete with different mineral admixtures. *Construction and Building Materials*, 50, 710–717. <http://doi.org/10.1016/j.conbuildmat.2013.10.025>
- Rao, G. A., & Prasad, B. K. R. (2002). Fracture energy and softening behavior of high-strength concrete. *Cement and Concrete Research*, 32(September 2000), 247–252. [http://doi.org/10.1016/S0008-8846\(01\)00667-6](http://doi.org/10.1016/S0008-8846(01)00667-6)

- Rizwan, S. A., Ahmad, S., & Bier, T. A. (2012). Application of packing concepts to high performance self-consolidating mortar (SCM) systems. In *American Concrete Institute, ACI Special Publication (SP-289.22)* (pp. 299–315). <http://doi.org/10.14359/51684271>
- Sakaray, H., Togati, N. V. V. K., & Reddy, I. V. R. (2012). Investigation on properties of bamboo as reinforcing material in concrete. *International Journal of Engineering Research and Applications*, 2(1), 77–83.
- Sassoni, E., Manzi, S., Motori, A., Montecchi, M., & Canti, M. (2014). Novel sustainable hemp-based composites for application in the building industry: Physical, thermal and mechanical characterization. *Energy and Buildings*, 77, 219–226. <http://doi.org/10.1016/j.enbuild.2014.03.033>
- Sawant, S. Y., Somani, R. S., Panda, A. B., & Bajaj, H. C. (2013). Formation and characterization of onions shaped carbon soot from plastic wastes. *Materials Letters*, 94, 132–135. <http://doi.org/10.1016/j.matlet.2012.12.035>
- Scrivener, K. L., Crumby, A. K., & Laugesen, P. (2004). The Interfacial Transition Zone (ITZ) Between Cement Paste and Aggregate in Concrete. *Interface Science*, 12(4), 411–421. <http://doi.org/10.1023/B:INTS.0000042339.92990.4c>
- Sedan, D., Pagnoux, C., Smith, A., & Chotard, T. (2008). Mechanical properties of hemp fibre reinforced cement: Influence of the fibre/matrix interaction. *Journal of the European Ceramic Society*, 28(1), 183–192. <http://doi.org/10.1016/j.jeurceramsoc.2007.05.019>
- Shah, S. P., Swartz, S. E., & Ouyang, C. (1995). *Fracture mechanics of Concrete: Applications of fracture mechanics to concrete, rock and other quasi-brittle materials*. John Wiley & Sons, Inc.
- Siddique, R., & Mehta, A. (2014). Effect of carbon nanotubes on properties of cement mortars. *Construction and Building Materials*, 50, 116–129. <http://doi.org/10.1016/j.conbuildmat.2013.09.019>

- Sinsiri, T., Kroehong, W., Jaturapitakkul, C., & Chindaprasirt, P. (2012). Assessing the effect of biomass ashes with different finenesses on the compressive strength of blended cement paste. *Materials & Design*, *42*, 424–433. <http://doi.org/10.1016/j.matdes.2012.06.030>
- Société Nouvelle du Littoral. (2014). Standard sand. Retrieved from <http://www.s-n-l.fr.html>
- Stark, J. (2011). Recent advances in the field of cement hydration and microstructure analysis. *Cement and Concrete Research*, *41*(7), 666–678. <http://doi.org/10.1016/j.cemconres.2011.03.028>
- Stevulova, N., Kidalova, L., Junak, J., Cigasova, J., & Terpakova, E. (2012). Effect of Hemp Shive Sizes on Mechanical Properties of Lightweight Fibrous Composites. *Procedia Engineering*, *42*, 496–500. <http://doi.org/10.1016/j.proeng.2012.07.441>
- Tangpagasit, J., Cheerarot, R., Jaturapitakkul, C., & Kiattikomol, K. (2005). Packing effect and pozzolanic reaction of fly ash in mortar. *Cement and Concrete Research*, *35*(6), 1145–1151. <http://doi.org/10.1016/j.cemconres.2004.09.030>
- Topçu, İ. B. (1997). Assessment of the brittleness index of rubberized concretes. *Cement and Concrete Research*, *27*(2), 177–183. [http://doi.org/10.1016/S0008-8846\(96\)00199-8](http://doi.org/10.1016/S0008-8846(96)00199-8)
- Tsamba, A. J., Yang, W., & Blasiak, W. (2006). Pyrolysis characteristics and global kinetics of coconut and cashew nut shells. *Fuel Processing Technology*, *87*(6), 523–530. <http://doi.org/10.1016/j.fuproc.2005.12.002>
- Ulm, F. (2009). What's the matter with concrete? From atoms to structures: A first cut. In *Convegno Nazionale IGF XX* (pp. 1–44).
- Vandamme, M., & Ulm, F.-J. (2009). Nanogranular origin of concrete creep. *Proceedings of the National Academy of Sciences of the United States of America*, *106*(26), 10552–10557. <http://doi.org/10.1073/pnas.0901033106>

- Wang, C., Yang, C., Liu, F., Wan, C., & Pu, X. (2012). Preparation of Ultra-High Performance Concrete with common technology and materials. *Cement and Concrete Composites*, 34(4), 538–544.
<http://doi.org/10.1016/j.cemconcomp.2011.11.005>
- Wang, X., Wang, K., Taylor, P., & Morcou, G. (2014). Assessing particle packing based self-consolidating concrete mix design method. *Construction and Building Materials*, 70, 439–452.
<http://doi.org/10.1016/j.conbuildmat.2014.08.002>
- Worrell, E., Price, L., Martin, N., Hendriks, C., & Meida, L. O. (2001). Carbon dioxide emissions from the global cement industry. *Annual Review of Energy and the Environment*, 26, 303–329.
- Yahia, A., Tanimura, M., & Shimoyama, Y. (2005). Rheological properties of highly flowable mortar containing limestone filler-effect of powder content and W/C ratio. *Cement and Concrete Research*, 35(3), 532–539.
<http://doi.org/10.1016/j.cemconres.2004.05.008>
- Yang, E.-H., & Li, V. C. (2014). Strain-rate effects on the tensile behavior of strain-hardening cementitious composites. *Construction and Building Materials*, 52, 96–104. <http://doi.org/10.1016/j.conbuildmat.2013.11.013>
- Yi, S., Huang, Z., Huang, J., Fang, M., Liu, Y., & Zhang, S. (2014). Novel calcium hexaluminate/spinel-alumina composites with graded microstructures and mechanical properties. *Scientific Reports*, 4, 4333.
<http://doi.org/10.1038/srep04333>
- Zhang, J., & Ju, X. (2011). Investigation on stress-crack opening relationship of engineered cementitious composites using inverse approach. *Cement and Concrete Research*, 41(8), 903–912.
<http://doi.org/10.1016/j.cemconres.2011.04.010>
- Zhao, S., & Sun, W. (2014). Nano-mechanical behavior of a green ultra-high performance concrete. *Construction and Building Materials*, 63, 150–160.
<http://doi.org/10.1016/j.conbuildmat.2014.04.029>

- Zhu, W., Hughes, J. J., Bicanic, N., & Pearce, C. J. (2007). Nanoindentation mapping of mechanical properties of cement paste and natural rocks. *Materials Characterization*, 58(11-12 SPEC. ISS.), 1189–1198.
<http://doi.org/10.1016/j.matchar.2007.05.018>